



UNIVERSITY OF OKLAHOMA

GRADUATE COLLEGE

SAND THICKNESS ESTIMATION

USING

SPECTRAL DECOMPOSITION

A THESIS

SUBMITTED TO THE GRADUATE FACULTY

in partial fulfillment of the requirements for the

degree of

Master of Science

By

Sara K. Tirado

Norman, Oklahoma

2004

ESIS  
A  
12



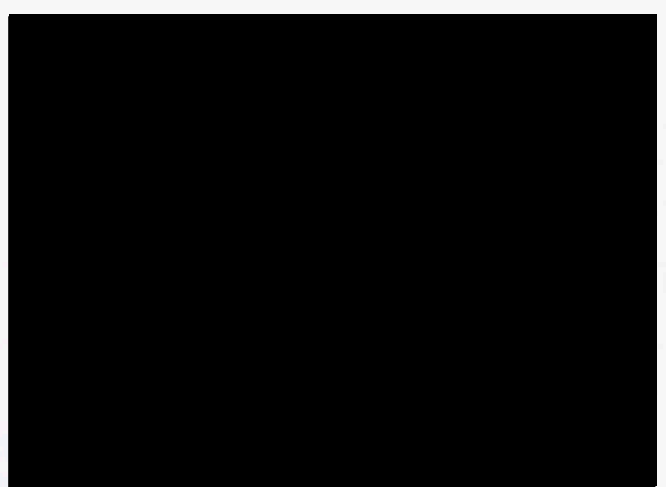
# Sand Thickness Estimation Using Spectral Decomposition

A THESIS

APPROVED FOR

THE SCHOOL OF GEOLOGY AND GEOPHYSICS

BY



## Acknowledgements

I would not have been able to complete this thesis without the help of many people. I would like to thank my advisor Dr. John Castagna for helping me with nearly every aspect of this thesis. And of course he kept coming up with new things for me to do, allowing me to learn even more.

I would like to thank the Shell Central Imaging Facility for the use of its workstations and software: GSI and Kingdom. I would like to especially thank Joe Duda for all of her help. It would have been impossible for me to finish without her. I also want to thank Mohamed El-Tass for his individual help. And, of course, I want to thank my other committee members, Dr. Judson Ahern and Dr. Alan Whitten, for their time and suggestions for my thesis.

I would like to thank the University of Oklahoma School of Geology and Geophysics for providing me with financial help through both my undergraduate years and my graduate years. I would like to acknowledge the use of seismic data from Tetra, Inc.

I would also like to thank friends that I made here at the University that provided me with encouragement, knowledge, and diversion while I worked on my thesis. I want to also thank all the teachers I have had over the years that piqued my interest and allowed me to learn.



## Acknowledgements

I would not have been able to complete this thesis without the help of many people. I would like to thank my advisor Dr. John Castagna for helping me with nearly every aspect of this thesis. And of course he kept coming up with new things for me to do, allowing me to learn even more.

I would like to thank the Shell Crustal Imaging Facility for the use of the workstations and software: GX2 and Kingdom. I would like to especially thank Jan Dodson for all of her help. It would have been impossible for me to finish without her. I also want to thank Muhammad Eissa for his individual help. And, of course, I want to thank my other committee members, Dr. Judson Ahern and Dr. Alan Witten, for their time and suggestions for my thesis.

I would like to thank the University of Oklahoma School of Geology and Geophysics for providing me with financial help through both my undergraduate years and my graduate years. I would like to acknowledge the use of seismic data from Texaco, Inc.

I would also like to thank friends that I made here at the University that provided me with encouragement, knowledge, and diversions while I worked on my thesis. I want to also thank all the teachers I have had over the years that piqued my interest and allowed me to learn.

Lastly, but probably most importantly, I would like to express my gratitude towards my husband Esteban for all of his love, support, and time taking care of our baby when we both had hectic schedules. I want to thank both my parents and my in-laws for all the encouragement and prayers that I received through the years. Thank you so much, I love you.

Abstract	1
Chapter 1: Introduction	1
Purpose of Study	1
Organization of thesis	1
Chapter 2: Background	2
Introduction	2
Geologic Background	2
Stratigraphy	2
Tectonics	2
Survey Parameters	2
Study Sites	2
Tying Wells to Seismic	2
Well A Discussion	2
Well C Discussion	2
Chapter 3: Spectral Decomposition of Seismic Data	2
Introduction	2

# Table of Contents

Acknowledgements.....	iv
Table of Contents.....	vi
Table of Figures.....	ix
Table of Tables.....	xii
Abstract.....	xiii
Chapter 1: Introduction.....	1
Purpose of Study.....	1
Organization of thesis.....	2
Chapter 2: Background.....	4
Introduction.....	4
Geologic Background.....	5
Stratigraphy.....	5
Tectonics.....	7
Survey Parameters.....	9
Study Sands.....	15
Tying Wells to Seismic.....	16
Sand A Discussion.....	18
Sand C Discussion.....	19
Chapter 3: Spectral Decomposition of Seismic Data.....	20
Introduction.....	20

Fourier Transform.....	20
Spectral Decomposition Methods.....	22
InSpect™ Program.....	25
Frequency Range and Increment .....	26
Interpreting Frequency Content for Sand A.....	28
Chapter 4: Peak Frequency versus Bed Thickness .....	29
Introduction.....	29
Sand A.....	29
Modeling Sand A .....	33
Sand C.....	40
Modeling Sand C .....	42
Chapter 5: Modeling Sand A .....	47
Introduction.....	47
Green’s Function.....	47
Frequency Characteristics for Sand A Model.....	52
Models.....	56
Chapter 6: Conclusions and Discussion.....	64
Conclusions.....	64
Discussion .....	65
References.....	66
Appendix.....	69
Appendix A: Tuning Charts.....	69

Appendix B: Spectrums .....	78
Appendix C: Frequency Spectra for Sands A and C at each well .....	87
Appendix D: Well Logs in study interval .....	97
Figure 2.3 Fault trends during the Tertiary (Barnard, 1999) .....	9
Figure 2.6 Base map of seismic data .....	12
Figure 2.7 Arbitrary line used for trends .....	13
Figure 2.8 Arbitrary line seismic .....	14
Figure 3.1 Chirp signal with two hyperbolic sweep frequencies using STFT (Stula, 2007) .....	23
Figure 3.2 Chirp signal with two hyperbolic sweep frequencies using CWT (Stula, 2007) .....	25
Figure 3.4 Frequency Spectrum for seismic survey .....	27
Figure 4.1 Cross plot of Peak Frequency (Hz) and Bed Thickness (ft) for Sand A ..	32
Figure 4.2 Wedge Model used for Sand A, annotated with reflection coefficients and velocities .....	34
Figure 4.3 Traces created in GX1 for Sand A, Wavelet extracted from original seismic data .....	35
Figure 4.4 Peak Frequency versus Bed Thickness for Modeled Sand A .....	36
Figure 4.5 Graph showing Peak Frequency and Bed Thickness relationship modeled and observed for Sand A .....	37
Figure 4.6 Graph showing Peak Frequency and Bed Thickness using second highest peak frequency for Sand A for wells #40499, #511, #312, #40477 .....	38

## Table of Figures

Figure 2.1 Location of Seismic Survey (Barncord, 1999).....	5
Figure 2.2 Generalized geologic column for Gulf of Mexico (Murray, 1961).....	7
Figure 2.3 Fault trends during the Tertiary (Barncord, 1999) .....	9
Figure 2.6 Base map of seismic data .....	12
Figure 2.7 Arbitrary line used for thesis .....	13
Figure 2.8 Arbitrary line seismic .....	14
Figure 3.1 Chirp signal with two hyperbolic sweep frequencies using STFT (Sinha, 2002) .....	23
Figure 3.2 Chirp signal with two hyperbolic sweep frequencies using CWT (Sinha, 2002) .....	23
Figure 3.4 Frequency Spectrum for seismic survey.....	27
Figure 4.1 Cross plot of Peak Frequency (Hz) and Bed Thickness (ft) for Sand A ...	32
Figure 4.2 Wedge Model used for Sand A, annotated with reflection coefficients and velocities .....	34
Figure 4.3 Traces created In GX2 for Sand A, Wavelet extracted from original seismic data.....	35
Figure 4.4 Peak Frequency versus Bed Thickness for Modeled Sand A.....	36
Figure 4.5 Graph showing Peak Frequency and Bed Thickness relationship modeled and observed for Sand A.....	37
Figure 4.6 Graph showing Peak Frequency and Bed Thickness using second highest peak frequency for Sand A for wells #40400, #311, #312, #40477 .....	38

Figure 4.7 Graph showing Peak Frequency and Bed Thickness using average of peak frequency and second highest peak frequency for Sand A for wells #40400, #311, #312, #40477.....	39
Figure 4.8 Graph showing Peak Frequency and Bed Thickness using trough frequency between peak frequency and second highest peak frequency for Sand A for wells #40400, #311, and #40477.....	40
Figure 4.9 Peak Frequency plotted with Bed Thickness for Sand C .....	42
Figure 4.10 Wedge Model used for Sand C, annotated with reflection coefficients and velocities .....	43
Figure 4.11 Generated traces for Modeled Sand C .....	44
Figure 4.12 Graph showing Peak Frequency and Bed Thickness relationship modeled and observed for Sand C .....	45
Figure 4.13 Graph showing Peak Frequency and Bed Thickness using trough frequency between peak frequency and second highest peak frequency for Sand C for wells #40400, #311, #20066, #55, #83, and #40133.....	46
Figure 5.1 Model defining impulse response ( Marfurt and Kirlin, 2001) .....	48
Figure 5.2 Amplitude as a Function of Frequency for odd impulse pairs ( Marfurt and Kirlin, 2001).....	49
Figure 5.3 Amplitude as a Function of Frequency for even impulse pairs ( Marfurt and Kirlin, 2001).....	49
Figure 5.4 Wavelet Overprint on Frequency spectra (Partyka, 1999) .....	50

Figure 5.5 Frequency Amplitude of Modeled Sand A (Navy) compared with Green's Function (Magenta).....	51
Figure 5.6 Peak Frequency Response for Sand A Reflection Coefficients at Ricker Wavelet peak frequencies 15 Hz, 20 Hz, 25 Hz, 30 Hz, and 35 Hz. ....	54
Figure 5.7 Even and Odd Pairs for Sand A.....	56
Figure 5.8 Sand A Model Odd Component of Impulse Pair generated traces.....	57
Figure 5.9 Sand A Model Even Component of Impulse Pair generated traces .....	58
Figure 5.10 Peak Frequency Response for modeled Sand A Odd Part .....	59
Figure 5.11 Peak Frequency Response for modeled Sand A Even Part .....	59
Figure 5.12 Peak Frequency Response for Odd Reflection Coefficients at Ricker Wavelet peak frequencies 15 Hz, 20 Hz, 25 Hz, 30 Hz, and 35 Hz. ....	60
Figure 5.13 Peak Frequency Response for Even Reflection Coefficients at Ricker Wavelet peak frequencies 15 Hz, 20 Hz, 25 Hz, 30 Hz, and 35 Hz. ....	61
Figure 5.14 Amplitude for Sand A Model Odd Component of Impulse Pair.....	62
Figure 5.15 Amplitude for Sand A Model Even Component of Impulse Pair .....	63
Figure 5.16 Amplitude for Modeled Sand A .....	63

## Table of Tables

Table 2.1 Acquisition Parameters (Todd 1993).....	10
Table 2.2 Processing sequence on the OCS310 3D survey (Todd 1993). .....	11
Table 4.1 Thickness (ft) of Sand A at Well Locations .....	30
Table 4.2 Peak Frequency values for Sand A at well locations.....	31
Table 4.3 Thickness (ft) of Sand C at Well Locations.....	41
Table 4.4 Peak Frequency values for Sand C at well locations .....	41

has the highest amplitude value in the spectrum. The peak frequency at each location is then plotted against the thickness of the sand. The peak frequency response of the data is compared with a modeled case. Sand A shows significant correlation to the modeled case, however, several spectra confuse the relationship. Sand C shows no clear relationship and that case appears to have no relation to peak frequency. Both before the main frequency the two have closer relationship to the modeled and reference curve. The method of peak frequency as a tool for bed thickness estimation shows no simple relationship. For unequal odd impulse pairs there are two thicknesses for one peak frequency value.

## Chapter 1: Introduction

### Abstract

Spectral decomposition of seismic data has been used to identify thin beds and other possible changes subsurface sand layers. Spectral decomposition can be used as a tool for estimating bed thickness. This thesis uses a 3-D Seismic data set in the Shelf Gulf of Mexico. Two Sands were identified and designated, sands A and C in a traditional 3-D seismic survey with the use of nine well logs. For each sand the frequency spectrum is extracted and the peak frequency found. Peak frequency is the frequency that has the highest amplitude value in the spectrum. The peak frequency at each location is then plotted against the thickness of the sand. The peak frequency response of the data is compared with a modeled case. Sand A shows some correlation to the modeled case; however, bimodal spectra confuse the relationship. Sand C shows no clear relationship and thickness appears to have no relation to peak frequency. Sands below the tuning frequency for the bed have clearer relationship to the modeled and theoretic curves. The method of peak frequency as a tool for bed thickness estimation shows no simple relationship. For unequal odd impulse pairs there are two thicknesses for one peak frequency value.

*Abstract* This document is intended for a general relationship between

thickness and peak frequency. The relationship is then compared to theoretical

models.

# Chapter 1: Introduction

## *Purpose of Study*

Sedimentary bed thickness is a very important measure for geophysicists, geologists, and engineers. It affects the way a bed may appear on seismic data, feasibility of a reservoir, and the net volume of a reservoir. Being able to identify changes in thickness of a potential reservoir can identify new possible drilling sites as well as lower the risk involved in finding a producible reservoirs. The question asked in this thesis is: Can the frequency content, or more specifically the peak frequency in a layer or horizon, be used to estimate the thickness of the sand layer?

The intent of this thesis is to attempt to find a correlation between peak frequency and bed thickness. Ideally, such a correlation could lead to a simple way of estimating the thickness in a unit of sand, assuming that each sand may be different in content and thickness variation. In order to better understand the problem, a case study of frequency variations is performed on a real seismic dataset using spectral decomposition. Two sand units are analyzed for empirical relationships between thickness and peak frequency. These observations are then compared to theoretical predictions.

## **Organization of thesis**

Chapter 2 will address the particulars of the seismic survey. A general background for the location of the survey in near offshore Louisiana and geologic history is presented. This chapter will also describe the considerations and reasoning for choosing the sands in the study. Finally, Chapter 2 will describe the spectral decomposition method and use of frequency data.

Chapter 3 begins the analysis of the data. Particularly, this chapter will focus on how peak frequency was gathered and analyzed. The gathered data is compared to the theoretical Green's Function.

Next Chapter 4 will demonstrate the importance of unequal impulse pairs and show the outcome of modeling even and odd impulse pairs for the study sand. This was done to give an explanation for the drop in peak frequency for very thin sands.

Finally, Chapter 5 will conclude the thesis with a discussion of peak frequency as a tool for determining sand thickness. Further questions are presented here along with possible future research.

Appendix A contains the seismic survey parameters and processing steps. Appendix B has the tuning charts for each well in the survey. Appendix C contains the time-frequency charts for Sand A at each well location. Appendix D has the time-frequency charts for Sand C at each well location.

## Chapter 2: Background

### *Introduction*

As with any study it is important to begin with an understanding of the location of the seismic data as well as how the seismic were acquired. This chapter will give a brief background of the geologic setting of the seismic survey. It will begin with a summary of the geologic history of north central Gulf of Mexico and summarize the stratigraphy to be expected in the area. The survey parameters are discussed later in the chapter. The study area is located offshore Louisiana, south of Marsh Island (Figure 2.1).

### *Geologic Background*

#### *Stratigraphy*

The survey area is in the Gulf of Mexico north of the North American continent.

Underlying the Gulf of Mexico is a series of sedimentary basins.

These basins are composed of sand, silt, and clay.

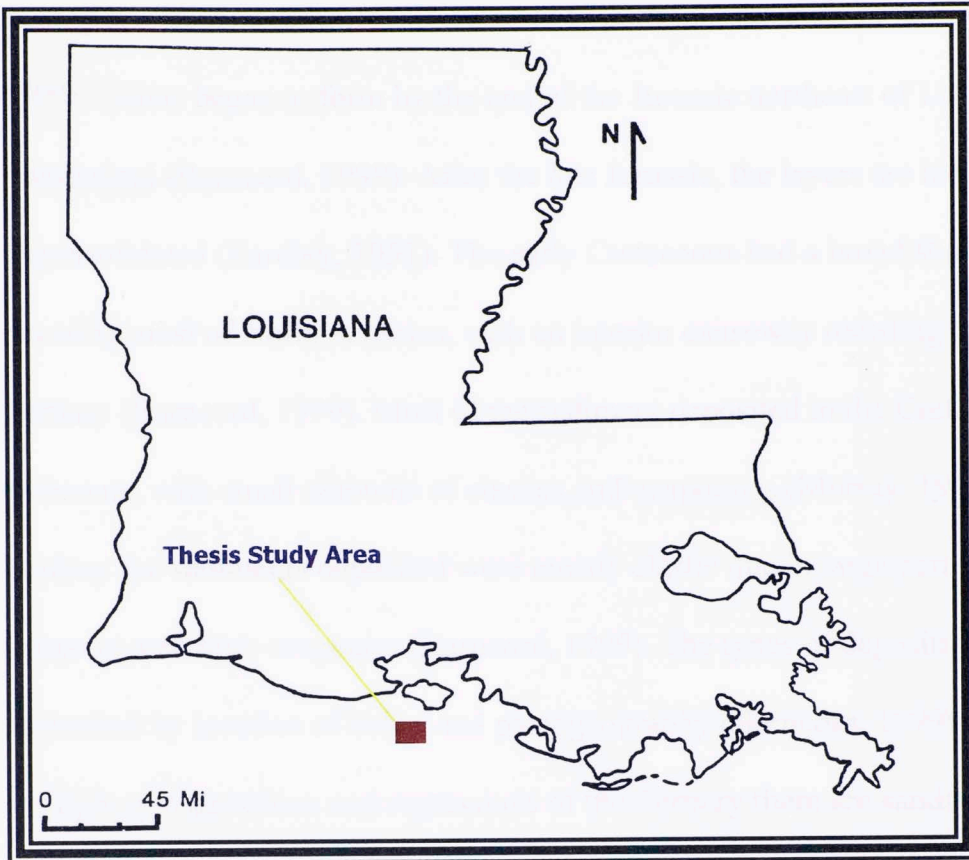


*Figure 2.1 Location of Seismic Survey (Barncord, 1999)*

## ***Geologic Background***

### **Stratigraphy**

The survey area is in the gulf coastal plain of the North American continent. Underlying the gulf coastal plain is a series of sedimentary formations mostly composed of sand, clay, marl, limestone, and chalk (Eardley, 1951).

During the Triassic sediment first started to pour into the Gulf of Mexico (Barncord, 1999). Deltas began to form by the end of the Jurassic northeast of Louisiana and Mississippi (Barncord, 1999). After the late Jurassic, the layers are largely unconsolidated (Eardley, 1951). The early Cretaceous had a broad shallow sea covering most of North America, with an interior causeway receding by the early Tertiary (Barncord, 1999). Most of the sediment deposited in the Cretaceous was carbonate, with small amounts of clastics and evaporates (Murray, 1961). In the Tertiary the sediments deposited were mostly clastic due in large part to the Laramide Orogeny and other orogenies (Barncord, 1999). The types of deposits were mostly controlled by location of deltas and paleogeography (Barncord, 1999) Due to the multiple transgressions and regressions of the Tertiary there are sandstones and shales laid alternately (Murray, 1961). The beds are interfingering with each other and very commonly difficult to correlate because columnar sections can be dissimilar unless closely spaced. Sands, silts, and clay were transported and deposited in the Gulf by the rivers draining the central part of the continent. (Eardley, 1951)

## Tertiary

The eastern Gulf of Mexico was part of the shallowly flooded part of the Atlantic Ocean, which, in late Tertiary, beginning approximately 10 million years ago, was closed off by the formation of the Isthmus of Panama. The resulting isolation of the Gulf basin was critical to the development of the Gulf of Mexico as a sedimentary basin. The Gulf basin was created by the subsidence of the continental shelf and the warping (Barncord, 1999).

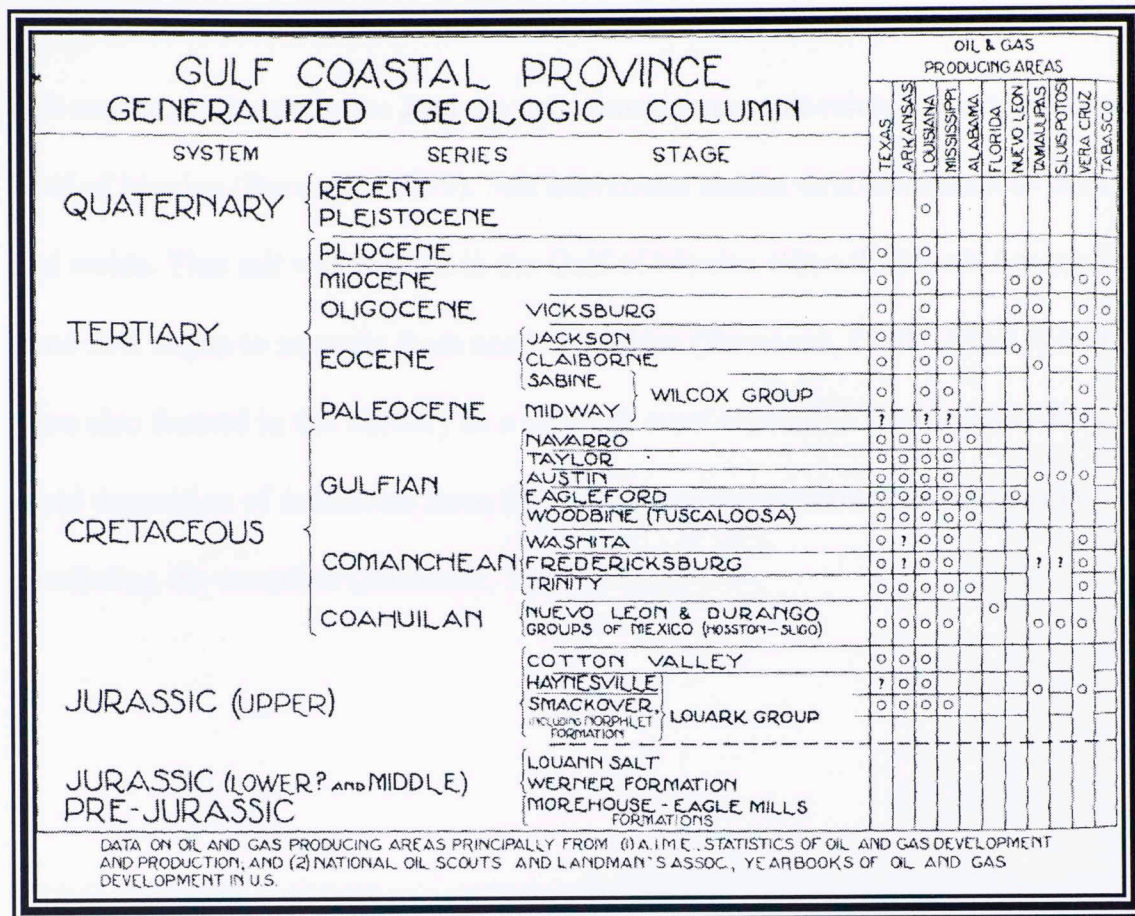


Figure 2.2 Generalized geologic column for Gulf of Mexico (Murray, 1961)

## Tectonics

The northern Gulf of Mexico was part of the landmass Pangea at the start of the Permian (Barncord, 1999). In late Triassic, the rifting began with the margin between Laurasia and Gondwana relaxing (Barncord, 1999). A system of grabens and half grabens were created from late Triassic to Cretaceous as the rifting led to subsidence and downwarping (Barncord, 1999).

Salt movement began in the Jurassic and caused many salt-related structures in the Gulf of Mexico (Barncord, 1999). Salt movement causes structures such as domes and welds. This salt was formed in the Gulf of Mexico when the North American plate first began to separate from northern Africa (Barncord, 1999). Fault systems were also formed in the Tertiary as a result of crust relaxation (Barncord, 1999). The rapid deposition of sediments from the Mississippi River caused growth faults paralleling the coastline (Barncord, 1999).

Figure 2.4 Peak growth during the Tertiary period

### Survey Parameters

The seismic survey was a part of the OCSIS (Offshore Coastal Seismic Investigation) program. It was conducted in June 1992 for Texas Energy Services. The survey was conducted in a depth of 70-100 ft and covered an area of 100-150 sq miles (Barnard, 1999). After processing the data, the results were presented in a report.

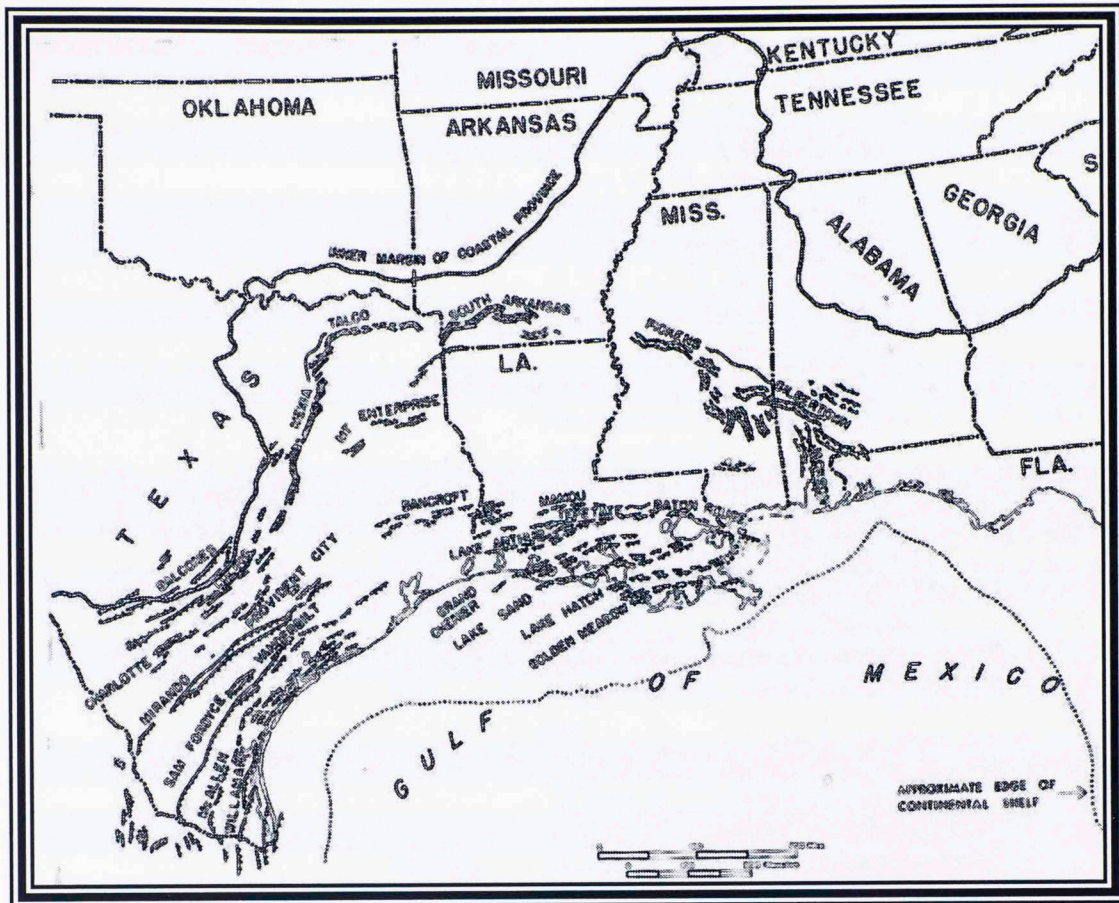


Figure 2.3 Fault trends during the Tertiary (Barncord, 1999)

### Survey Parameters

The seismic survey used was part of the OCS310 3D Survey acquired by Halliburton Geophysical Services in June 1990 for Texaco (Todd 1993). The grid for the survey was located at northing of 284392 ft and easting of 1695522 ft with an azimuth of 125 degrees (Todd 1993). After processing the bin size was 110 ft X 110 (Barncord, 1999).

<b>Inlines (production)</b>	
Receivers	22 parallel lines 2640 ft apart
	3 lines of 358 groups 220 ft apart
	16 lines of 579 groups 220 ft apart
	3 lines of 194 groups 220 ft apart
Shots	127 parallel lines 440 ft apart with a 220 ft offset between the receiver line and the nearest shot line
	18 lines of 358 shots 220 ft apart
	90 lines of 579 shots 220 ft apart
	19 lines of 194 shots 220 ft apart
NOTES	Shot records were 120 trace split-spread
	Shot stations had an inline offset of 110 ft from the receiver stations
<b>Crosslines (quality control)</b>	
Receivers	16 parallel lines 1.5 miles apart
	5 lines of 241 groups 220 ft apart
	7 lines of 277 groups 220 ft apart
	4 lines of 313 groups 220 ft apart
Shots	32 parallel lines with pairs 220 ft from each receiver line
	10 lines of 241 groups 220 ft apart
	14 lines of 277 groups 220 ft apart
	8 lines of 313 groups 220 ft apart
NOTES	Shot records were 120 trace split-spread
	Shot stations had an inline offset of 110 ft from receiver stations

**Table 2.1 Acquisition Parameters (Todd 1993).**

<b>A) Without DMO</b>	
1) Demultiplex	
2) Navigation Processing	
3) Prestack Enhancement	
4) Geometry	
5) Refraction Statics	
6) Coarse Velocity Grid	
7) First Pass Residual Statics	
8) Final Velocity Grid	
9) Second Pass Residual Statics	
10) Final Pre-DMO Stack	
11) Interpolation to Final Grid	
12) Migration	
13) Scale	
14) Filter	
15) Phase Rotation (-30 degrees)	
16) Final Pre-DMO Product	
<b>B) With DMO</b>	
17) Trim Statics	
18) DMO	
19) Trace Interpolation 1	
20) Trace Interpolation 2	
21) Migration	
22) FX Deconvolution	
23) Phase Rotation	
24) Filter	
25) Final DMO Product	

**Table 2.2 Processing sequence on the OCS310 3D survey (Todd 1993).**

The survey was loaded into SMT's Kingdom © for interpretation. Figure 2.6 shows the basemap for the seismic. For this study, one arbitrary line through nine wells was considered (figure 2.7). Figure 2.8 shows the arbitrary line seismic. (Red represents negative reflection coefficients.)

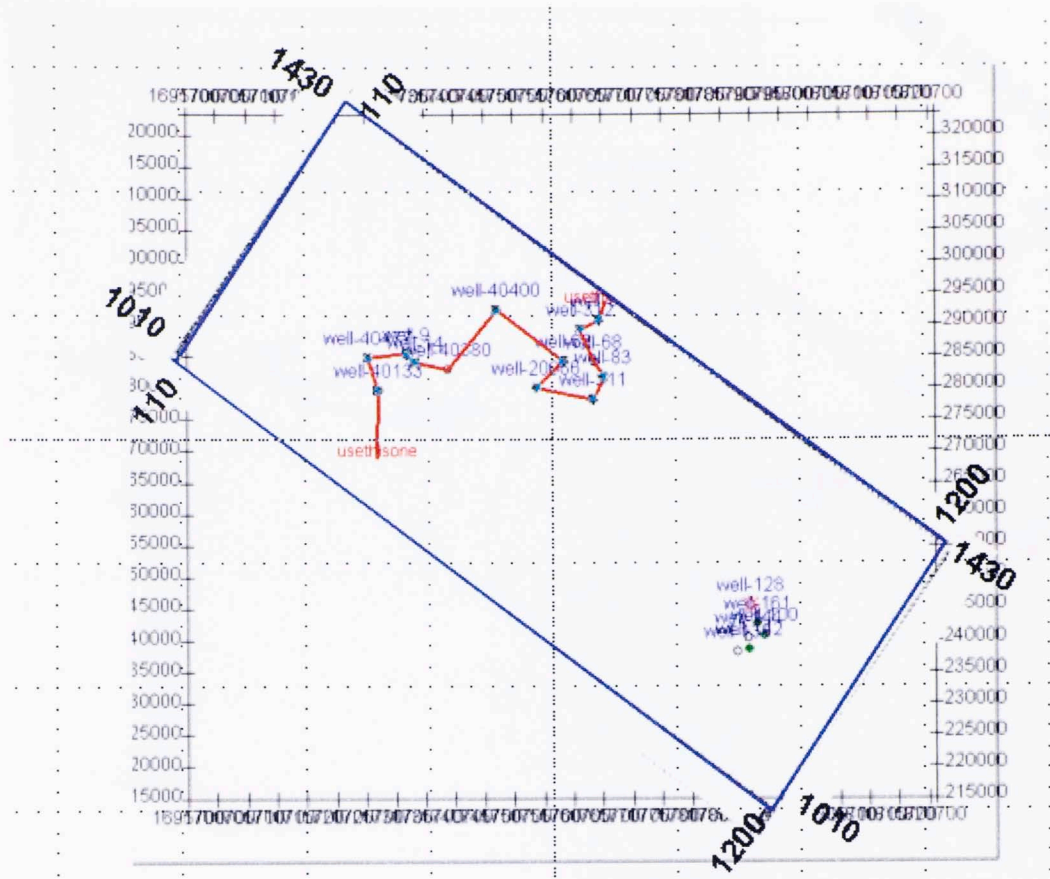


**Figure 2.6 Base map of seismic data**

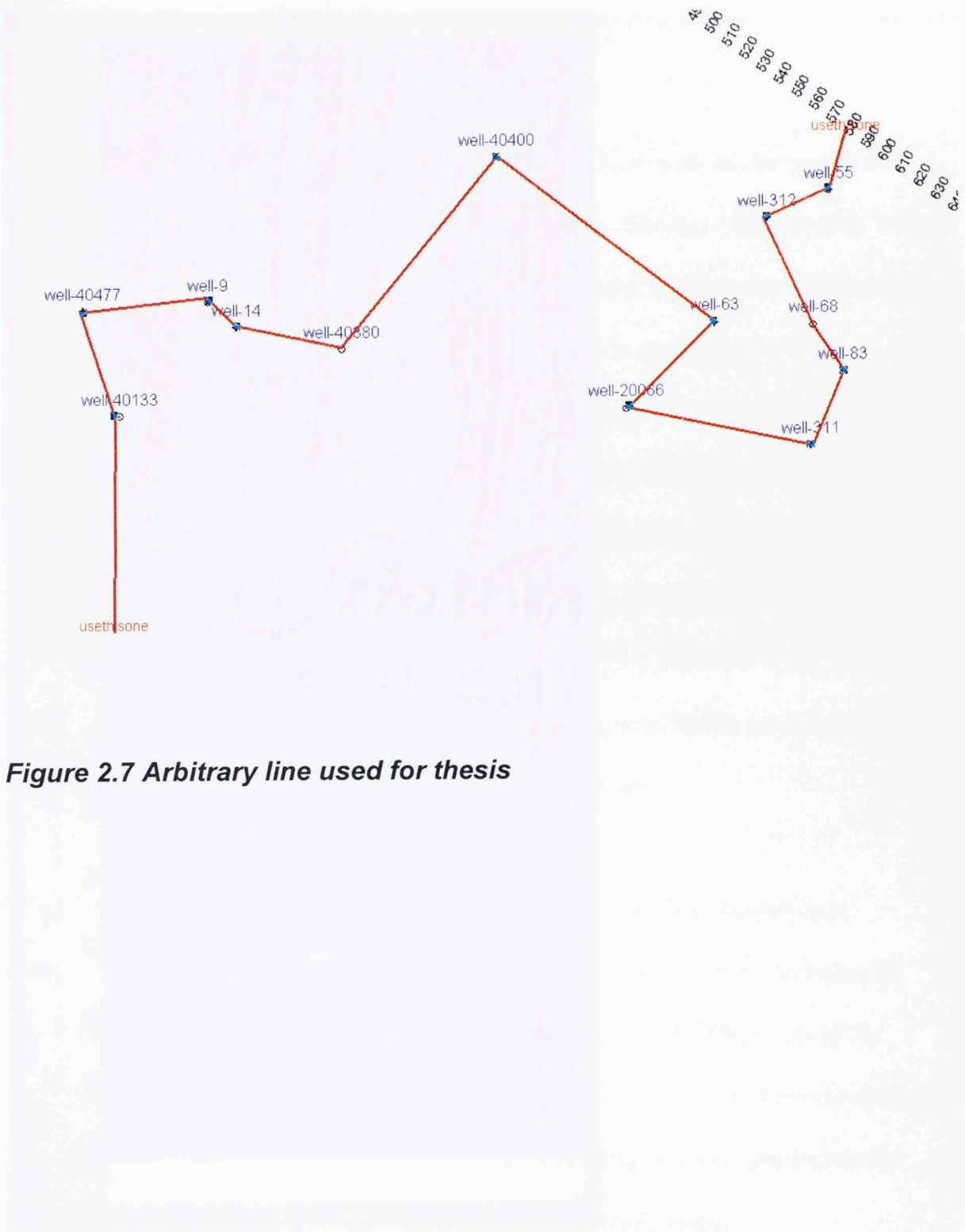


**Figure 2.7 Arbitrary line used for thesis**

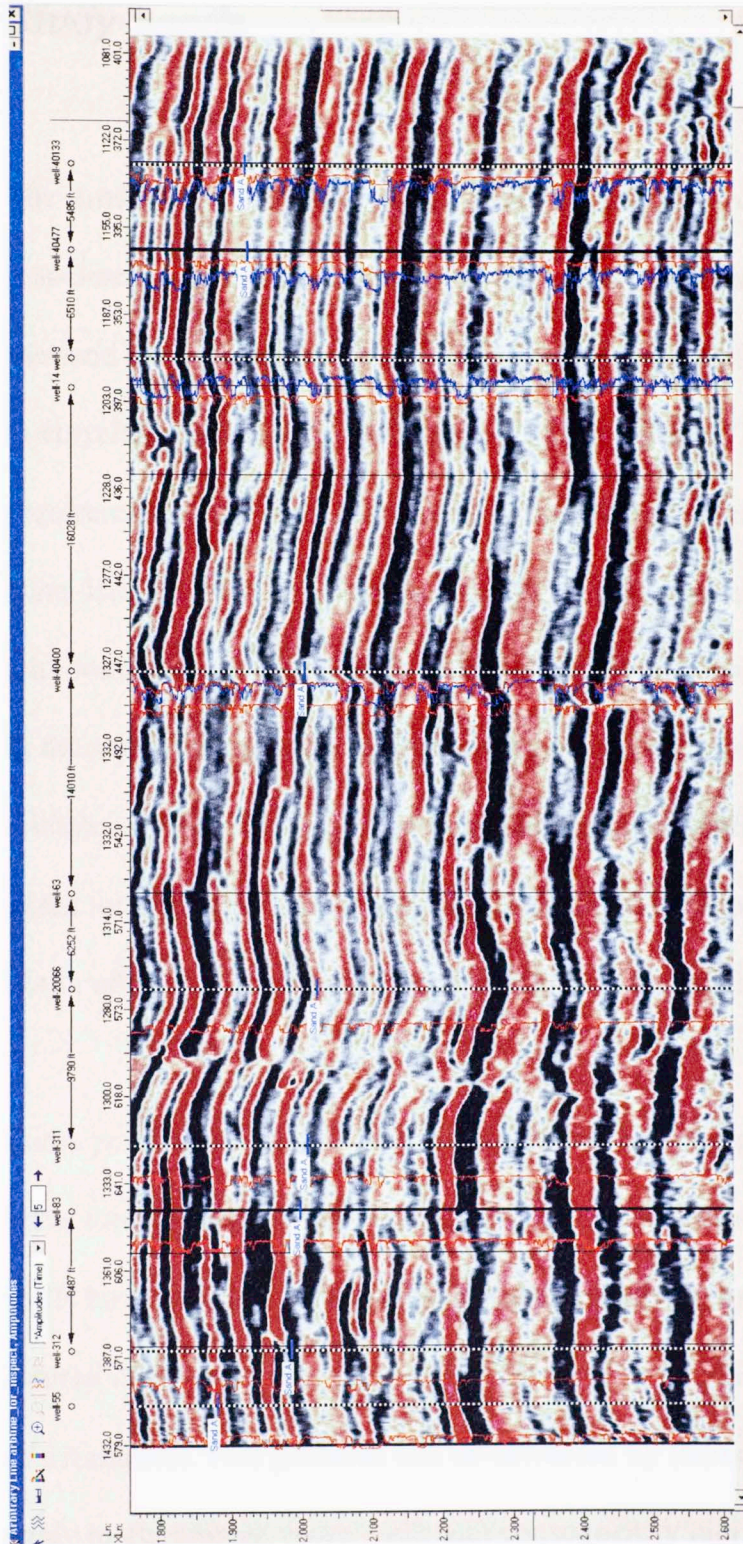


Figure 2.8 Arbitrary line seismic

## **Study Sands**

The sands that will be used in the study are required to have several characteristics associated with them in order to be useful for this thesis. The first characteristic is that the sand be continuous. This is a requirement of simplicity. It makes the sands easier to correlate from well to well and across the seismic. This should not be a requirement of the thickness versus frequency relationship, but is merely a consideration for a first look at identifying the relationship. The main characteristic I am looking for in the sands is variable thickness. This requirement is self explanatory in the sense that in order to do a study on sand thicknesses, one must first have thicknesses that change. Other considerations in identifying sands for study were, again for simplicity, easily correlated sands on well logs and blocky sand units, so as not to affect the frequency with gradations in the sand units.

Some possible problems with this thesis can be anticipated. The first and most influential problem is the limited number of data points. Only a limited number of wells have well logs to identify the sands and thicknesses from. The result of the limited data points is a less precise relationship and ultimately a less accurate method of estimation. This problem can be corrected by increasing the area covered in the study to encompass more wells and consequently more data points

Paleo markers were used to restrict the search for sands to the shallower sands. The paleo data helped me to determine that the shallower sands were much more continuous than the deeper sands. As you go deeper in the seismic record the horizons are less continuous and are more complicated by faulting. Although, it can probably be assumed that useful information can be gained by looking at deeper sands with regard to their frequency content.

Once the search was restricted to shallow sands, well logs were used to correlate sands. The logs used were the gamma ray log and the spontaneous potential log, primarily. When these were not available induction logs were used. The paleo markers identified by a previous interpreter were not identified in every well in the survey area so other sands were correlated in the wells with the paleo markers so other sands could be correlated in the remaining well logs. Several sands were identified in the wells. These were arbitrarily named A-G. They are in no specific order other than the order in which they were identified. Although only sands A and C were used in this study.

### ***Tying Wells to Seismic***

There were several check shot surveys associated with wells in the survey area. The first step in tying the wells to the seismic was to apply these surveys to the wells that

were associated with them. Unfortunately, there was not a check shot survey for each well in the study area. Fortunately, there was a previous interpreter that applied time-depth charts to the majority of the wells. Several of the check shot surveys had been altered and applied to wells considerably distant from the original well.

#### Associated with the check shot survey

The time-depth charts needed to be verified. To do this I displayed the interpreted sands as markers on the seismic data. After noticing inconsistencies I iterated changes in the time-depth charts for the well. As a control I applied the original check shot surveys at the wells they originated from. I changed the check shot surveys applied at distant wells to surveys that were from wells closer to the well without a specific survey. I tried not to alter the time-depth charts too much so as not to over correct the models. Also as a control for the velocity model I displayed the Gamma Ray and SP curves next to the wells on the seismic. This gave me some idea as to the location of different lithologies and I was able then to compare the well logs to the seismic.

I was not interested in getting a perfect velocity model for the entire length of the seismic record. Since I was primarily interested in two or three sands, I focused on tying the wells to the seismic in the specific range of 1.0-2.5 seconds. Figure 2.7 shows the tied wells and seismic. Well number 55 presented a problem in tying to seismic. Well number 55 did not have a check shot survey associated with it, and the wells in the proximity could not provide a close representation of the time-depth chart needed for well number 55. I was not able to accurately tie well number 55 to the

seismic section. The well log correlation, however, was done with confidence. After interpreting the seismic horizons associated with the markers for the other wells, the conclusion was drawn that since the horizons were consistent between the wells next to well number 55 and well number 55 itself, there was no doubt of the horizons associated with the markers in the well.

(Correlations are included in the appendix.)

Seismic horizons were interpreted for three sands: Sand A, Sand C, and Sand E. Sand A and C were continuous for all wells involved. Sand E was only determined for wells on one side of the interpreted fault. Wells numbered 14, 40400, 40477, and 40133, did not have Sand E identified in the log data. Sand E was not included in this study.

### ***Sand A Discussion***

Sand A was identified at 7100 Ft MD on Well # 40400. This sand was correlated onto the eight other wells #55, #63, #83, #311, #312, #20066, #40477, and #40133. The average thickness for Sand A is 44 ft. There are two wells with Sand A thickness above the tuning frequency, and the remaining with Sand A thickness below the tuning frequency. Sand A appears to have thin intermixed shale bed throughout. Different wells have slightly different sand character on the logs. Wells #40477, #83, and #20066 show Sand A as a blocky sand with not much influence of shales on the

SP log in the sand interval. Wells #63 and #311 show Sand A as a mostly block sand and one notch in the curve. This is assumed to be a thin shale bed. The remaining wells #40133, #40400, #55, and #312 show Sand A with mostly sandstone but several thin shale beds intermixed. For the purpose of this thesis the sand thickness was the net thickness and any shale content was not considered or subtracted. (The log interpretations are included in the appendix.)

### ***Sand C Discussion***

Sand C was correlated on well logs for nine wells: #55, #63, #83, #311, #312, #20066, #40477, and #40133. On well #40400 it was at 5600 ft MD. The average thickness for this sand is 120 ft. Only one of the wells showed Sand C below tuning thickness. Sand C is a fairly clean sand. It shows increasing shale content upwards for wells #63, #312, #20066, and #40477. The remaining wells show a blocky sand. The net thickness was used in this thesis for comparison and the thinning upwards sequence was included as part of the whole sand. Because many of the wells showed sands above tuning thickness for the sand extensive analysis was restricted to Sand A. (The log interpretations are included in the appendix.)

## Chapter 3: Spectral Decomposition of Seismic Data

### *Introduction*

The seismic data was decomposed into the frequency content according to the parameters outlined in Chapter 2. The section will describe the methodology and rationale in using spectral decomposition in this thesis. Frequency content and frequency character of reflections has been studied to some extent in past years (Partyka et al., 1998 and 1999, Chakraborty and Okaya, 1995, Castagna, 2003, Marfurt and Kirlin, 2001). Spectral analysis has been used to identify thin beds and as a hydrocarbon indicator. (Partyka et al., 1999, Castagna, 2003) This thesis will use the spectral decomposition to find the peak frequency of the seismic data at Sand A for different sand thicknesses.

### *Fourier Transform*

Fourier analysis in  $\mathbb{R}^n$  is used to decompose arbitrary functions into usually continuous sums of characters (Hormander, 1990). A character is defined as a function  $f$  such that for every  $y \in \mathbb{R}^n$

$$f(x+y) = f(x) c(y), x \in \mathbb{R}^n, \quad (3.1)$$

for some  $c(y)$ . The characters needed to expand a given function  $u$  depends on the properties of  $u$  (Hormander, 1990). For a function  $f \in \mathbb{R}^n$  the Fourier transform  $\mathbf{F}$  is defined as

$$\mathbf{F}(\xi) = \int e^{-\langle x, \xi \rangle} f(x) dx, \quad \xi \in \mathbb{R}^n. \quad (3.2)$$

Or for our purposes,

$$\mathbf{F}(\omega) = \int e^{-i\omega t} f(t) dt, \quad \omega \in \mathbb{R}^n. \quad (3.3)$$

If  $\mathbf{F}$  is also integrable then,

$$f(t) = (2\pi)^{-n} \int e^{i\omega t} \mathbf{F}(\omega) d\omega, \quad \omega \in \mathbb{R}^n, \quad (3.4)$$

by the Fourier inversion formula. (Hormander, 1990)

The function  $f(t)$  can also be written in terms of the Fourier transform as the sum of sines and cosines. This is expressed as

$$f(t) = \frac{a_0}{2} + \sum_{n=1}^{\infty} (a_n \cos \omega t + b_n \sin \omega t). \quad (3.5)$$

Equation 3.5 can be rewritten in terms of only cosines:

$$f(t) = c_0 + \sum_{n=1}^{\infty} c_n \cos (\omega t + \theta_n), \quad (3.6)$$

where  $c_n = \sqrt{a_n^2 + b_n^2}$  and  $\theta_n = \arctan(b_n / a_n) = \omega t_0$ , called the phase. (Sinha, 2002)

## ***Spectral Decomposition Methods***

Frequency information can be obtained either as the frequency content of the entire signal or as time localized frequencies. It is more useful in seismic geophysics to have time localized frequency information. One method of having time localized frequency information is using the short-time Fourier transform (STFT). The STFT is performed by windowing the time domain and performing the Fourier transform over that window (Sinha, 2002). The window is defined such that the signal remains periodic (Sinha, 2002). This gives a time-frequency map known as a spectrogram (Sinha, 2002). Figure 3.1 shows a synthetic example of a chirp signal with two hyperbolic sweep frequencies from Sinha (2002) transformed using the STFT.

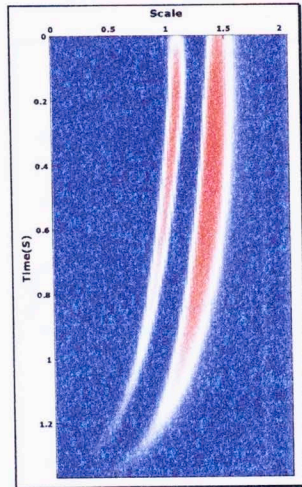
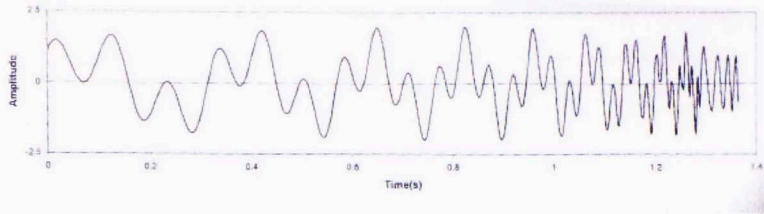


**Figure 3.1 Chirp signal with two hyperbolic sweep frequencies using STFT (Sinha, 2002)**

Many times the STFT cannot accurately represent the frequency with time because the structure of the signal can be non-stationary (Sinha, 2002). The continuous wavelet transform chooses atoms such that the time window changes for different frequencies (Sinha, 2002). Figure 3.2 shows the same chirp signal from the previous transformed using the CWT.

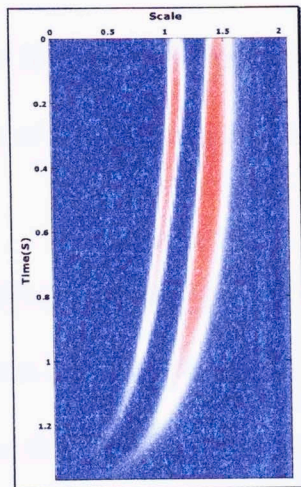
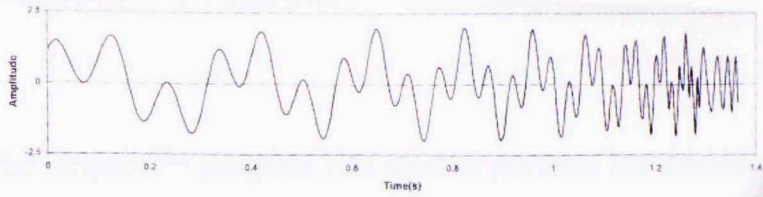


**Figure 3.2 Chirp signal with two hyperbolic sweep frequencies using CWT (Sinha, 2002)**

The program InSpect™ used to transform the seismic in this thesis uses a variation of the continuous wavelet transform method called matching pursuit decomposition. Once the event was identified on the seismic section, the frequency content could be determined by looking at the time-frequency map and locating the same time for the event.

## **InSpect™ Program**

The InSpect™ program was used to perform the decomposition. This program uses the continuous wavelet transform method of decomposition. The inputs of the program were as follows: SEGY seismic data, frequency range, and frequency increment. Each of these inputs will be addressed.

The InSpect™ program has the capability of decomposing both 2-D and 3-D seismic data. The program creates several frequency traces for each trace of SEGY seismic data. This means that there is a volume of traces equal to the original seismic for each frequency value. This presented the problem of loading spectral decomposition output into Kingdom in a useful manner.

For a 3-D volume the InSpect™ data would need to be loaded either by line with all the corresponding frequencies to that line or by frequency with the whole volume of lines associated. Either way there would need to be multiple (nearly 100) volumes loaded into the project. It was decided that an arbitrary line connecting the wells in the study would be used for interpretation. (refer to figure 2.6)

The arbitrary line spectral decomposition results were loaded as lines of constant frequency. The consequence of this loading method is that the arbitrary line cannot be associated with the accurate world coordinates, meaning that the wells cannot be

simply viewed with the data. The benefit of this loading method is that by taking crosslines through the volume you can see all the frequencies associated with one trace. Also, by viewing an inline you can see the section with only one frequency.

## Frequency Range and Increment

Frequency range for the spectral decomposition was determined by extracting the frequency content of the Texaco seismic data set. Kingdom has a tool that extracts the frequency content. This plot is shown in figure 3.4. The main band of data falls between 0 and 60 Hz. The range was selected between 0 and 80 Hz. The frequency increment was set to 1 Hz.

Figure 3-4 Frequency Spectrum for seismic survey acquired over study area

The seismic data acquisition results were loaded into the main Kingdom project file. The seismic data was set additional memory. The world coordinates of the seismic data were set manually in the master of traces in the 7-D SEGY seismic loading routine of Kingdom software package. There were 913 traces and 15 frequency. The data were checked according to the frequency.

## Interpreting Frequency Content for Sand A

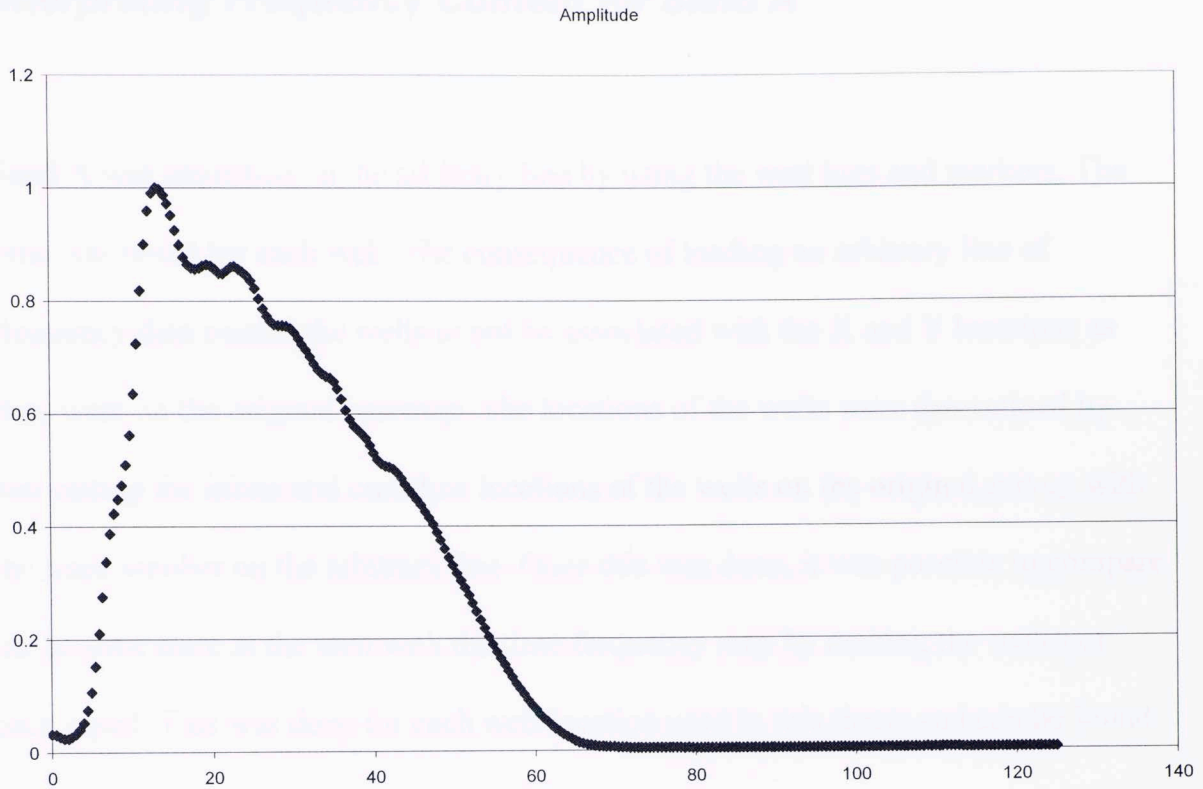


**Figure 3.4 Frequency Spectrum for seismic survey centered over study sands**

The spectral decomposition results were loaded into the same Kingdom project with the original seismic as an additional survey. The world coordinates of the InSpect survey were determined by the number of traces in the 2-D SEG Y seismic and the number of frequency volumes produced. There were 815 traces and 80 frequencies. The lines were ordered according to the frequencies.

## **Interpreting Frequency Content for Sand A**

Sand A was identified on the arbitrary line by using the well logs and markers. The time was noted for each well. The consequence of loading an arbitrary line of frequency data caused the wells to not be associated with the X and Y locations as they were on the original basemap. The locations of the wells were determined by associating the inline and crossline locations of the wells on the original survey with the trace number on the arbitrary line. Once this was done, it was possible to compare the seismic trace at the well with the time-frequency map by making the scales of each equal. This was done for each well location used in this thesis and can be found in the appendix.

### **Sand A**

Figure 4.1 shows the average thickness of Sand A. The values range from and indicate the average thickness of the Sand A. The average velocity over the interval is 2000 ft/sec. The well logs used for this study are listed in the appendix. Table 4.1 lists the locations of the wells used in this study. This is the net thickness of sand and gravel in the interval.

## Chapter 4: Peak Frequency versus Bed Thickness

### *Introduction*

This chapter will compare the sand thickness for the nine wells in the study to the peak frequency observed in the frequency spectra for two sands: Sand A and Sand C. Peak frequency is defined and used in this thesis as the frequency with the maximum amplitude in the frequency domain (Chung and Lawton, 1995). The thicknesses of the beds were estimated from the well logs for nine wells in the survey area. The plotted points are compared to expected outcomes from modeling sands with similar reflection coefficients.

### *Sand A*

Sand A has an average thickness of 40 ft. The values range above and below the tuning thickness of 66 ft. The average velocity over the interval is 8800 ft/sec. The well logs over the interval can be found in the appendix. Table 4.1 lists the thickness of Sand A at each well location. This is the net thickness of sand and does not factor in any shale content.

Well Number	Sand A Thickness (ft)
55	40
312	40
83	25
311	50
20066	35
63	64
40400	45
40477	20
40133	75

***Table 4.1 Thickness (ft) of Sand A at Well Locations***

The peak frequency was taken as the highest amplitude value on the frequency spectrum. The frequency spectrum was extracted from the frequency dataset at the time of the sand reflection. Table 4.2 shows the peak frequency for Sand A at each well location.

Well Number	Peak Frequency (Hz)
55	32
312	22
83	30
311	15
20066	29
63	21
40400	18
40477	18
40133	26

**Table 4.2 Peak Frequency values for Sand A at well locations**

The peak frequency was then plotted against the thickness of Sand A to determine a relationship. Frequency spectra for Sand A can be found in the appendix. Figure 4.1 shows the cross plot. The red line is the tuning thickness.

Bed Thickness Vs Peak Frequency for Sand A

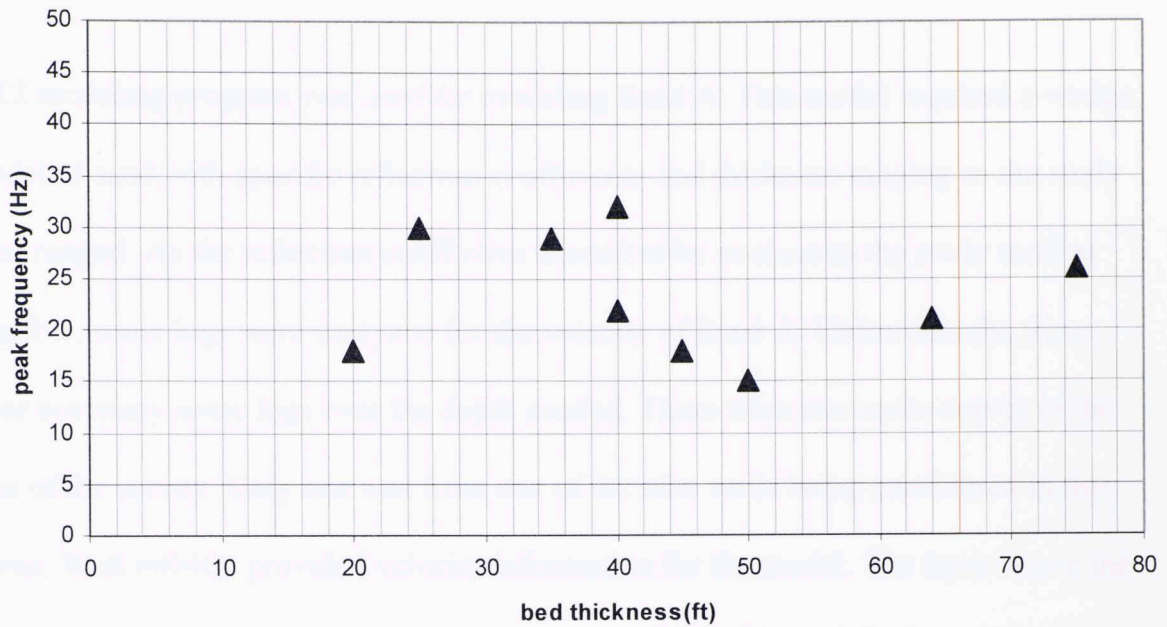


**Figure 4.1 Cross plot of Peak Frequency (Hz) and Bed Thickness (ft) for Sand A**

There was little observed relationship between the peak frequency and the bed thickness for Sand A. It was decided that the best approach would be to model the expected behavior for a sand with similar reflection coefficients. By modeling the sand as a wedge model and determining the frequency content of the assumed sand, more information could be learned about the study sand and peak frequency.

## Modeling Sand A

GX2 modeling program was used for modeling Sand A. This model required a wedge model of sand with specific reflection coefficients and thickness ranging as the study sand ranged. As the reflection coefficient needed to be as close to the study sand as possible, sonic logs were analyzed for the velocity of Sand A. Unfortunately, there were not many sonic logs over the depth needed. There were two sonic curves in the area of the survey. Only one was from one of the nine wells being considered in this thesis. Well #40400 provided velocity information for the model. The layer above the sand was averaged to 10,000 ft/s, with the sand at 8,800 ft/s, and the layer below 9,600 ft/s. The density used was the default value given by the program, as no density curves were found in the nine wells over the depth range of the study sand. The reflection coefficients were mostly odd but not equal. (figure 4.2)

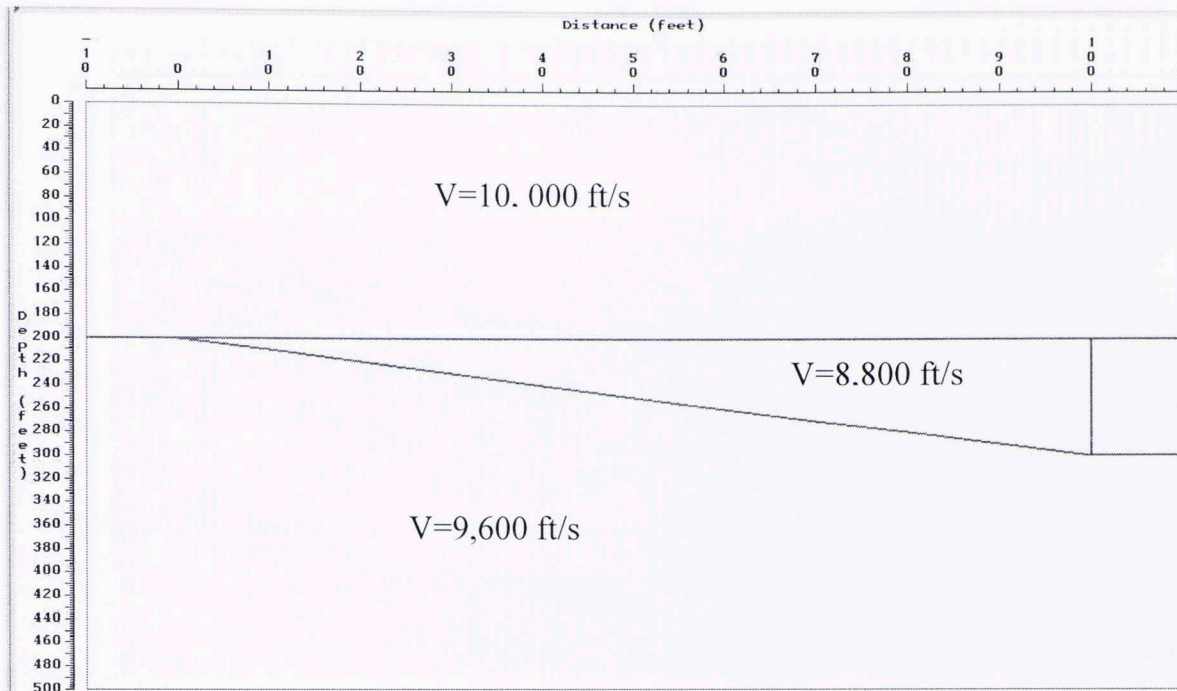


**Figure 4.2 Wedge Model used for Sand A, annotated with velocities (ft/s)**

Vertical ray paths were used to simulate the seismic response. An extracted wavelet from the 3-D seismic was used as a filter for the synthetics. A trace was generated at 1 ft intervals such that the wedge could represent the peak frequency at every integer value of thickness as needed. This was done in order to compare the frequency content of the synthetics with the frequency content of the 3-D seismic and have the same original wavelet. The resulting synthetic traces were exported to Kingdom for further analysis. (figure4.3)

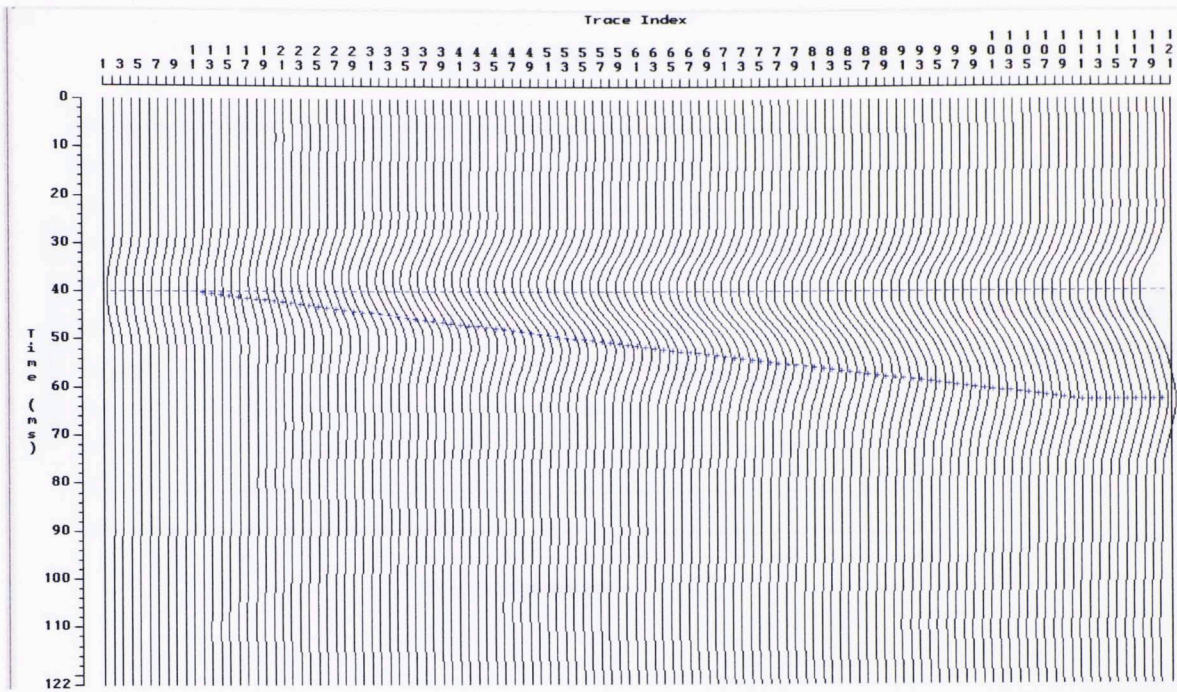


**Figure 4.3** *Traces created In GX2 for Sand A, Wavelet extracted from original seismic data*

InSpect™ was utilized to create the frequency spectra for the modeled case. The same parameters to spectrally decompose the 3-D seismic were used for the synthetics.

Spectra were extracted at 5 ft thickness intervals for comparison of peak frequency.

Figure 4.4 shows the results of the modeling.

Bed Thickness Vs Peak Frequency for Sand A

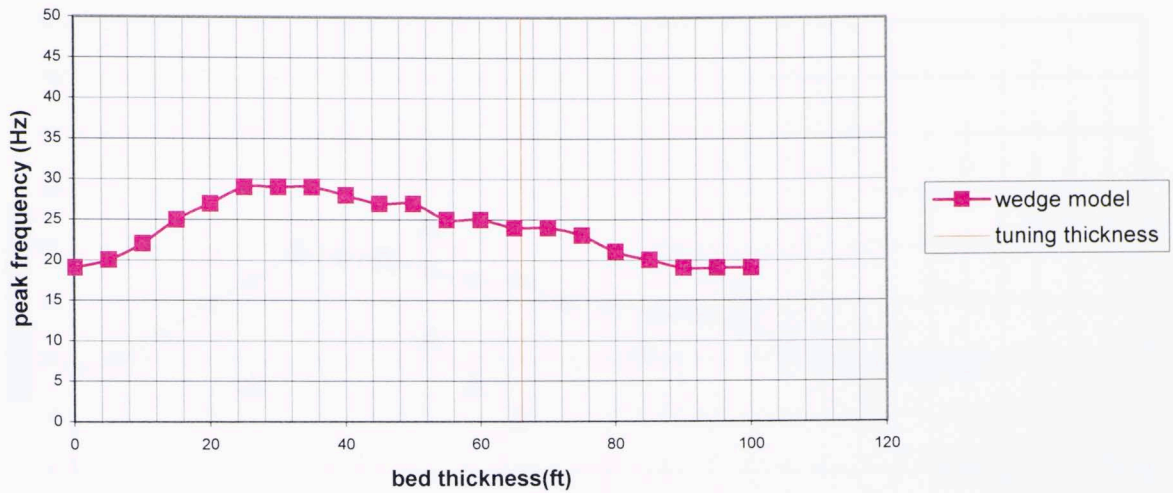


**Figure 4.4 Peak Frequency versus Bed Thickness for Modeled Sand A**

The peak frequency observed in the seismic data was then plotted with the modeled data in order to clarify the peak frequency relationship of the real data. This is shown in Figure 4.5. The pink line is the modeled results. The red line is the tuning thickness.

Bed Thickness Vs Peak Frequency for Sand A

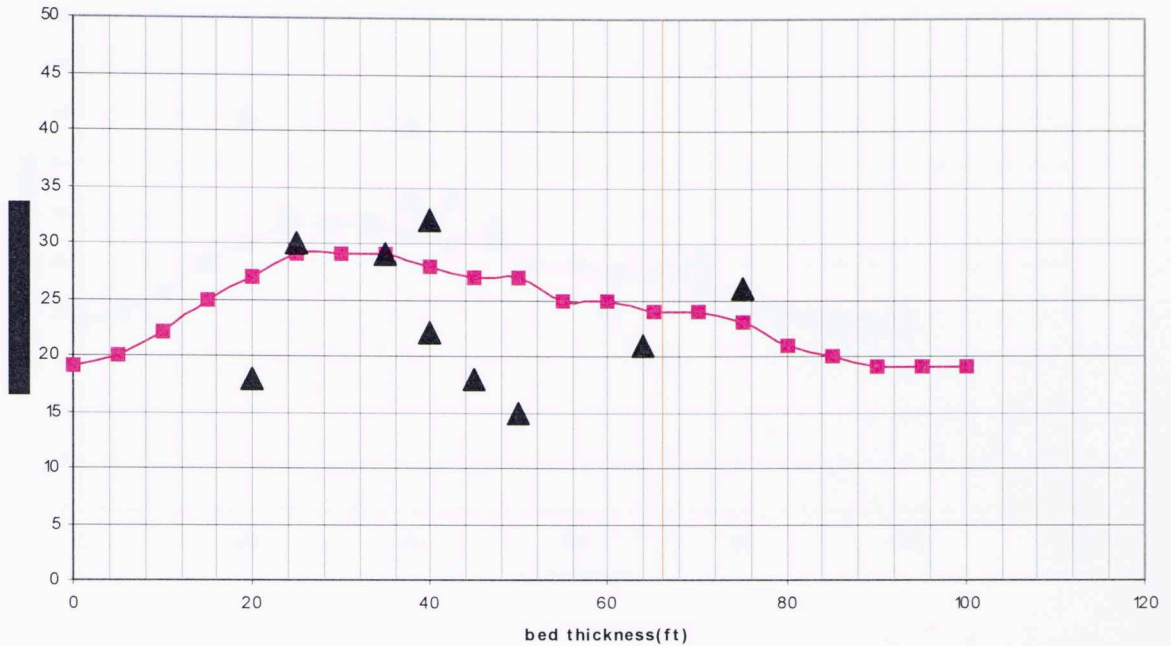
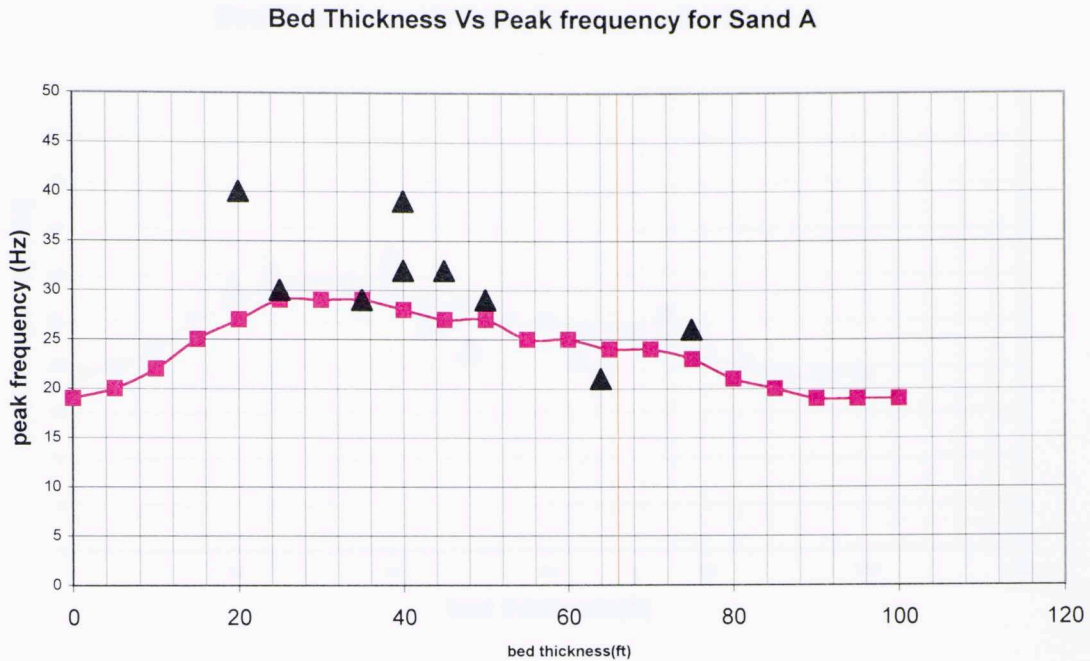


Figure 4.5 Graph showing Peak Frequency and Bed Thickness relationship modeled and observed for Sand A

Figure 4.5 Graph showing Peak Frequency and Bed Thickness relationship modeled and observed for Sand A

Next, the number of the year is plotted on the frequency spectrum of

Wells #40400, #311, #312, and #40477 have peak frequencies that fall well below the expected frequency as given in the model. Also noted in the frequency spectrum of the sand at these wells is presence of a second frequency with high amplitude associated with it. This second highest peak frequency was plotted with the peak frequency in the other wells in Figure 4.6. The values of this second peak plot higher than the modeled values.



**Figure 4.6 Graph showing Peak Frequency and Bed Thickness using second highest peak frequency for Sand A for wells #40400, #311, #312, #40477**

Next, the average of the two frequencies in the bimodal spectrum wells was performed (Figure 4.7). These values were not surprisingly closer to the modeled value. Although, there is no reason to believe this average is the correct operation to use for this estimate other than the fact that it would be close to the average frequency. A trough in the spectrum for wells #40400, #311, and #40477 has a frequency value that is very close to the average of the two peak frequencies in each. This is shown in Figure 4.8. It is evident that the simple wedge model is probably not adequate to describe the true reflectivity.

### Bed Thickness Vs Peak frequency for Sand A

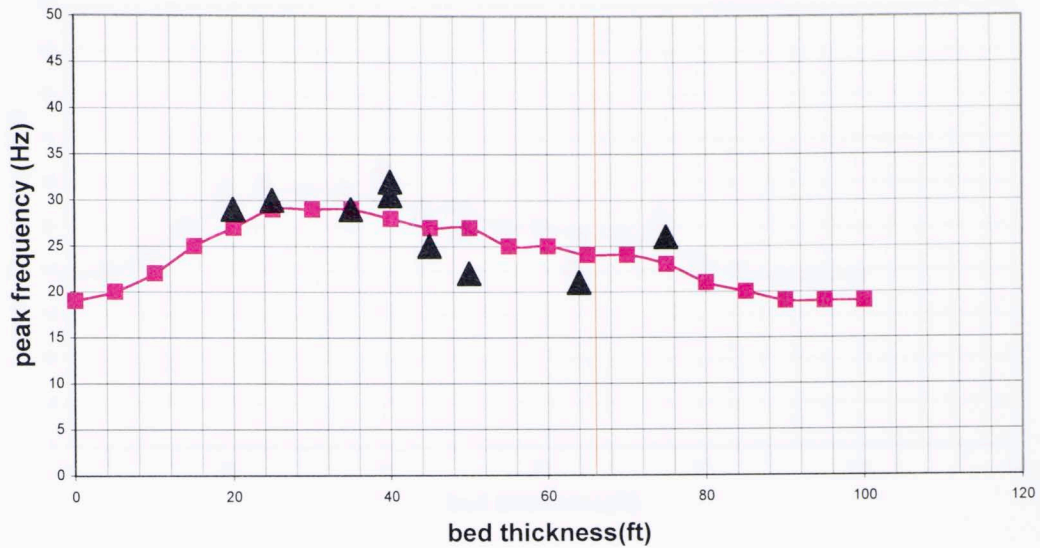


**Figure 4.7 Graph showing Peak Frequency and Bed Thickness using average of peak frequency and second highest peak frequency for Sand A for wells #40400, #311, #312, #40477**

### Sand C

Well #40477 was analyzed with same curve as Sand A. The difference mainly being that Sand C was analyzed under that is being thickness of 65 ft. The average thickness was 130 ft. Table 4.5 shows the thickness of Sand C along well.

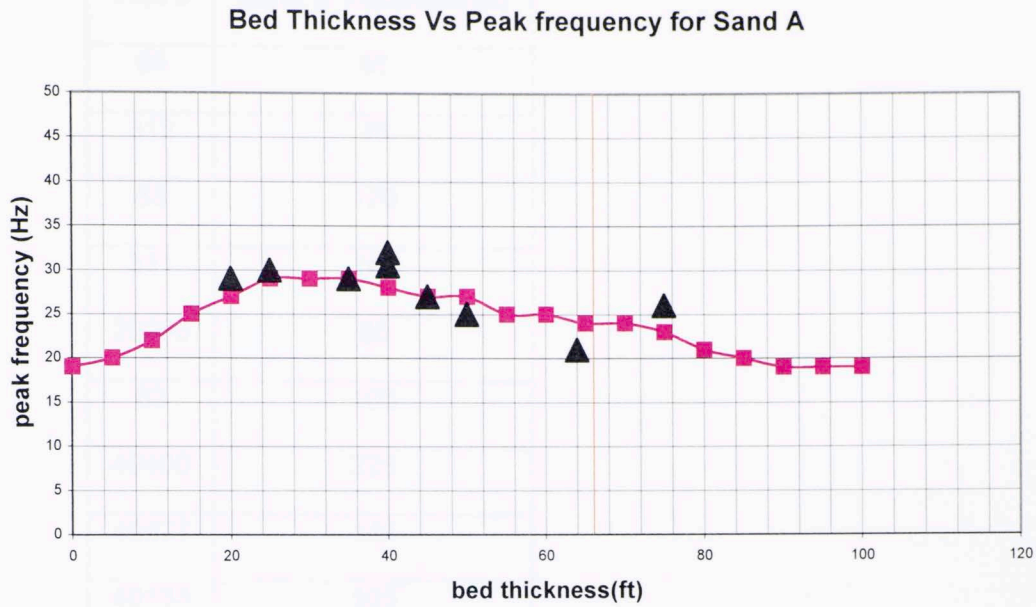


**Figure 4.8 Graph showing Peak Frequency and Bed Thickness using trough frequency between peak frequency and second highest peak frequency for Sand A for wells #40400, #311, and #40477.**

### **Sand C**

Sand C was approached in the same manner as Sand A. The difference mainly being that Sand C was mostly thicker than its tuning thickness of 63 ft. The average thickness was 120 ft. Table 4.3 shows the thickness of Sand C at each well.

Well #	Sand C Thickness (ft)
55	95
312	35
83	120
311	145
20066	85
63	105
40400	225
40477	145
40133	105

**Table 4.3 Thickness (ft) of Sand C at Well Locations**

Well #	Peak Frequency (Hz)
55	23
312	26
83	23
311	35
20066	34
63	25
40400	18
40477	26
40133	19

**Table 4.4 Peak Frequency values for Sand C at well locations**

The peak frequencies for each location were plotted against the bed thickness. Figure 4.9 show the cross plot. The values show no trend and for some wells with the same thickness the peak frequency is different.

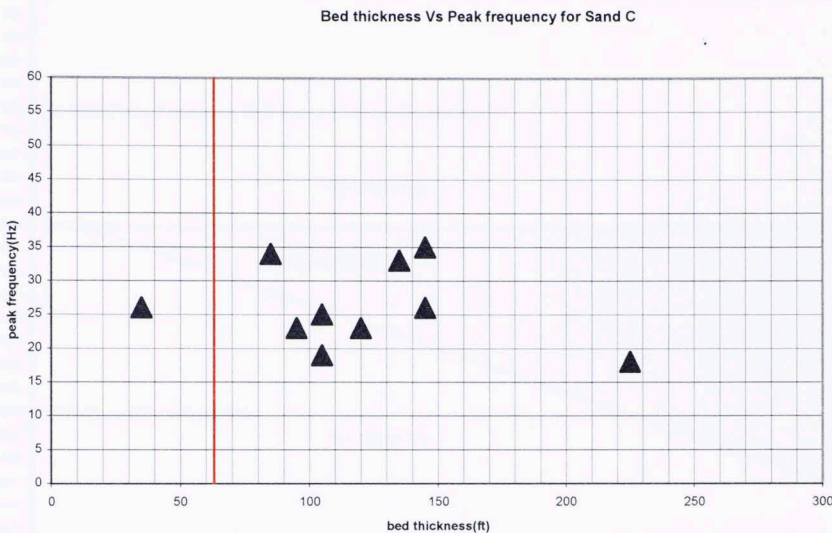


**Figure 4.9 Peak Frequency plotted with Bed Thickness for Sand C**

## Modeling Sand C

GX2 modeling program was again used for modeling Sand C. A sonic log from well # 40400 provided the velocity information for the model. The layer above the sand was averaged to 7,700 ft/s, with the sand at 8,550 ft/s, and the layer below 6,600 ft/s. The density used was the default value given by the program, as no density curves were found in the nine wells over the depth range of the study sand. The reflection coefficients were mostly odd but not equal (figure 4.10). The wedge model was

increased to range from 0 to 300 ft in thickness, due to the variation observed in the logs.

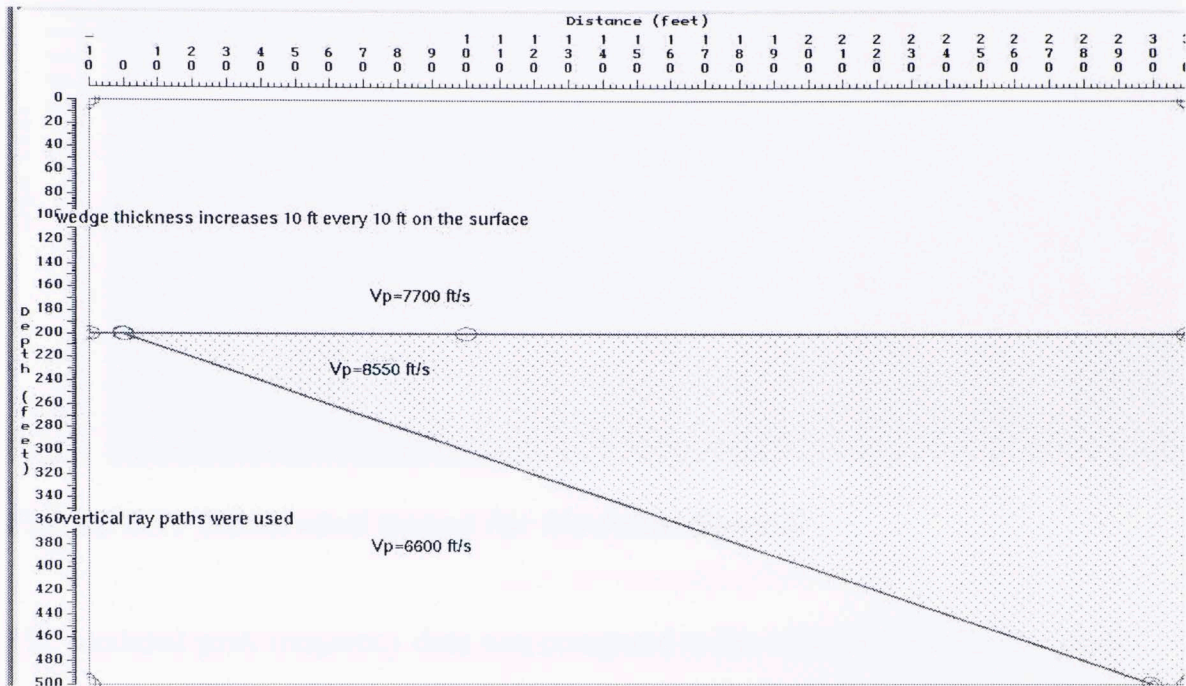


**Figure 4.10 Wedge Model used for Sand C, annotated with reflection coefficients and velocities**

Traces were generating using the extracted wavelet from the original seismic as the filter. The resulting traces were decomposed according to the same parameters as the original seismic. The frequency data was loaded into Kingdom for interpretation.

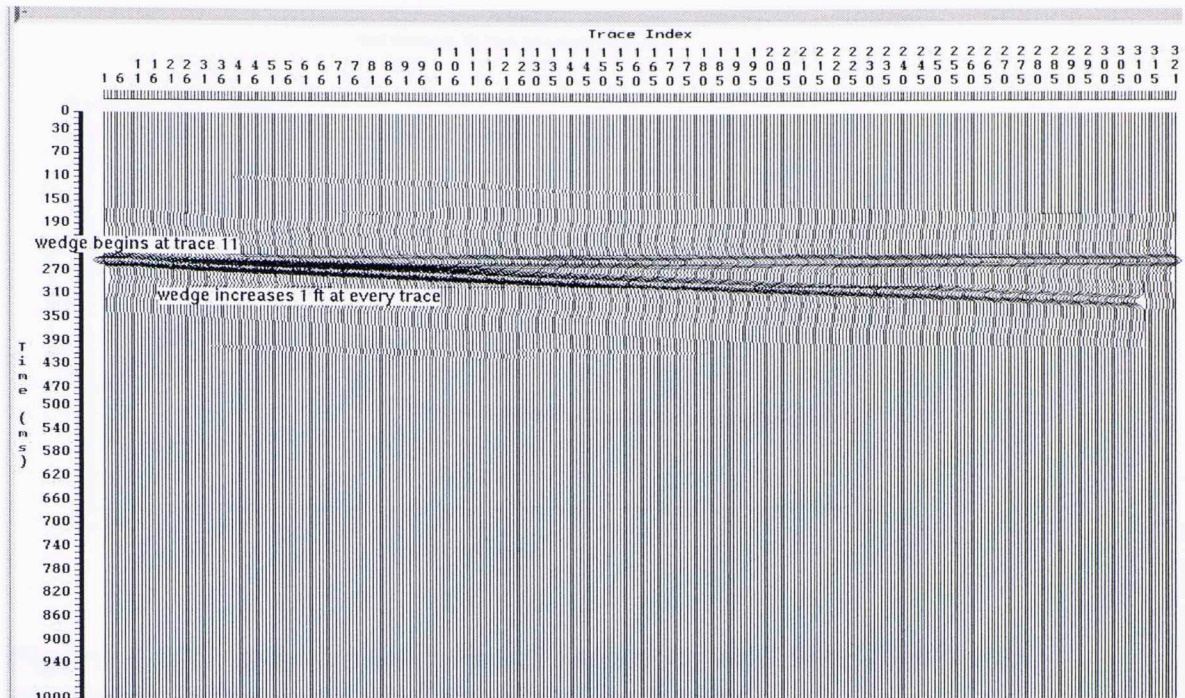


**Figure 4.11 Generated traces for Modeled Sand C**

The modeled peak frequency data was compared to the observed results for Sand C. These results showed a huge deviation from the expected modeled results. The only well to show an expected outcome was well #312. This was the only well with Sand C thickness below the tuning thickness.

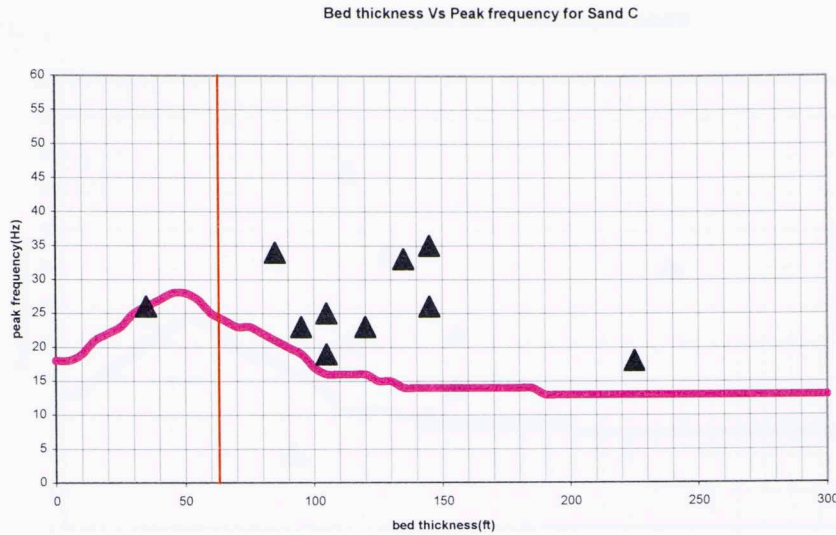


**Figure 4.12** Graph showing Peak Frequency and Bed Thickness relationship modeled and observed for Sand C

As with Sand A, several locations exhibited bimodal spectra. These wells however, were not located on the cross plot in any localized area. The second peak frequency was plotted against the thickness for Sand C to see whether the graph was improved by using the second highest peak frequency. Figure 4.13 shows the results. The graph was not improved by using this second frequency. The points were scattered farther apart and any relationship was further distorted.

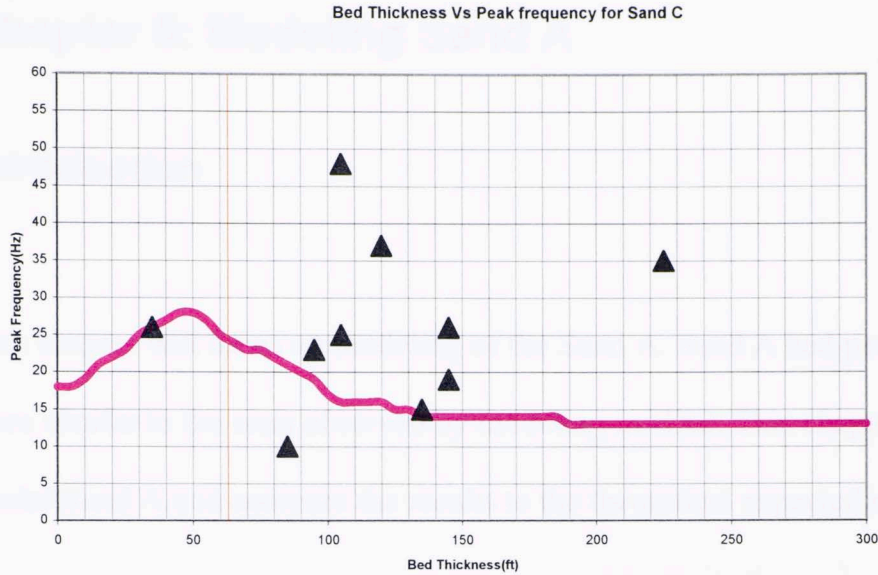


**Figure 4.13 Graph showing Peak Frequency and Bed Thickness using trough frequency between peak frequency and second highest peak frequency for Sand C for wells #40400, #311, #20066, #55, #83, and #40133.**

Sand C did not show any relationship to peak frequency. This is thought to be because the thickness of Sand C is predominantly above tuning thickness. At the thicknesses observed for Sand C no interference from the upper and lower boundaries of the sand is expected. The frequency content of Sand C could be impacted more by stratigraphic changes and less by thickness variation.

## Chapter 5: Modeling Sand A

### Introduction

This chapter will focus on modeling of the Sand A. Sand A had peak frequencies that were similar to the ones observed by modeling in GX2. This chapter will further model Sand A and compare the results to the theoretical expected results.

### Green's Function

The impulse response of the reflection off a thin bed can be expressed by the Green's function,  $g(t)$  where

$$g(t, \theta) = r_1 \delta(t - t_1) + r_2 \delta(t - t_1 - T) \quad (5.1)$$

Equation 3.1 is the time-domain impulse response. The frequency-domain impulse response is given by  $G(f)$ ,

$$G(f) = r_1(\theta) \exp(-2\pi f t_1) + r_2(\theta) \exp[-2\pi f(t_1 + T)] \quad (5.2)$$

Where  $t_1$  is the two-way time to the top of the thin bed,  $t_2$  is the two-way time to the

bottom of the thin bed,  $r_1$  is the reflection coefficient of the top of the thin bed,  $r_2$  is the reflection coefficient of the bottom of the thin bed,  $\theta$  is the angle determining reflection coefficients,  $T$  is the two-way time thickness of the thin bed,  $T = t_2 - t_1$ ,  $\delta(t)$  is the Dirac delta function, and  $f$  is the temporal frequency.

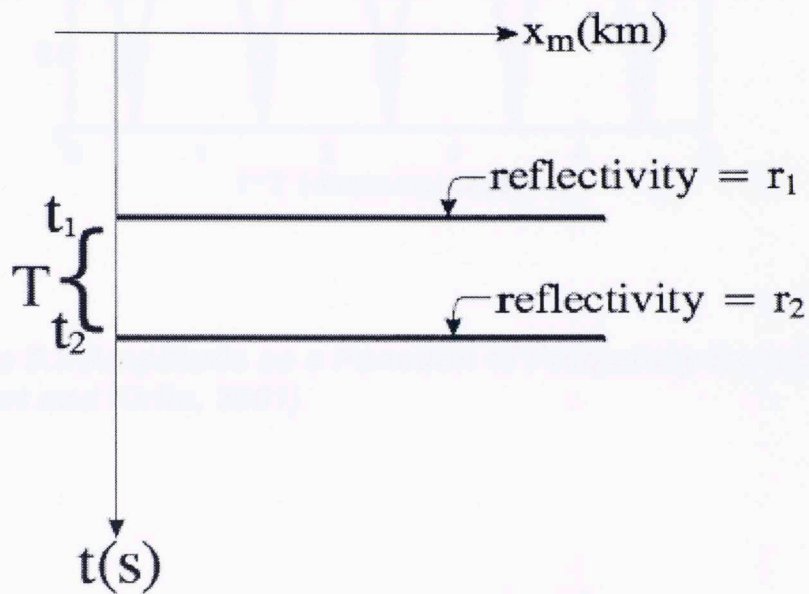


**Figure 5.1 Model defining impulse response ( Marfurt and Kirilin, 2001)**

Figures 5.2 and 5.3 show the theoretic curves given by equation 5.2. Figure 5.2 shows the case of  $r_1 / r_2 < 0$  which is the case seen for Sand A.

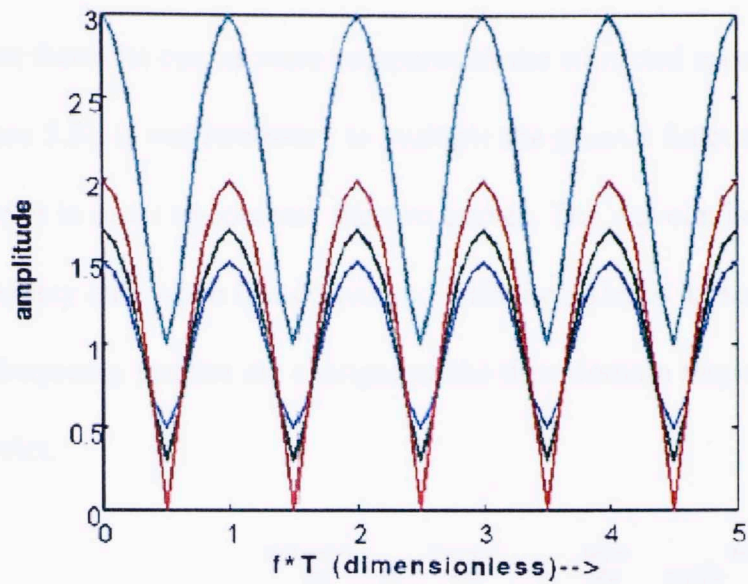


**Figure 5.2** Amplitude as a Function of Frequency for odd impulse pairs ( Marfurt and Kirilin, 2001)

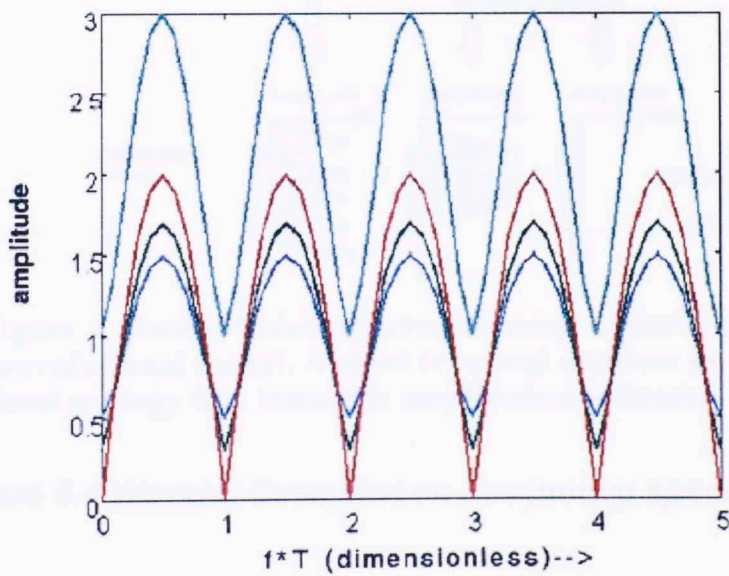


**Figure 5.3** Amplitude as a Function of Frequency for even impulse pairs ( Marfurt and Kirilin, 2001)

These theoretic curves were compared to the extracted spectra for the study sand (figure 5.5). It was necessary to multiple the green's function by the spectrum of the wavelet in order to compare the two curves. The wavelet is imprinted on the frequency data when it is convolved with the reflectivity series. Figure 5.4 shows how the frequency spectra are changed as the time domain response also changes with the wavelet.

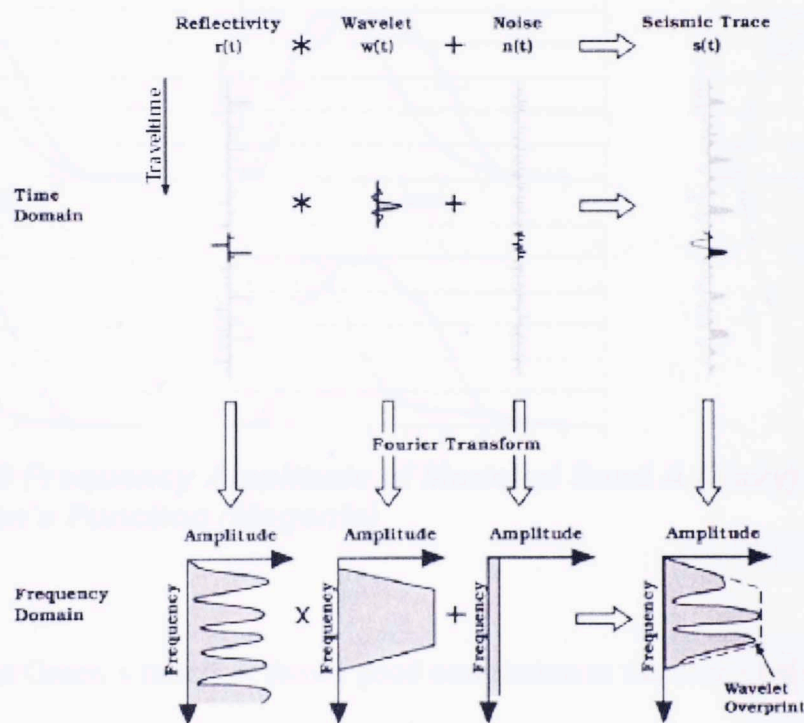
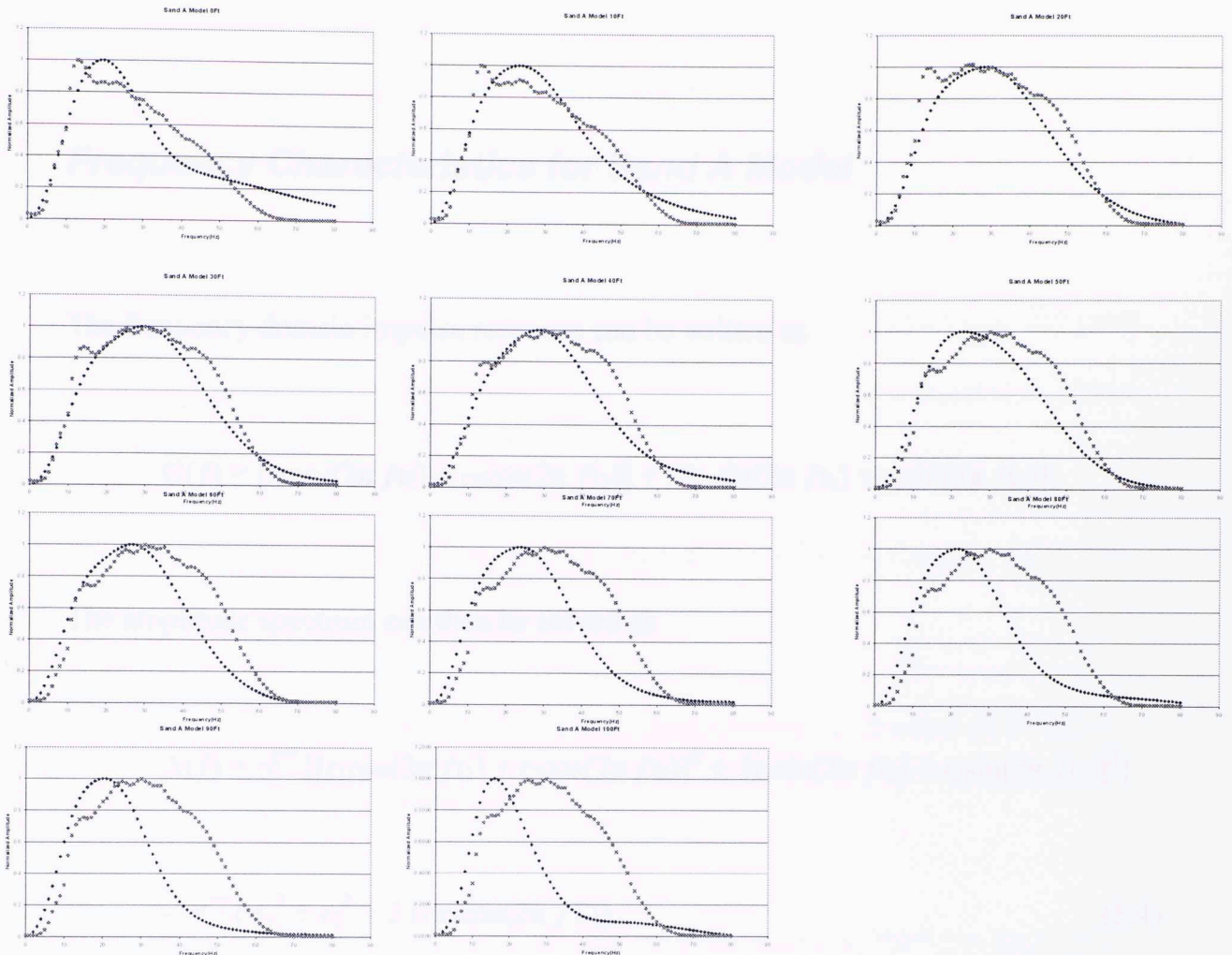


Figure 3. Short-window spectral decomposition and its relationship to the convolutional model. A short temporal window samples ordered (nonrandom) geology that tunes the amplitude spectrum.

Figure 5.4 Wavelet Overprint on Frequency spectra (Partyka, 1999)



**Figure 5.5 Frequency Amplitude of Modeled Sand A (Navy) compared with Green's Function (Magenta)**

The derived Green's function shows good correlation to the extracted spectra for thin sands. As the sands increase in thickness the correlation is less evident. This is expected because after a certain thickness there is no longer any noticeable interaction of the two wavelets for the real sand.

## Frequency Characteristics for Sand A Model

The frequency domain impulse response can be written as

$$G(f) = [r_1 \cos(2\pi f t_1) + r_2 \cos(2\pi f t_2)] + i [r_1 \sin(2\pi f t_1) + r_2 \sin(2\pi f t_2)].$$

The amplitude spectrum can then be solved as

$$\begin{aligned} A(f) &= \sqrt{\{[r_1 \cos(2\pi f t_1) + r_2 \cos(2\pi f t_2)]^2 + [r_1 \sin(2\pi f t_1) + r_2 \sin(2\pi f t_2)]^2\}} \\ &= \sqrt{\{r_1^2 + r_2^2 + 2 r_1 r_2 \cos(2\pi f T)\}}, \end{aligned} \quad (5.4)$$

where  $r_1$ ,  $r_2$ ,  $t_1$ ,  $t_2$ , and  $T$  are as defined as before. (Chung and Lawton, 1995)

A Ricker wavelet has the amplitude spectrum in terms of peak frequency ( $f_0$ ) as:

$$A_R(f) = (f/f_0)^2 \exp[-(f/f_0)^2], \quad (5.5)$$

So that the amplitude spectrum for a wavelet created by convolving the amplitude spectrum for the reflectivity series and the amplitude spectrum for the Ricker wavelet (Chung and Lawton, 1995). In the frequency domain this is done by multiplying

equation 5.4 and 5.5, so that:

$$C(f) = A(f) A_R(f), \quad (5.6)$$

The peak frequency can be found by taking the derivative of equation 5.6. The peak frequency would then be the value of  $f$  for which the derivative is equal to 0. Hence,

$$C'(f) = \frac{d}{df} \left\{ (f/f_0)^2 \exp[-(f/f_0)^2] * \sqrt{r_1^2 + r_2^2 + 2 r_1 r_2 \cos(2\pi fT)} \right\} = 0$$

Calculating this out gives peak frequency  $f$ , replaced with  $f_p$ , in terms of the peak frequency for a Ricker wavelet,  $f_0$ :

$$f_p = [r_1^2 + r_2^2 + 2 r_1 r_2 \cos(2\pi f_p T)] / [r_1 r_2 2\pi T \sin(2\pi f_p T)] * [1 - (f_p/f_0)^2], \quad (5.7)$$

Equation 5.7 is called the exact equation for peak frequency as defined by Chung and Lawton (1995). This equation was solved iteratively using Matlab.

The reflection coefficients for Sand A were  $r_1 = -0.09$  and  $r_2 = 0.06$ . Sand A was very nearly perfectly odd. Using equation 5.7 peak frequency was solved for Sand A with a Ricker peak frequency at 15 Hz, 20 Hz, 25 Hz, 30 Hz, and 35 Hz (Figure 5.6). At

this point it should be noted that the original seismic data does not have a theoretic Ricker wavelet and the generated traces from the model were not filtered with a Ricker wavelet but with the extracted wavelet. So, variation from the model and seismic data is expected.

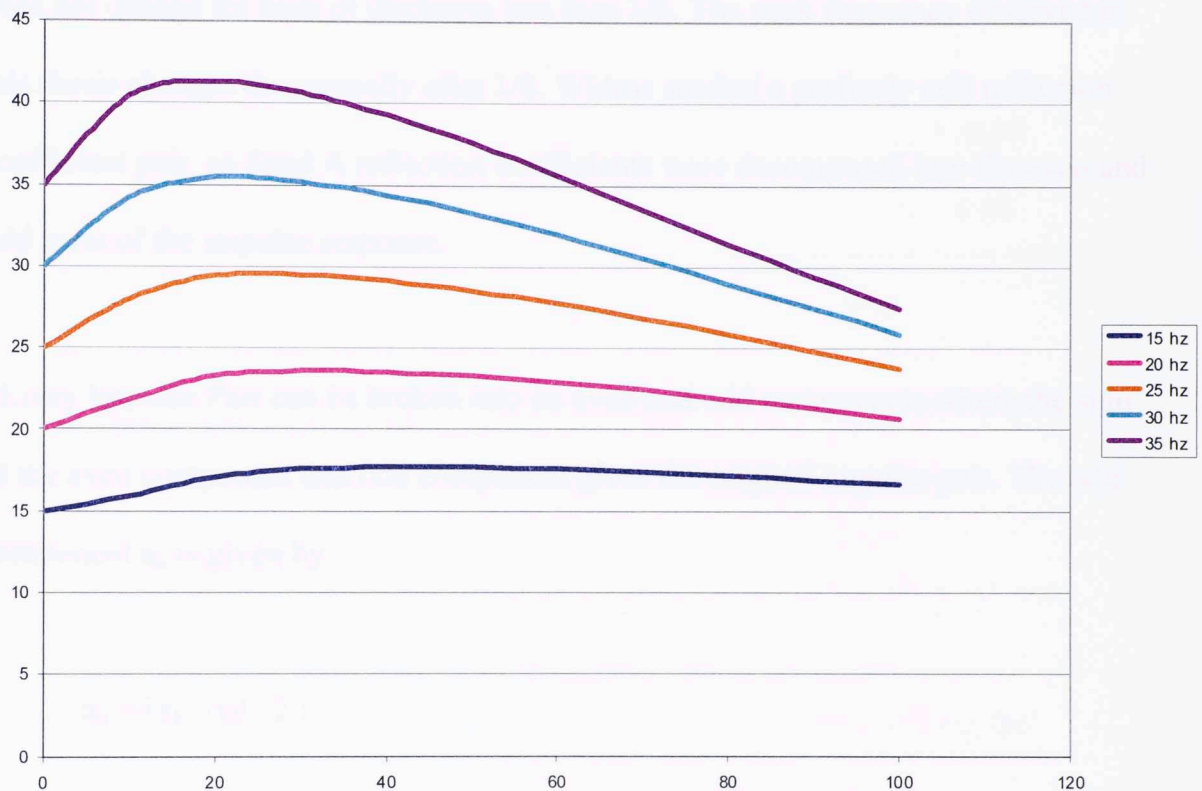


**Figure 5.6 Peak Frequency Response for Sand A Reflection Coefficients at Ricker Wavelet peak frequencies 15 Hz, 20 Hz, 25 Hz, 30 Hz, and 35 Hz.**

The shape of the curve in Figure 5.6 is consistent with the shape observed in the seismic survey and modeling data. A significant observation made by Chung and Lawton (1995) and also seen with this data is that with higher initial peak frequencies the distinction between frequencies for each thickness becomes greater. So that it can

be assumed that with higher input frequency the tool of peak frequency content may become more useful for distinguishing bed thickness.

Interestingly, the peak frequency drops to lower frequencies as bed thickness decreases. Widess, in *How Thin is a Thin Bed*, states that the character of a reflection does not change for beds of thickness less than  $\lambda/8$ . The peak frequency observed in this thesis changes dramatically after  $\lambda/8$ . Widess studied a perfectly odd reflection coefficient pair, so Sand A reflection coefficients were decomposed into the even and odd parts of the impulse response.

Figure 5.7 Even and Odd Parts for Sand A

Every Impulse Pair can be broken into its even and odd components where the sum of the even component and odd component gives the original impulse pair. The odd component  $a_o$  is given by

$$a_o = |r_1 - r_2| / 2 ;$$

and the even component is given by

$$a_e = |r_1 + r_2| / 2 .$$

For Sand A  $a_o = -0.075$  and  $a_e = -0.015$ . This is illustrated in the figure below (figure 5.7)

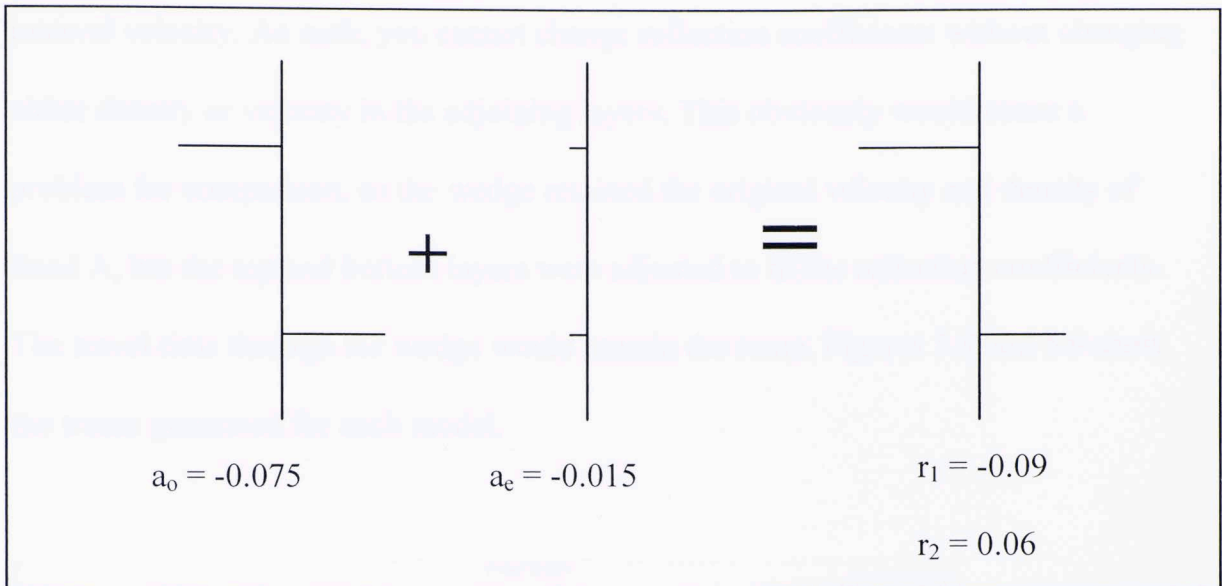


**Figure 5.7 Even and Odd Pairs for Sand A**

## **Models**

The even and odd impulse pairs were used to create models for modeling the frequency and amplitude of wavelets for each case. These models were created in the same fashion as previous Sand A models. For the Odd Impulse Model the top reflection coefficient was set to  $r_1 = -0.075$ , and the bottom reflection coefficient was set to  $r_2 = +0.075$ . Because Reflection Coefficients are calculated as

$$\text{R.C.} = \Delta I / I = (I_2 - I_1) / (I_2 + I_1),$$

where  $I$  is the acoustic impedance defined as  $I = \rho V$ ; and  $\rho$  is density, and  $V$  is interval velocity. As such, you cannot change reflection coefficients without changing either density or velocity in the adjoining layers. This obviously would cause a problem for comparison, so the wedge retained the original velocity and density of Sand A, but the top and bottom layers were adjusted to fit the reflection coefficients. The travel time through the wedge would remain the same. Figures 5.8 and 5.9 show the traces generated for each model.

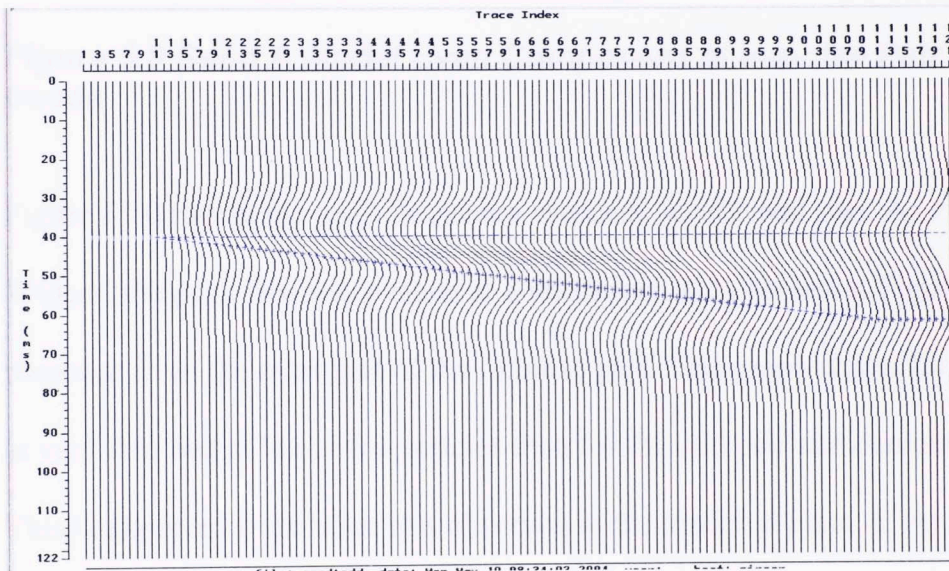


**Figure 5.8 Sand A Model Odd Component of Impulse Pair generated traces**

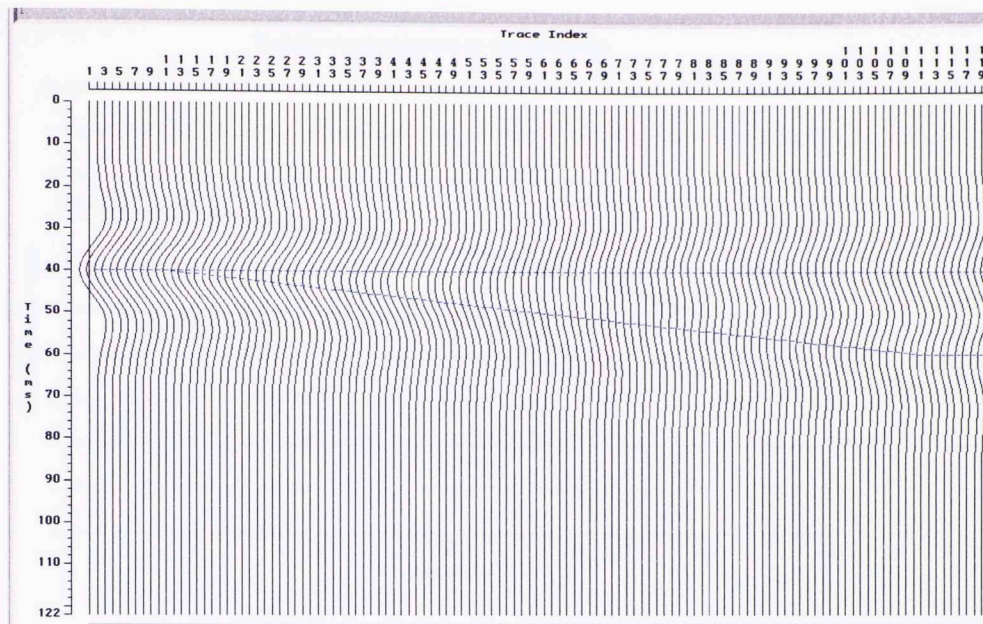


**Figure 5.9 Sand A Model Even Component of Impulse Pair generated traces**

Figure 5.10 shows the peak frequency response for the odd part. As expected from Widess, the peak frequency starts at a maximum and decreases. Figure 5.11 shows the response from the even part of the impulse pair. This graph shows the peak frequency at very thin bed at lower frequencies than for the odd pair and decreasing from there. This is expected from what was observed in the modeled Sand A. At around tuning thickness the character of the graph diverges strongly and peak frequency begins to increase again.

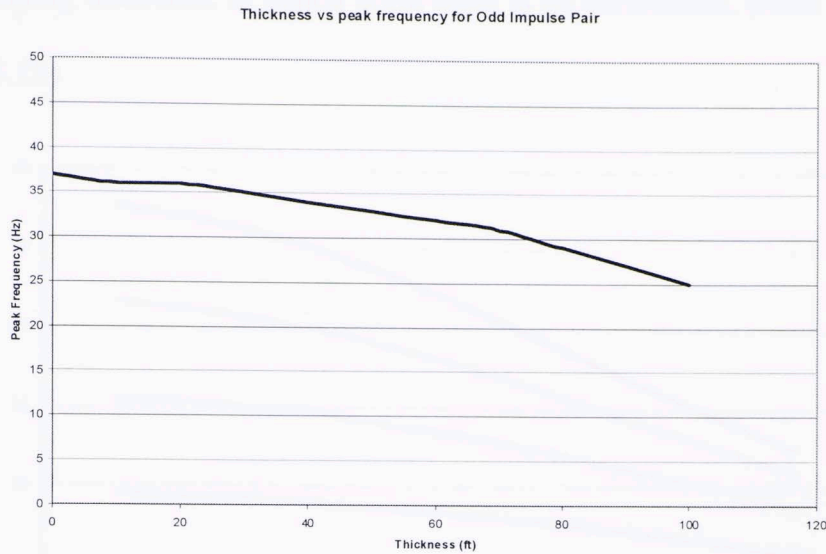


**Figure 5.10 Peak Frequency Response for modeled Sand A Odd Part**

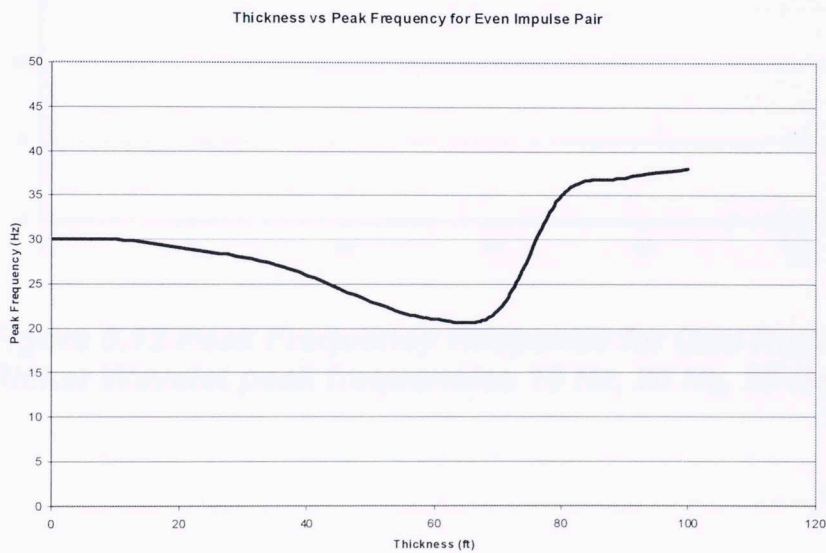


**Figure 5.11 Peak Frequency Response for modeled Sand A Even Part**

The exact equation (equation 5.7) for peak frequency response was applied using the reflection coefficients for the odd and even models. Again this was done for a range of Ricker wavelet peak frequencies. The odd model is fairly close in shape to the theoretic values. The even model shows resemblance of the theoretic values until

tuning thickness, at which point there is no correlation. (refer to figures 5.12 and 5.13)

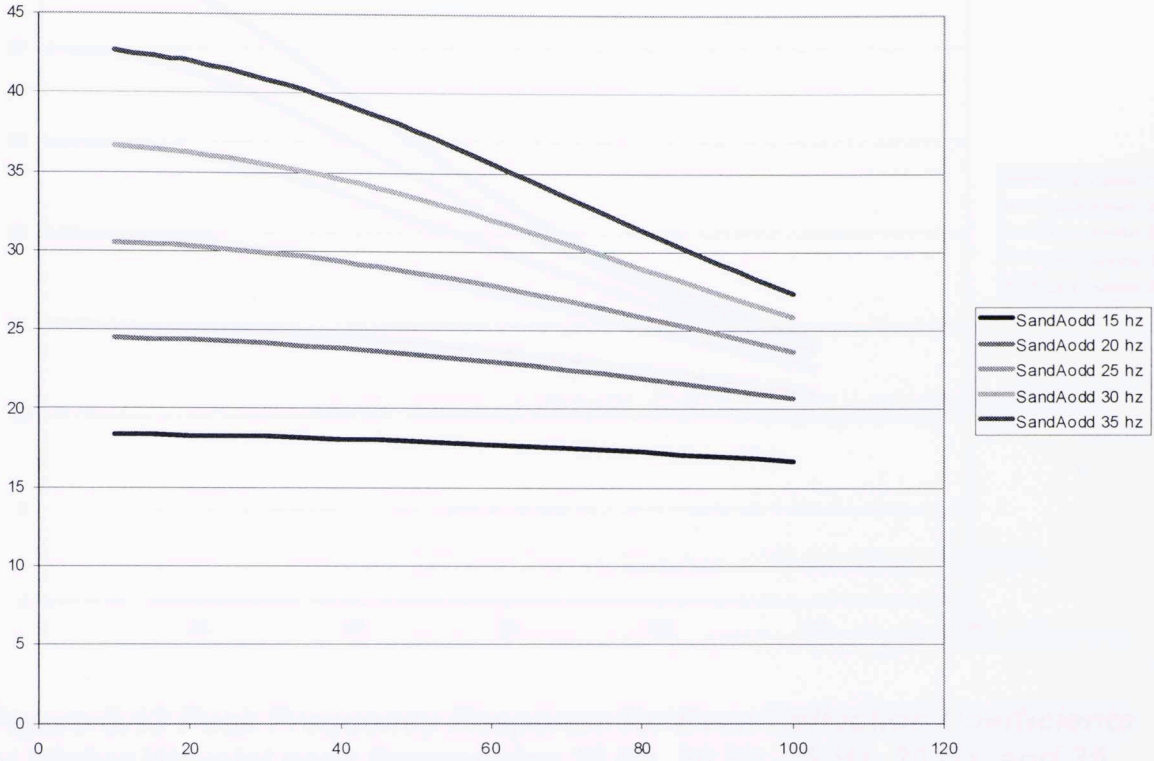


**Figure 5.12 Peak Frequency Response for Odd Reflection Coefficients at Ricker Wavelet peak frequencies 15 Hz, 20 Hz, 25 Hz, 30 Hz, and 35 Hz.**

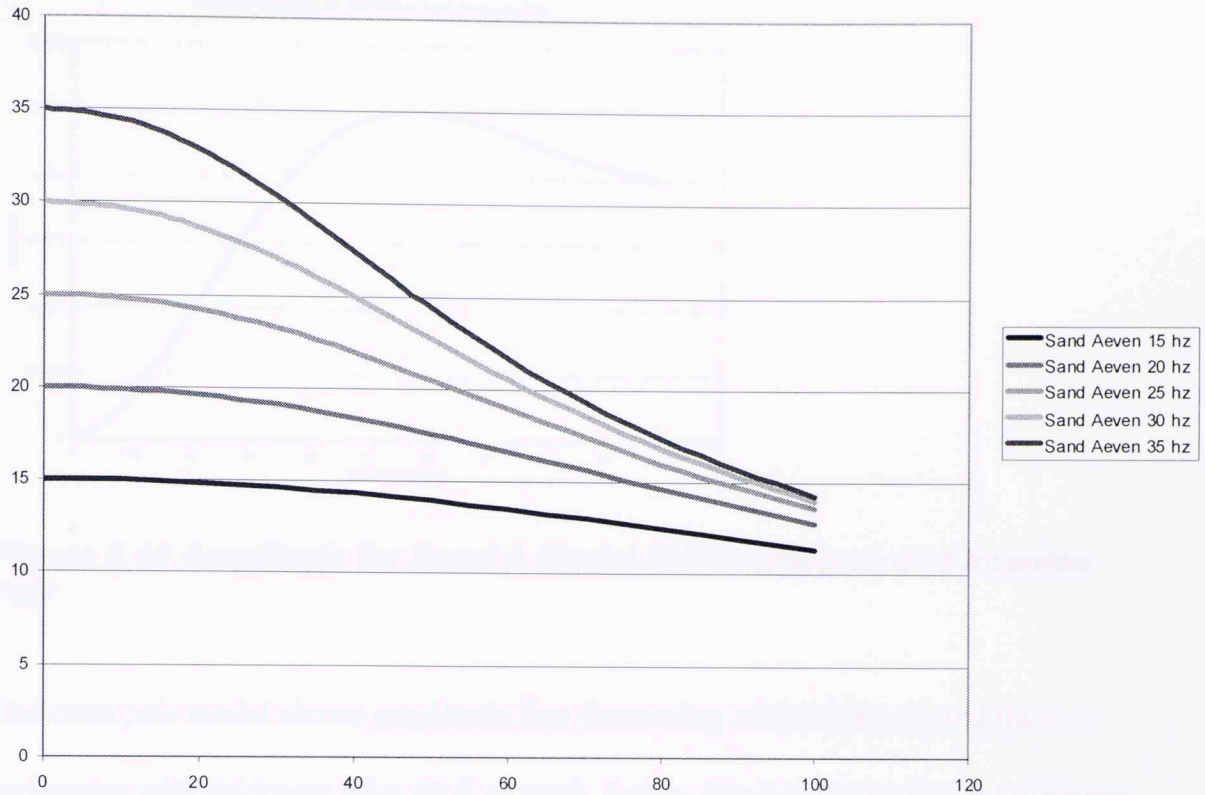


**Figure 5.13 Peak Frequency Response for Even Reflection Coefficients at Ricker Wavelet peak frequencies 15 Hz, 20 Hz, 25 Hz, 30 Hz, and 35 Hz.**

The even part appears to dominate the peak frequency for very thin beds with only a very small part of the total impulse pair. To investigate this further, the amplitude of the wavelets generated in the even and odd models were plotted for each thickness. For the odd impulse pair the amplitude goes to zero as the wedge decreases in thickness (figure 5.14). This is expected because of the destructive interference between opposite polarity wavelets.

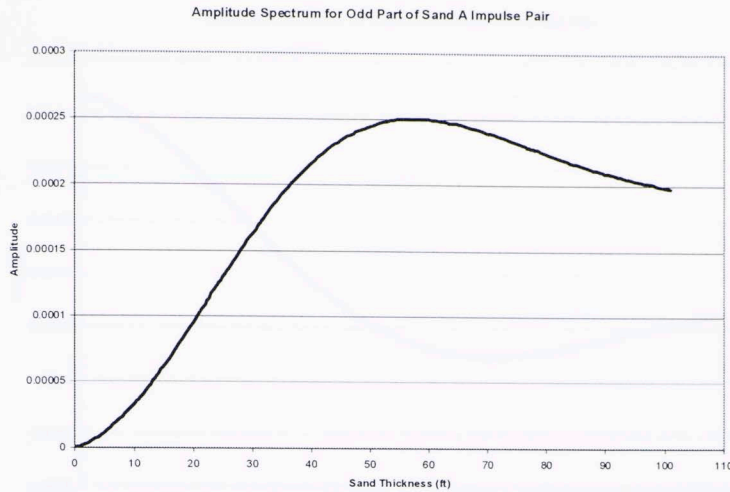


**Figure 5.14 Amplitude for Sand A Model Odd Component of Impulse Pair**

The even pair model shows amplitude first decreasing with thickness and then increasing with thickness after 60 ft of sand. Again, due to constructive interference the amplitude is expected to increase as the time between the reflections decreases.

(Figure 5.15)



**Figure 5.16 Amplitude for Modeled Sand A**

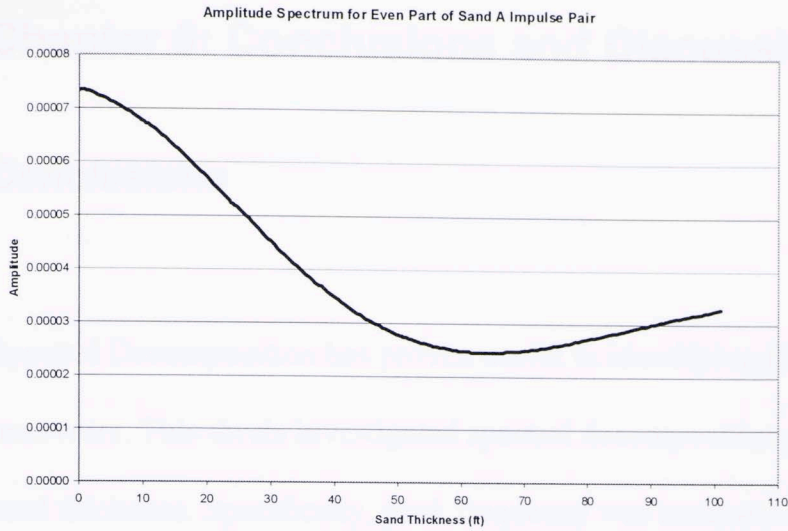


**Figure 5.15 Amplitude for Sand A Model Even Component of Impulse Pair**

Since the amplitude contribution of the odd part at very thin bed is very small, the even part plays a bigger role in the character of the peak frequency response (figure 4.4), while not impacting the amplitude spectrum as drastically. Figure 5.16 shows the Sand A model's amplitudes as the wedge increases.

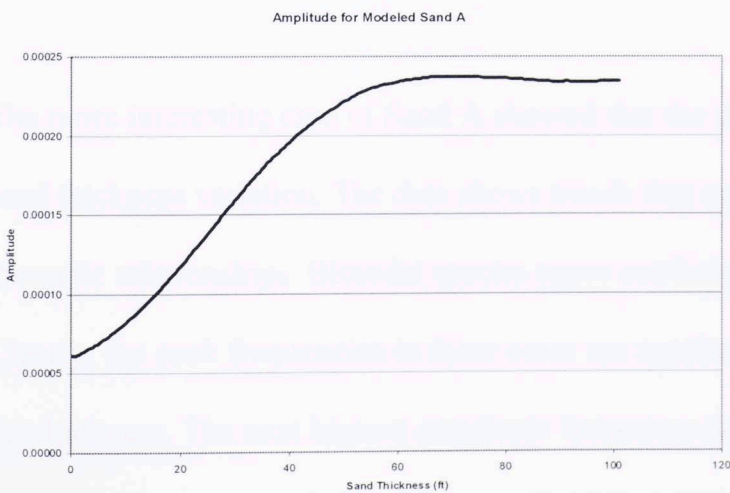


**Figure 5.16 Amplitude for Modeled Sand A**

## Chapter 6: Conclusions and Discussion

### *Conclusions*

Spectral Decomposition has proven useful in identifying thin beds and hydrocarbon reservoirs. This thesis investigated spectral decomposition as a tool for quantifying sand thickness. Specifically, peak frequency was analyzed as a method for determining bed thickness.

Sand C is an example of a thick sand. Modeling and data showed that the peak frequency does not work for thick sands (above tuning thickness). The values of peak frequency were random as far as thickness was concerned. There was no correlation of bimodal character in the spectrum to thickness. More than likely any variation of peak frequency observed in the data was due to stratigraphic changes in the sand.

The more interesting case of Sand A showed that the peak frequency may indicate sand thickness variation. The data shows trends that correspond to the modeled and theoretic relationships. Bimodal spectra cause confusion in the data, however.

Clearly, the peak frequencies in these cases are not the frequencies that correspond to the thickness. The next highest amplitude frequency does not represent the thickness either. In the absence of bimodal cases, the data points are fairly true to the relationship modeled and theoretic. However, as to the usefulness of peak frequency

as a quantitative tool, it does not appear to be very good.

The last chapter reviews theoretic relationships along with the modeled sands. Even in an ideal model there is not large variation in peak frequency. Higher frequencies give better distinction but the curves are still fairly flat. The most important hurdle for peak frequency as a quantitative tool is seen in the theoretic curves. For equal impulse pairs the curve associated with the peak frequency decreases with increasing thickness in both the even and odd cases. However, for the uneven odd case, such as sand A, there are two values of thickness for the same peak frequency. Without any stratigraphic changes and only comparing acoustic impedances, there is no decisive way to use peak frequency alone for bed thickness estimation.

## ***Discussion***

Frequency is impacted by the thickness of thin beds and as such there is more work to be done. This thesis only explored the peak frequency as a tool and not other aspects of the spectra. The presence of bimodal spectrum characteristics poses an interesting question. With more well control it may be possible to correlate more aspects of the frequency data with thickness. Also, as this thesis showed, sands are different and if peak frequency doesn't work for thin sands the peak frequency could give insight to the stratigraphic changes.

## References

- Barncord, L., The Application of petrophysical and seismic data for the interpretation of depositional environments and distribution of Miocene reservoir sandstones, Offshore central Louisiana, University of Oklahoma, 121 p., Thesis.
- Bassiouni, Z., 1994, Theory, Measurement, and Interpretation of Well Logs: Society of Petroleum Engineers Textbook Series, v. 4, SPE, Richardson, TX, 353 p.
- Castagna, J. P., Sun, S., and Siegfried, R. W., 2003, Instantaneous spectral analysis: Detection of low-frequency shadows associated with hydrocarbons: The Leading Edge, v. 22, p. 120-127
- Chakraborty, A. and Okaya, D., 1995, Frequency-time decomposition of seismic data using wavelet-based methods: Geophysics, v. 60, p. 1906-1919
- Chung, H. and Lawton, D. C., 1995, Amplitude responses of thin beds: Sinusoidal approximation versus Ricker approximation: Geophysics, v. 60, p. 223-230

Chung, H. and Lawton, D. C., 1995, Frequency characteristics of seismic reflections from thin beds: *Canadian Journal of Exploration Geophysicists*, v. 31, p. 32-37

Eardley, A. J., 1951, *Structural Geology of North America*, Second Edition: Harper & Row, New York, 743 p.

Goupillaud, P., Grossmann, A., and Morlet, J., 1984, Cycle-Octave and related transforms in seismic signal analysis: *Geoexploration*, v. 23, p. 85-102

Hormander, L., 1990, *The analysis of Linear Partial Differential Operators I*, Second Edition: Springer-Verlag, New York, 440 p.

Kallweit, R. S. and Wood, L. S., 1982, The limits of resolution of zero-phase wavelets: *Geophysics*, v. 47, p. 1035-1046

Knapp, R. W., 1990, Vertical resolution of thick beds, thin beds, and thin-bed cyclothem: *Geophysics*, v. 55, p. 1183-1190

Lloyd, J. A., 1991, *Regional Stratigraphic Well Log Analysis of Middle and Upper Miocene Sands of Offshore Central Louisiana*, University of New Orleans, 79 p., Thesis.

Marfurt, K. J. and Kirilin, R. L., 2001, Narrow-band spectral analysis and thin-bed tuning: *Geophysics*, v. 66, p. 1274-1283

Murray, G. E., 1961, *Geology of the Atlantic and Gulf Coastal Province of North America*: Harper, New York, 692 p.

Partyka, G. A., Gridley, J. M., and Lopez, J., 1999, Interpretational Applications of Spectral Decomposition: *The Leading Edge*, v. 18, p. 353-360

Robertson, J. D. and Nogami, H. H., 1984, Complex seismic trace analysis of thin beds: *Geophysics*, v. 49, p. 344-352

Ricker, N., 1953, Wavelet contraction, wavelet expansion and the control of seismic resolution: *Geophysics*, v. 18, p. 796-792

Sinha, S. K., 2002, *Time-Frequency Localization with Wavelet Transform and its Application in Seismic Data Analysis*, University of Oklahoma, 83 p., Thesis.

Widess, M.B., 1973, How thin is a thin bed?: *Geophysics*, v. 38, p. 1176-1180

# Appendix

## Appendix A: Tuning Charts

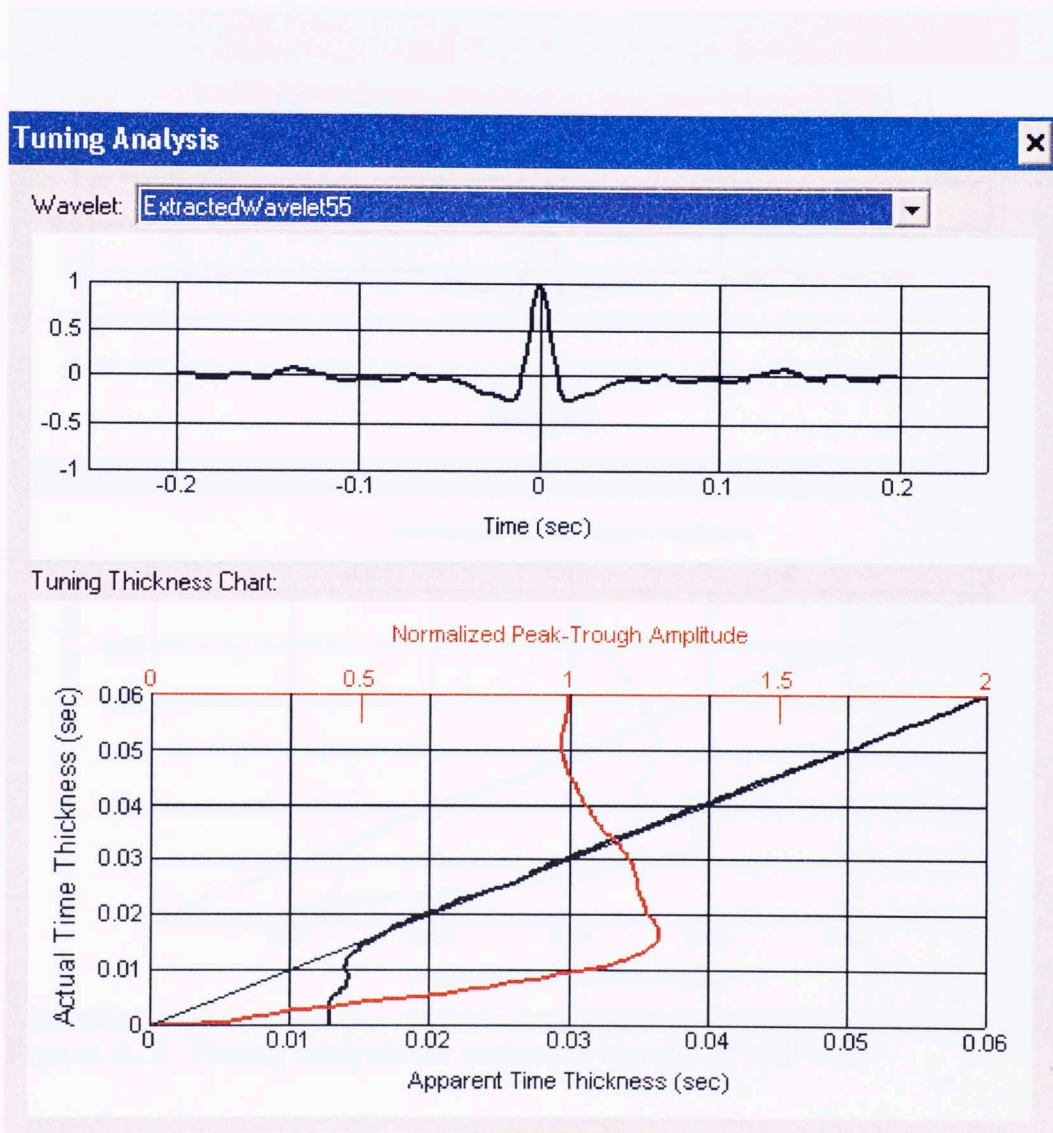
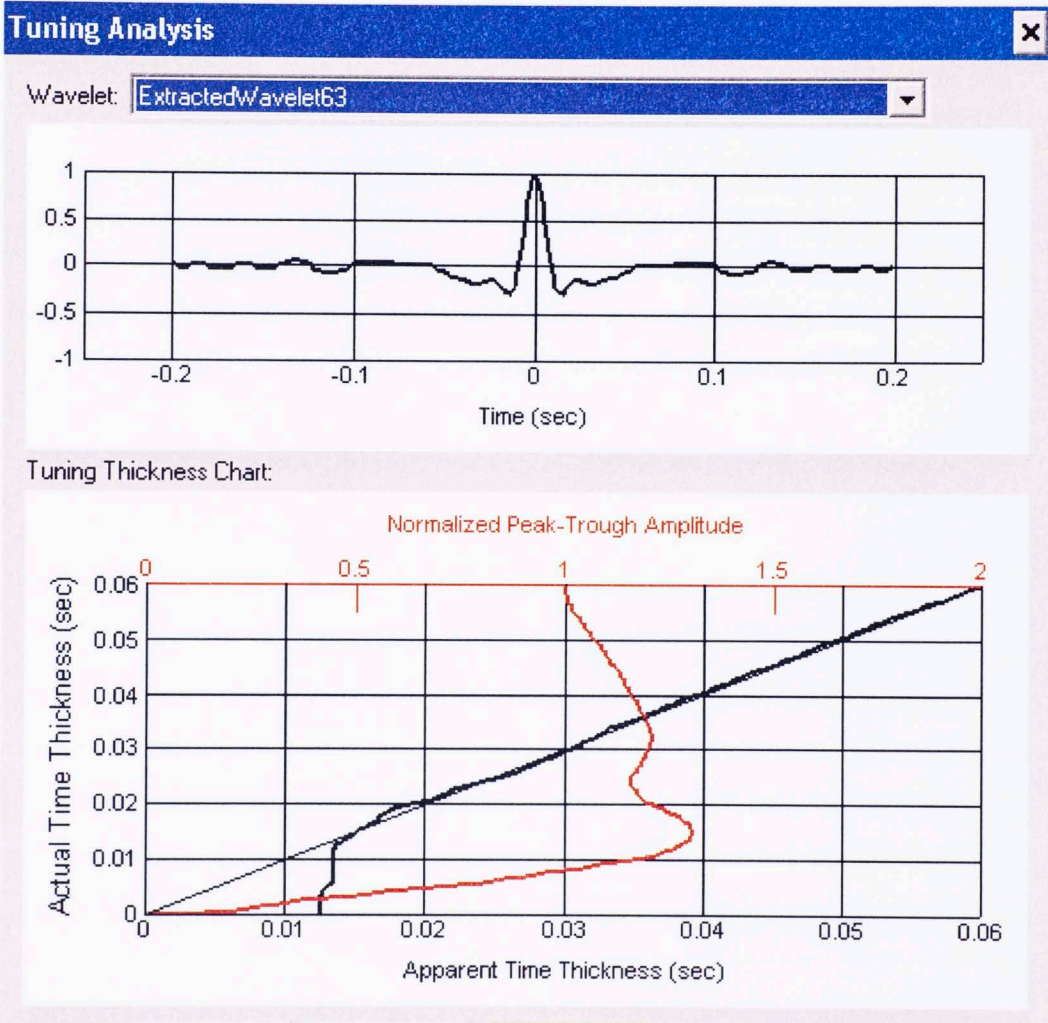
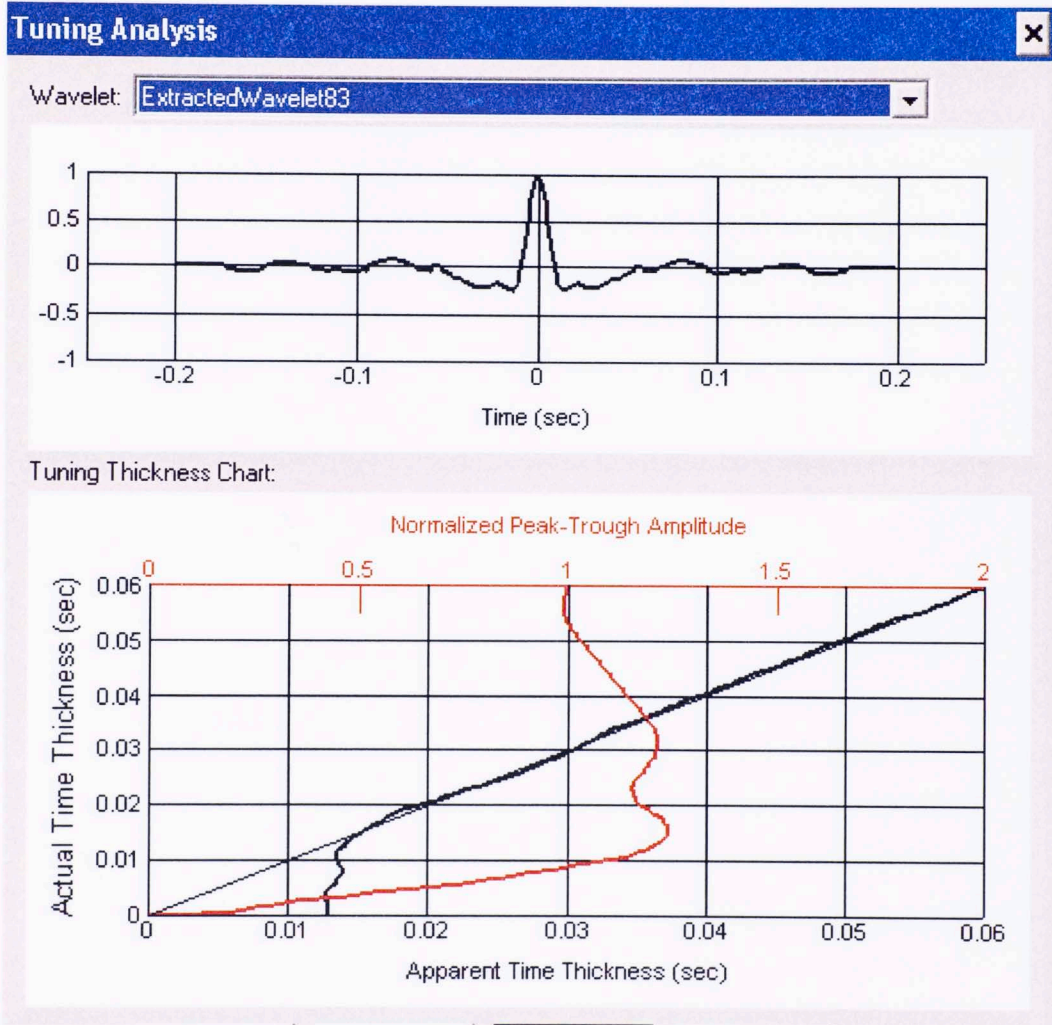


Figure A. 1 Tuning analysis for extracted wavelet at well # 55



**Figure A. 2** Tuning analysis for extracted wavelet at well # 63



**Figure A. 3** Tuning analysis for extracted wavelet at well # 83

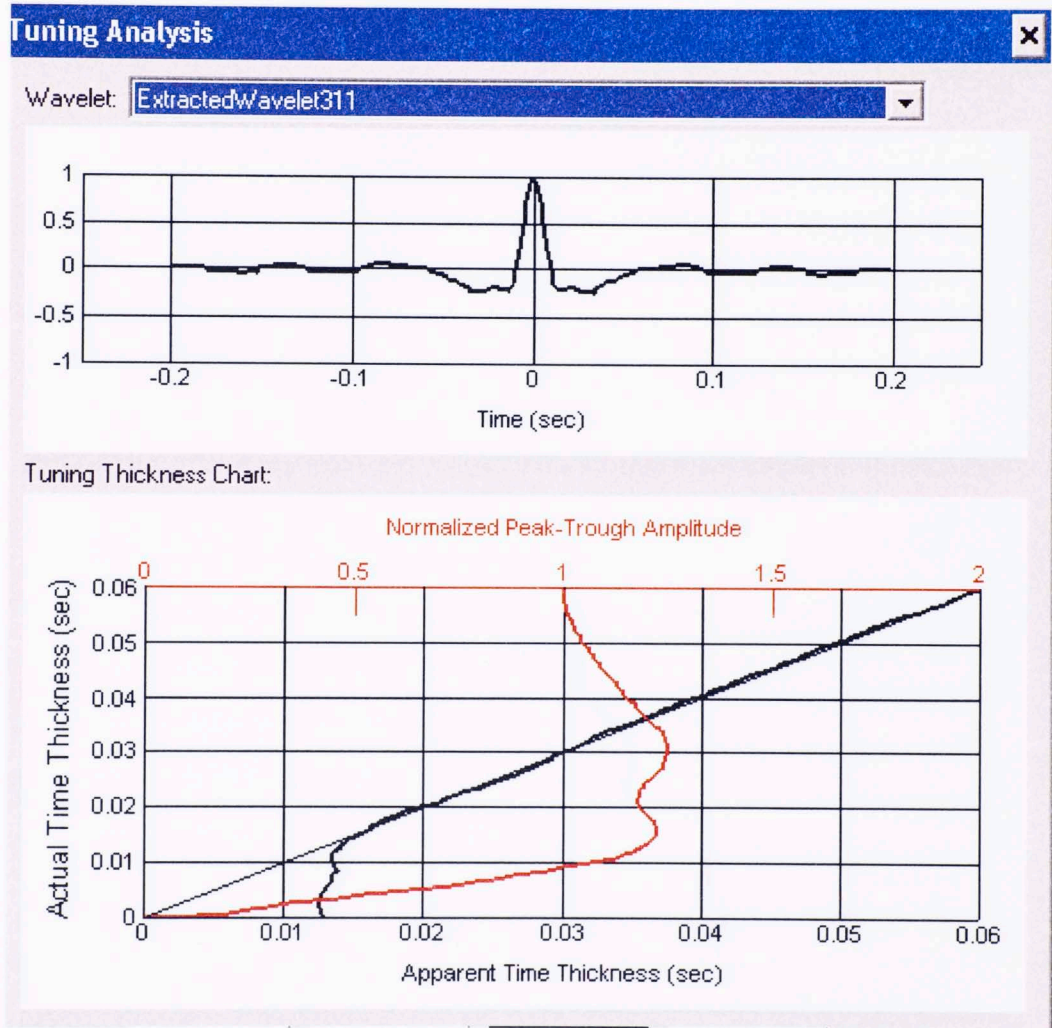


**Figure A. 4** Tuning analysis for extracted wavelet at well # 311

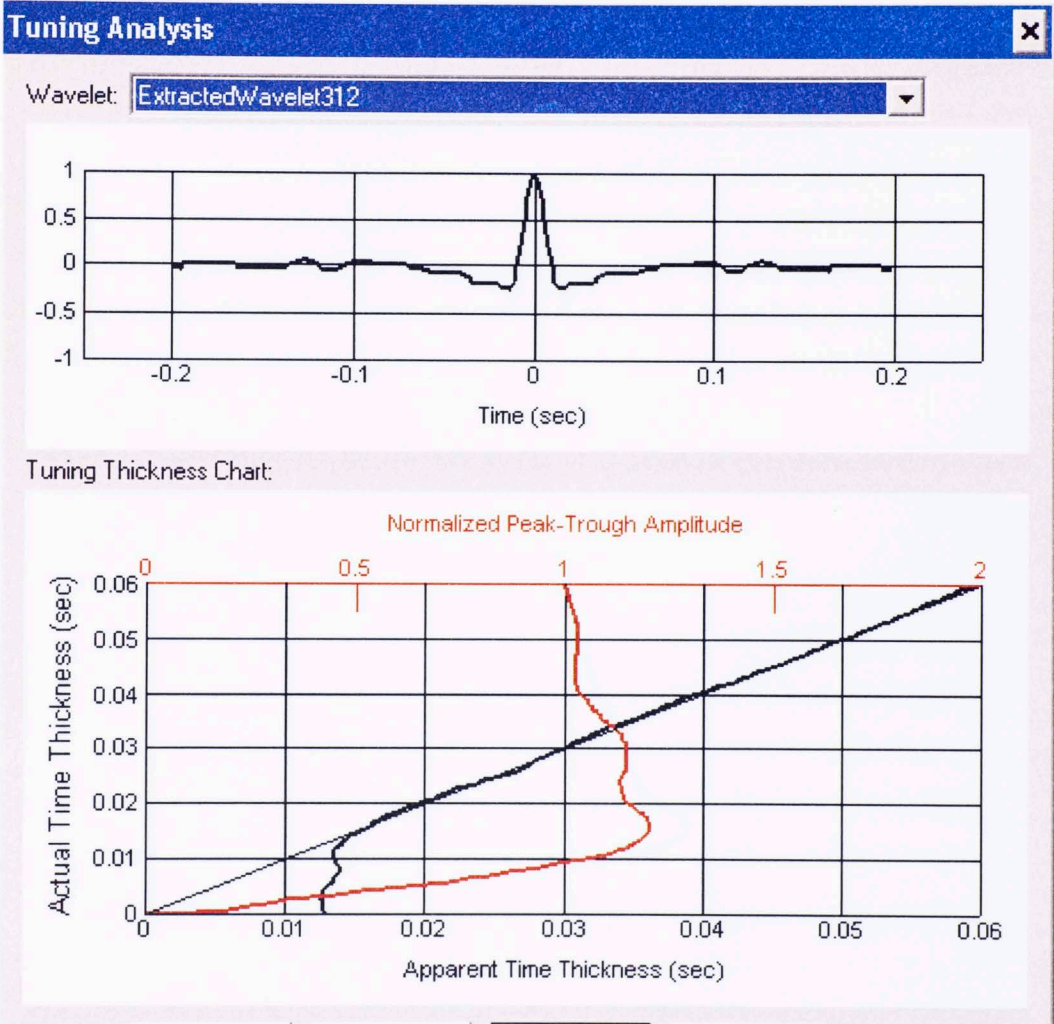


**Figure A. 5** Tuning analysis for extracted wavelet at well # 312



**Figure A. 6** Tuning analysis for extracted wavelet at well # 20066

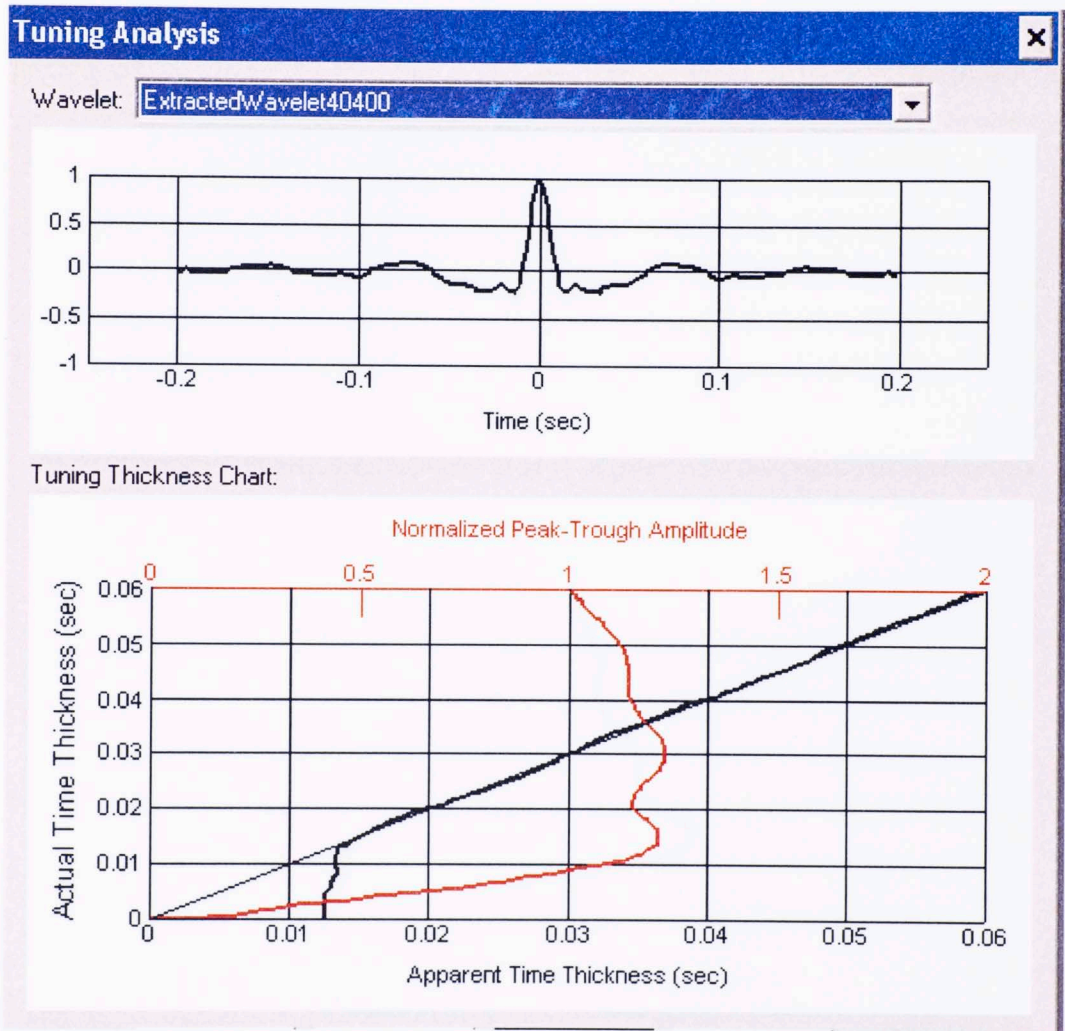
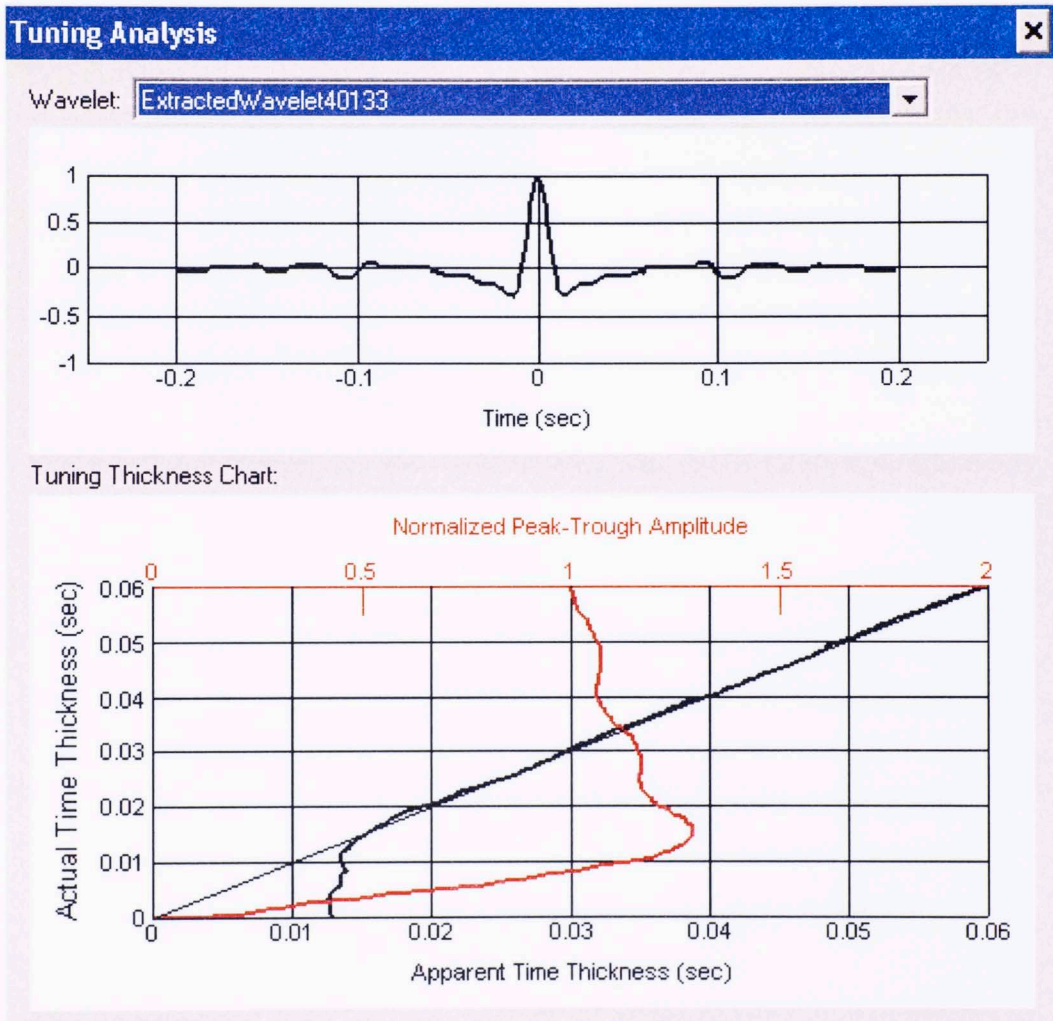


Figure A. 7 Tuning analysis for extracted wavelet at well # 40400



**Figure A. 8** Tuning analysis for extracted wavelet at well # 40133

## Appendix A: Spectrograms

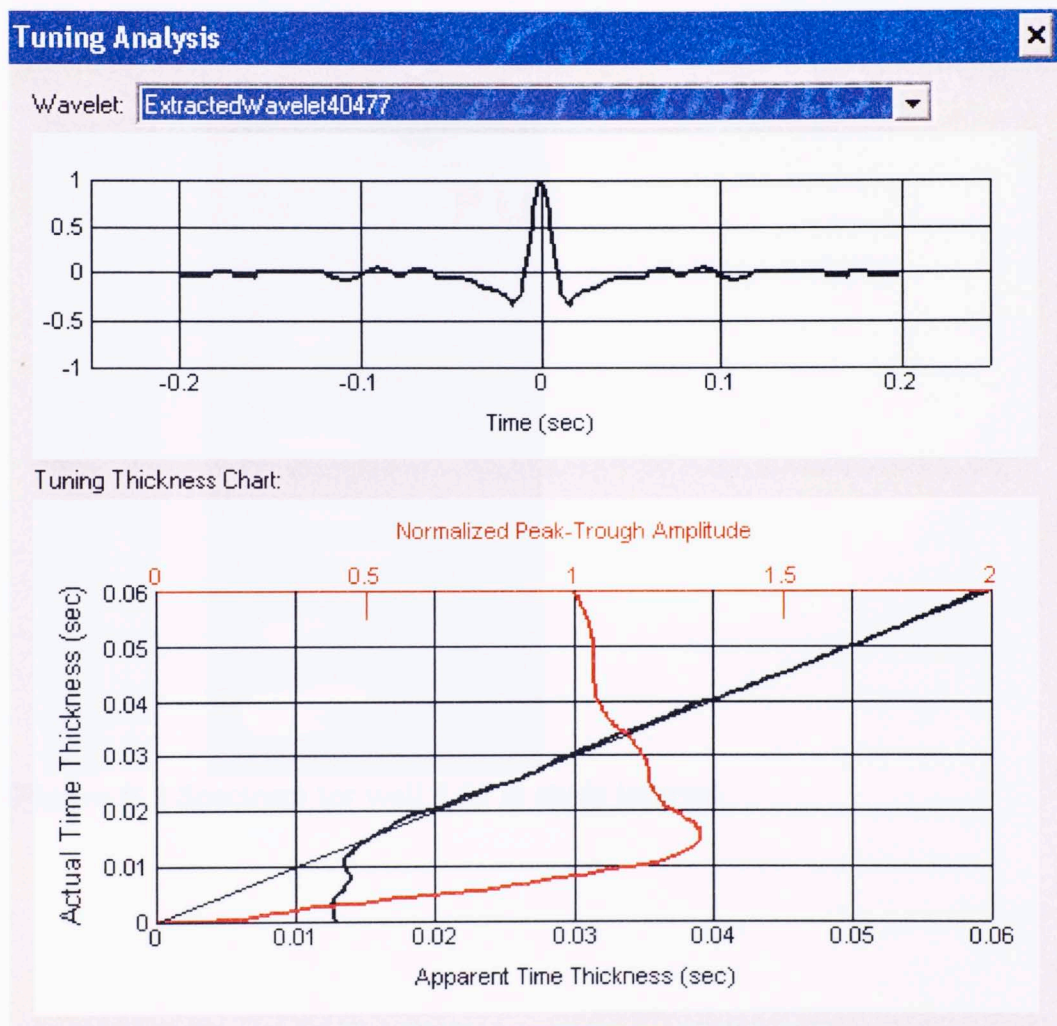


Figure A. 9 Tuning analysis for extracted wavelet at well # 40477

## Appendix B: Spectrums

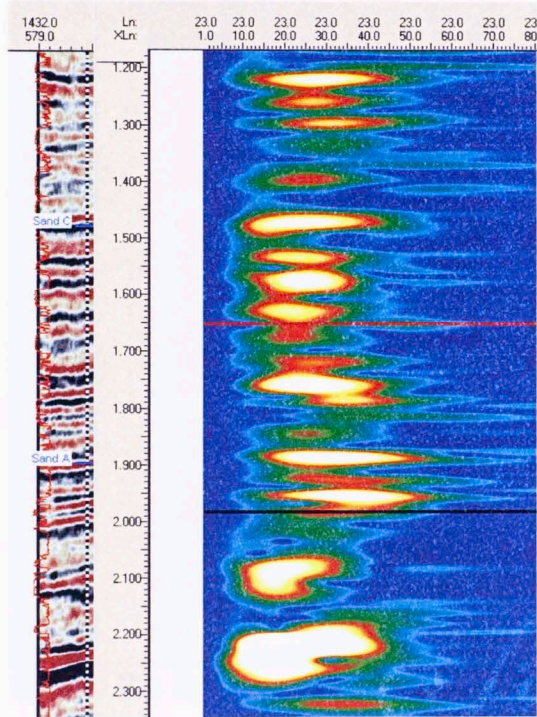
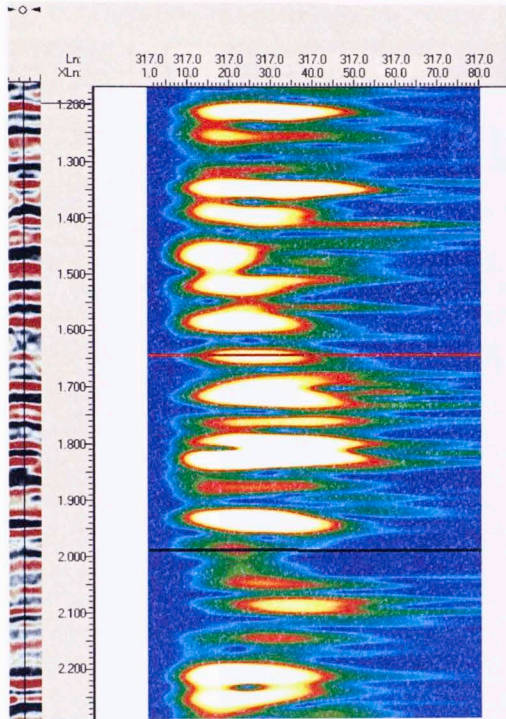


Figure B.1 Spectrum for well # 55 in study interval



**Figure B.2** Spectrum for well # 63 in study interval

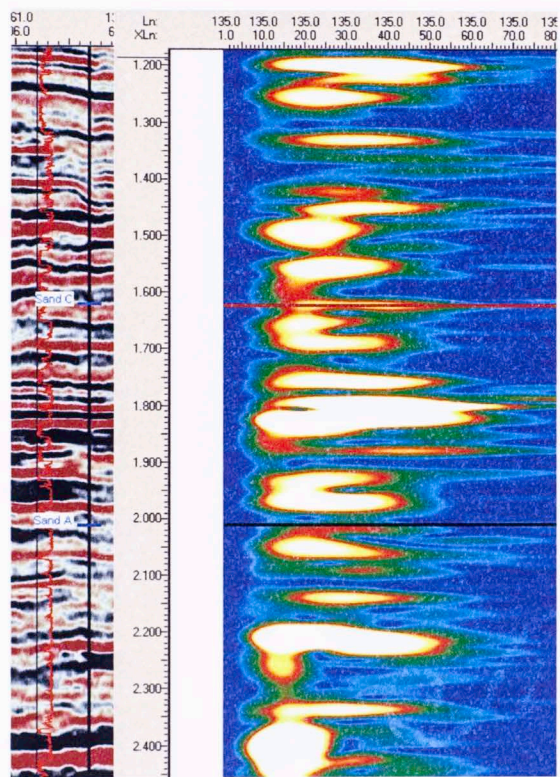


Figure B.3 Spectrum for well # 83 in study interval

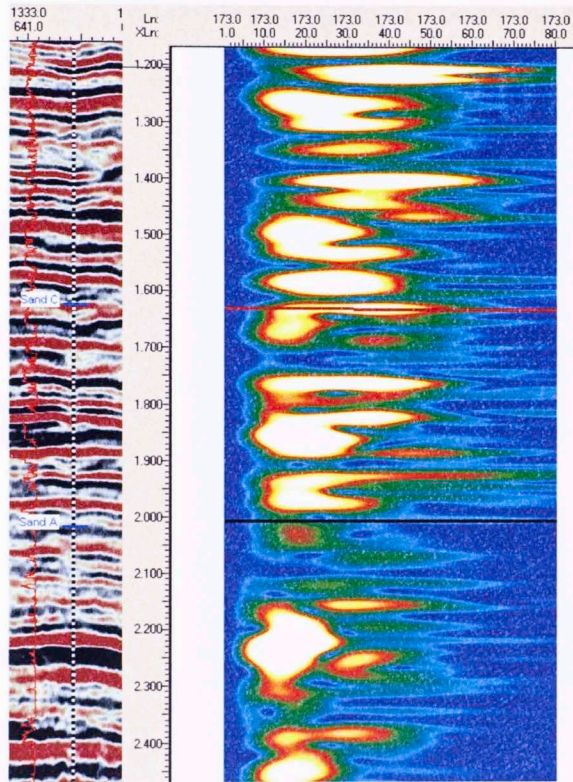


Figure B.4 Spectrum for well # 311 in study interval

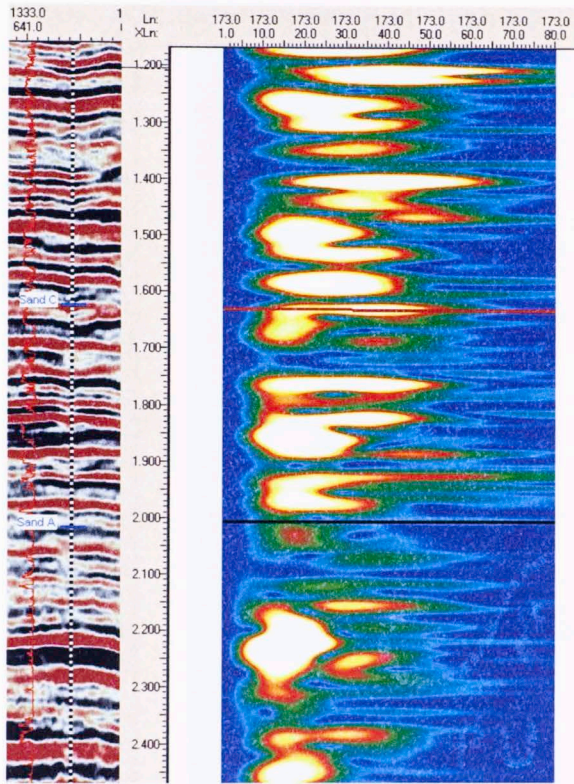
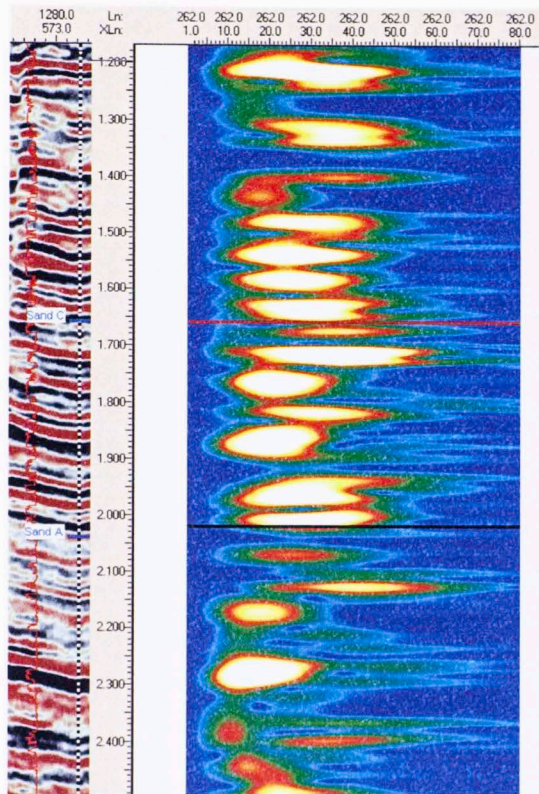


Figure B.5 Spectrum for well # 312 in study interval



**Figure B.6** Spectrum for well # 20066 in study interval

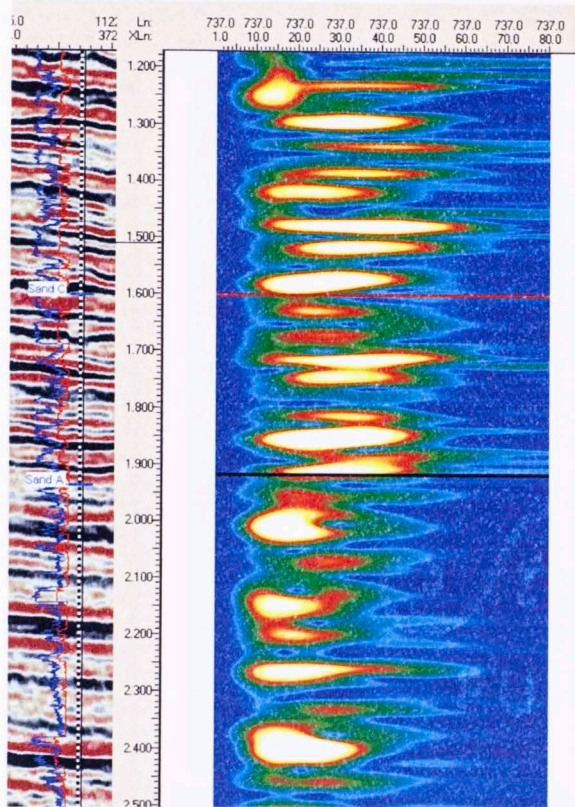
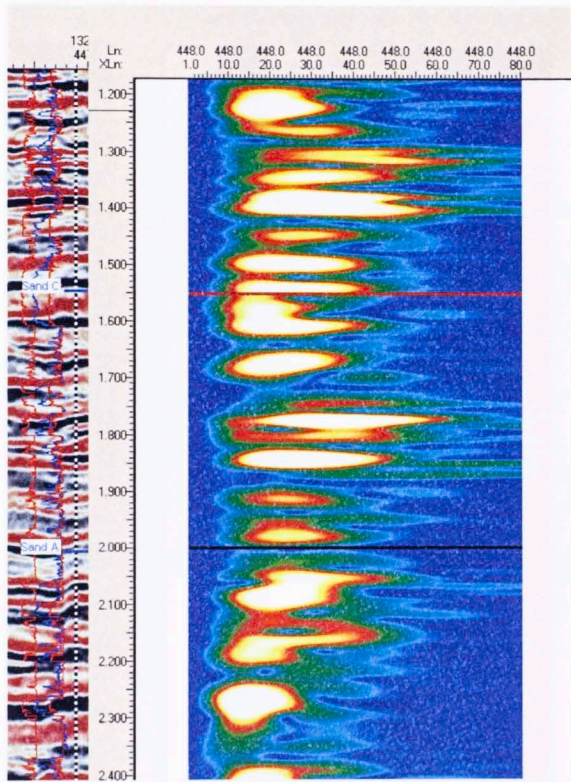


Figure B.7 Spectrum for well # 40133 in study interval



**Figure B.8** Spectrum for well # 40400 in study interval

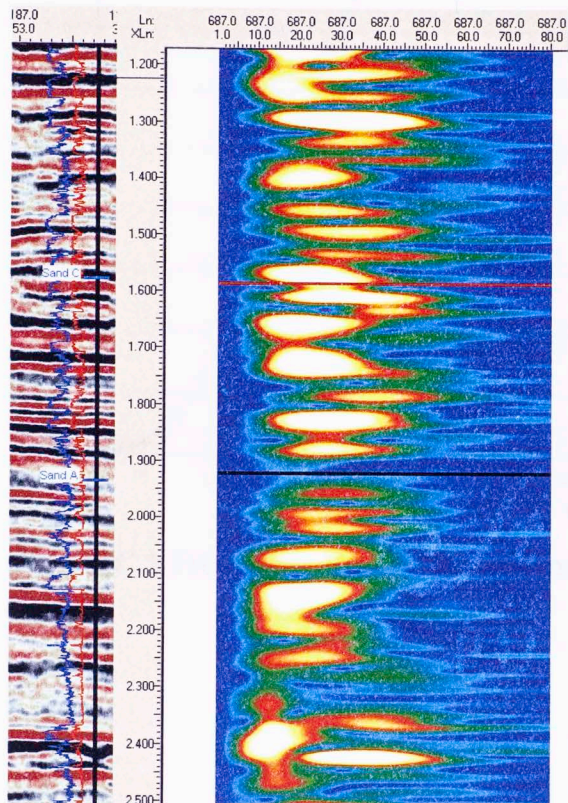


Figure B.9 Spectrum for well # 40477 in study interval

### Appendix C: Frequency Spectra for Sands A and C at each well

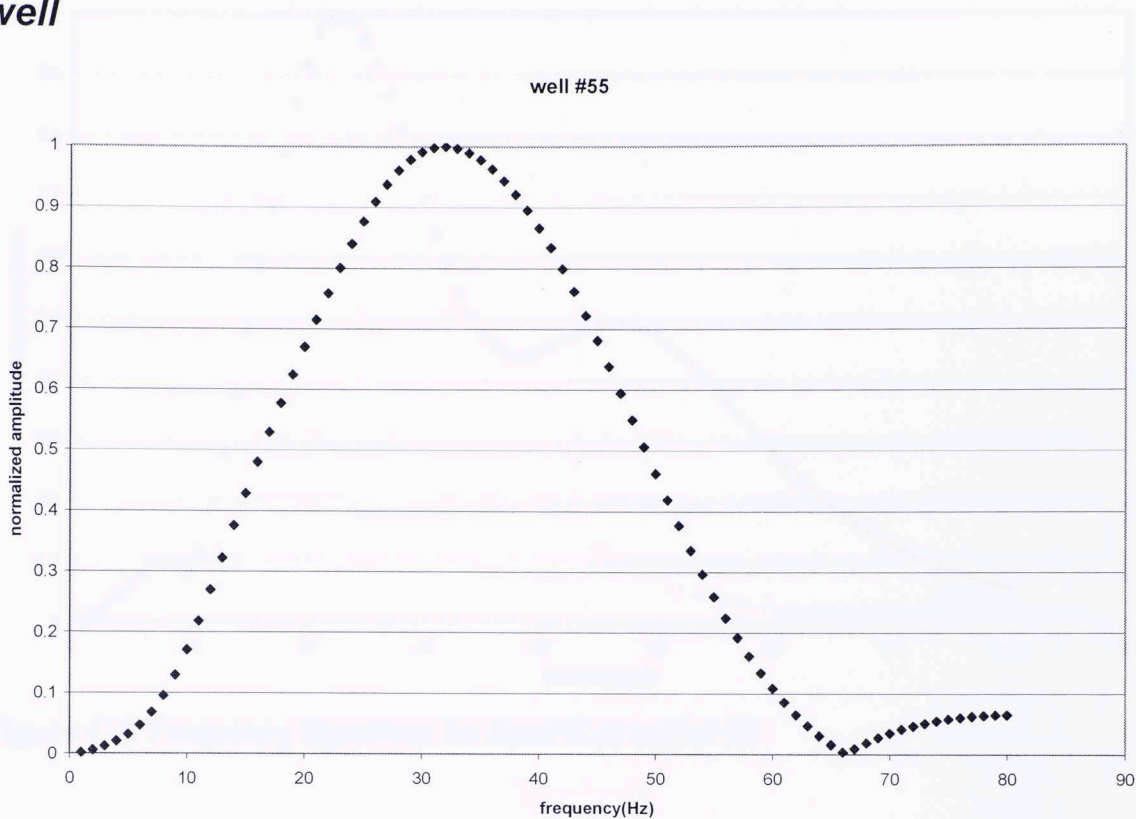
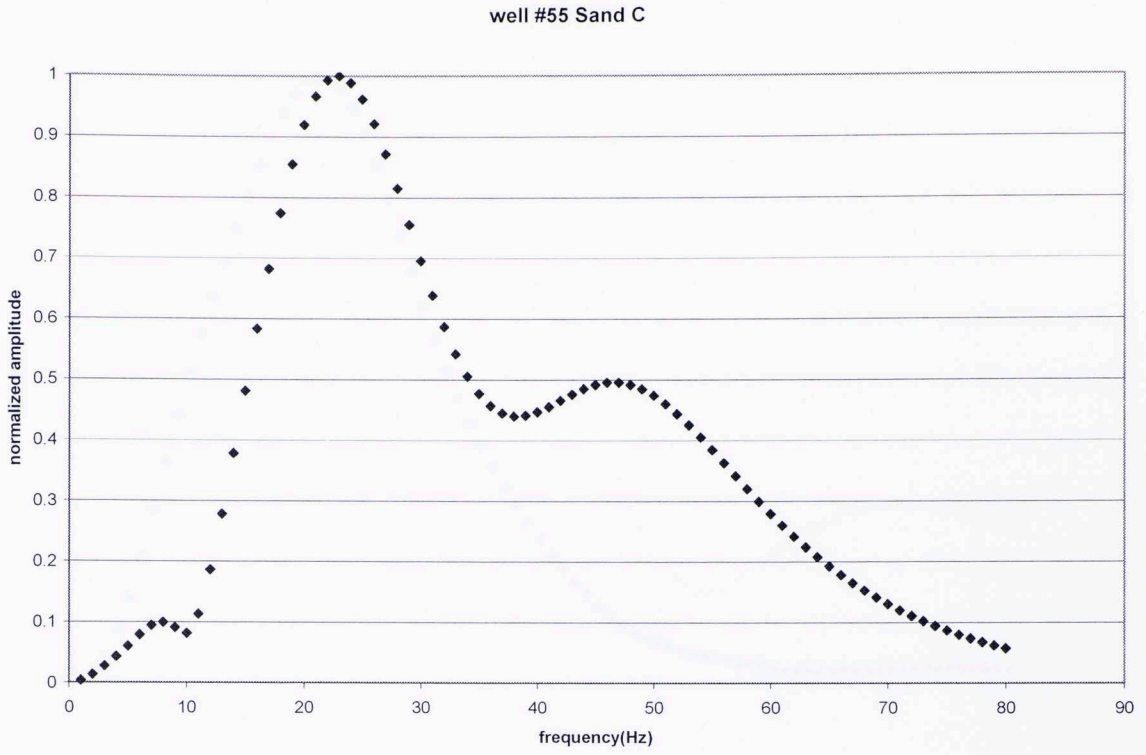


Figure C.1 Frequency Spectrum for Sand A at well # 55



**Figure C.2** Frequency Spectrum for Sand C at well # 55



**Figure C.4** Frequency Spectrum for Sand C at well #55

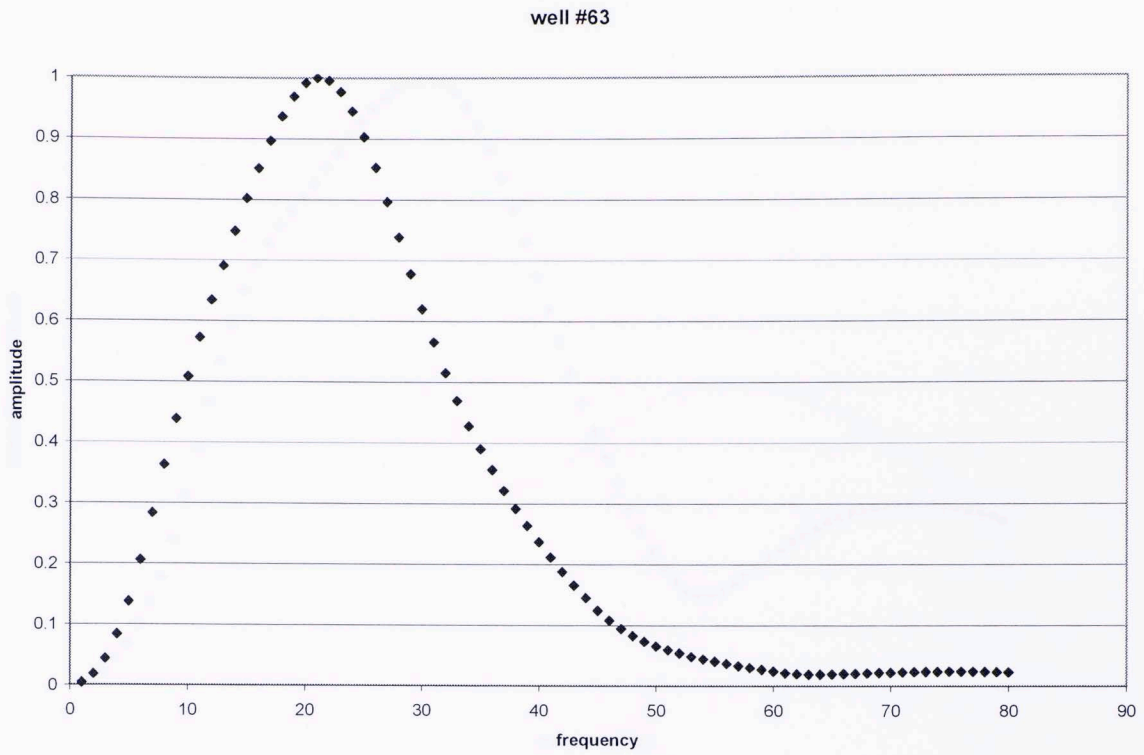


**Figure C.3** Frequency Spectrum for Sand A at well # 63

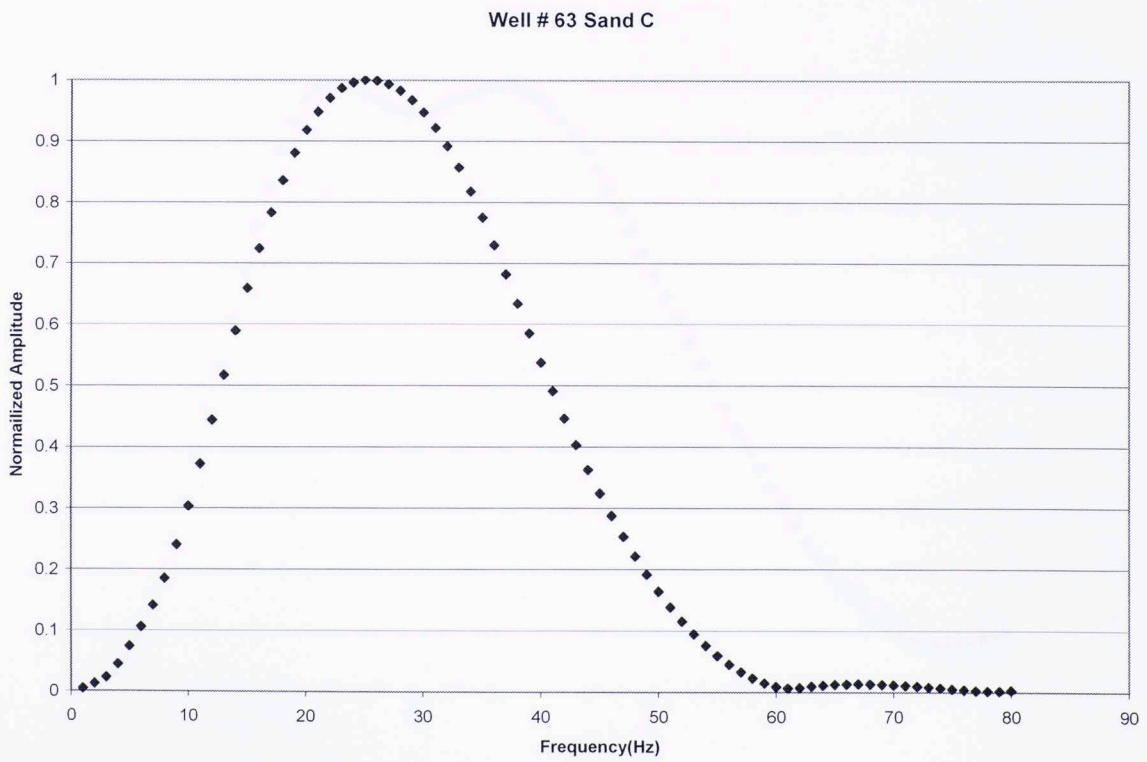


**Figure C.4** Frequency Spectrum for Sand C at well # 63

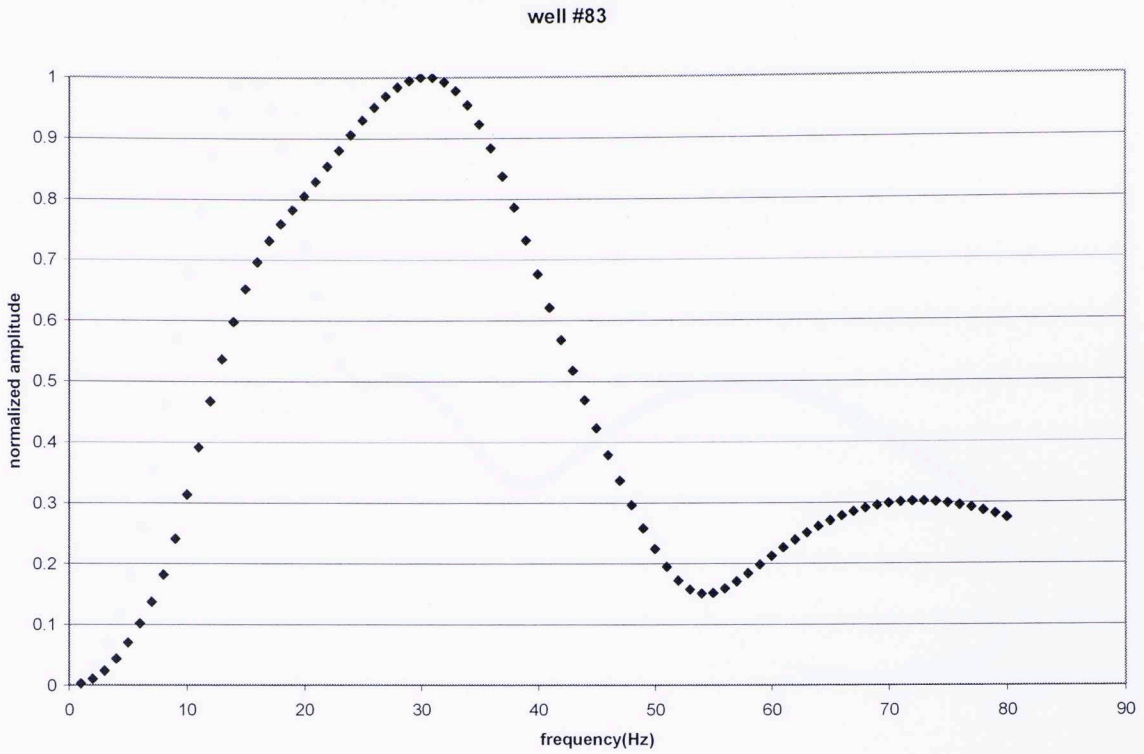


Figure C.5 Frequency Spectrum for Sand A at well # 83

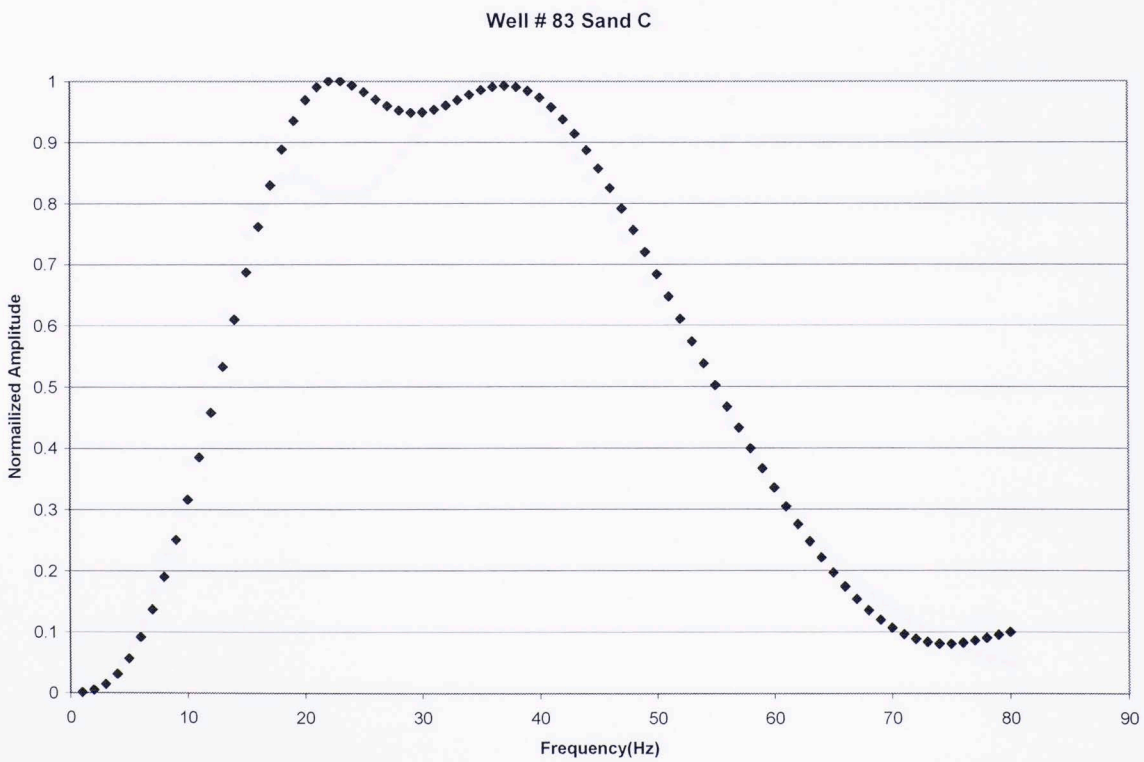
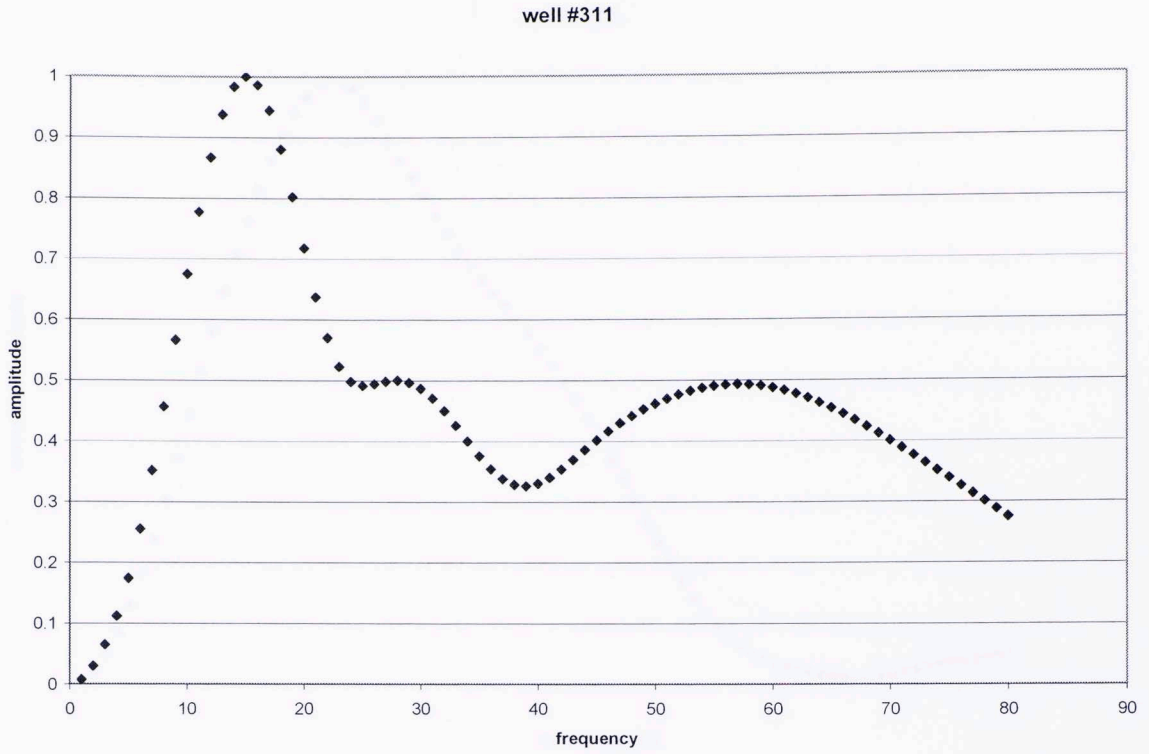
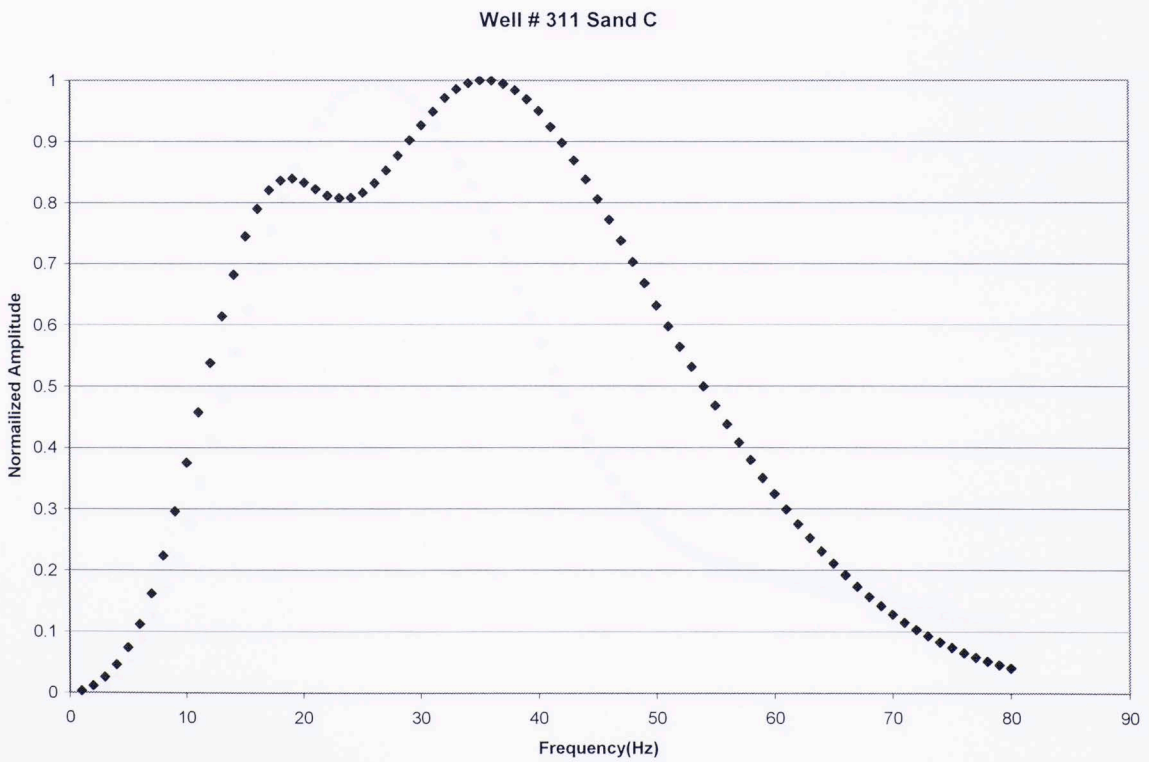


Figure C.6 Frequency Spectrum for Sand C at well # 83



**Figure C.7** Frequency Spectrum for Sand A at well # 311



**Figure C.8** Frequency Spectrum for Sand C at well # 311

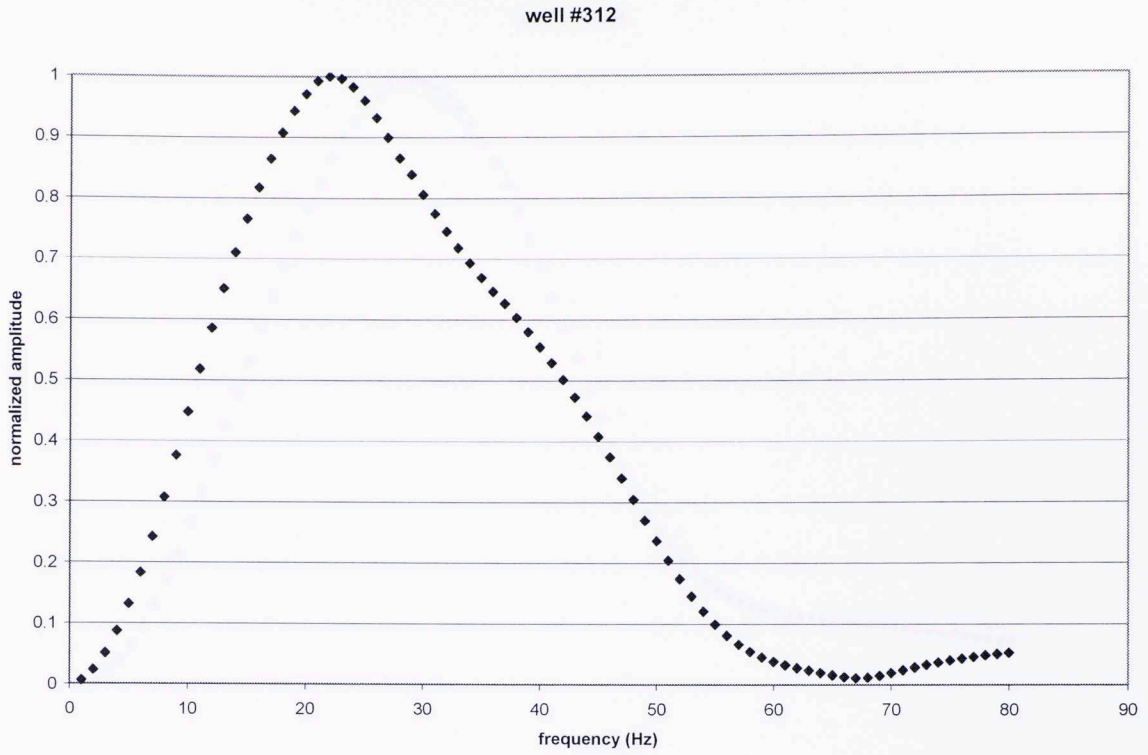


**Figure C.9** Frequency Spectrum for Sand A at well # 312

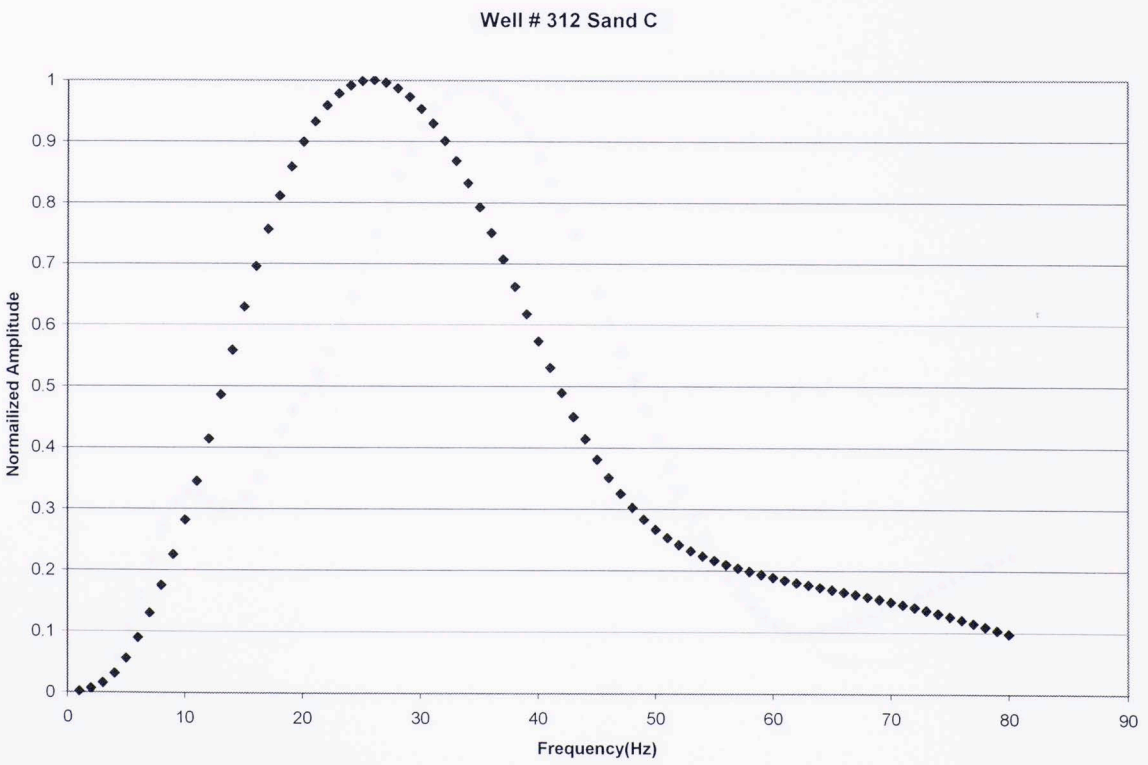


**Figure C.10** Frequency Spectrum for Sand C at well # 312

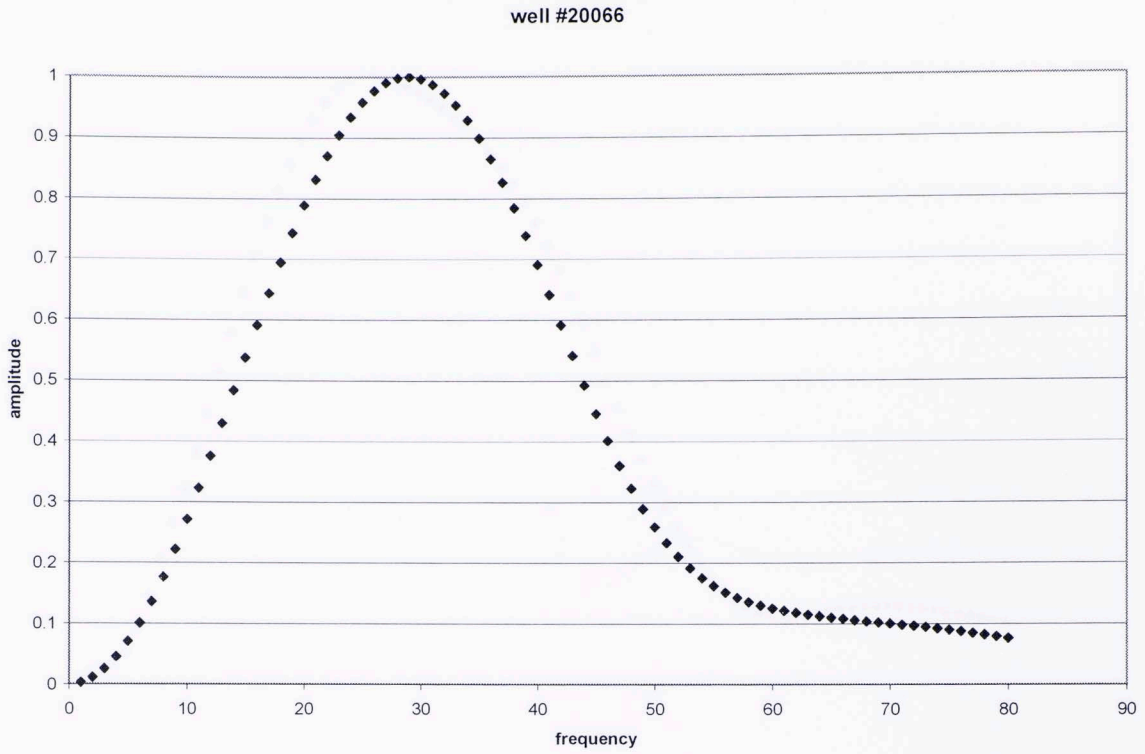


Figure C.11 Frequency Spectrum for Sand A at well # 20066

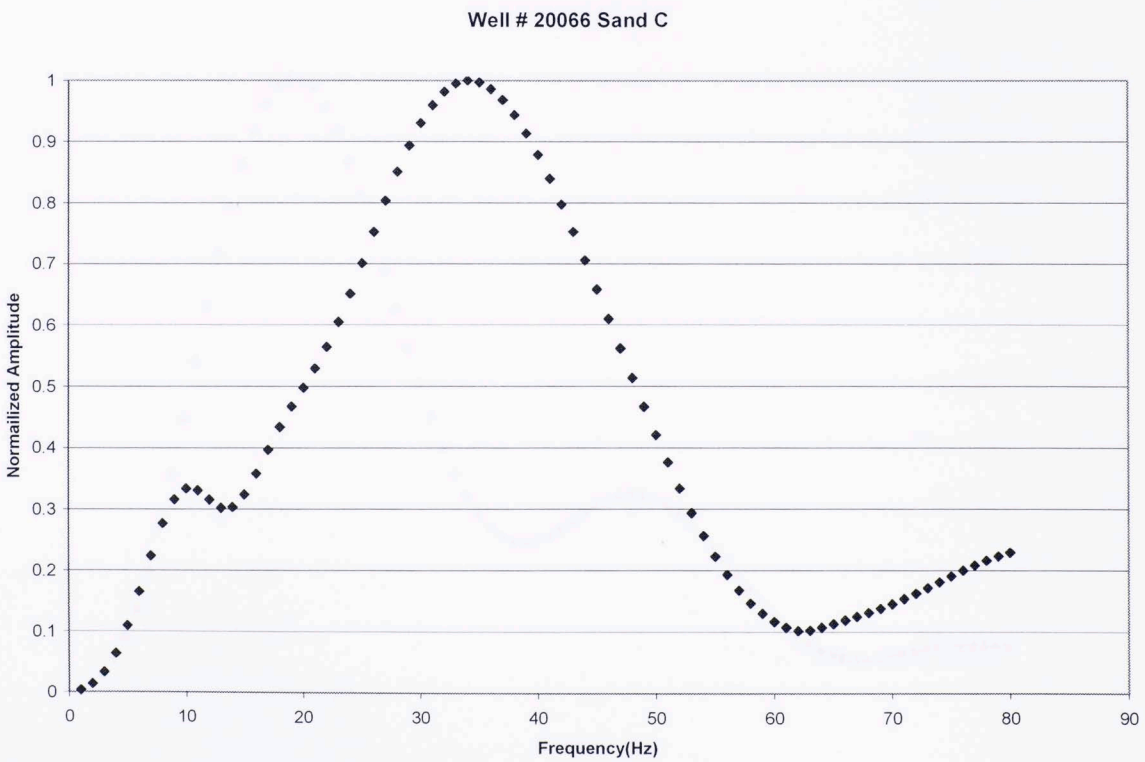
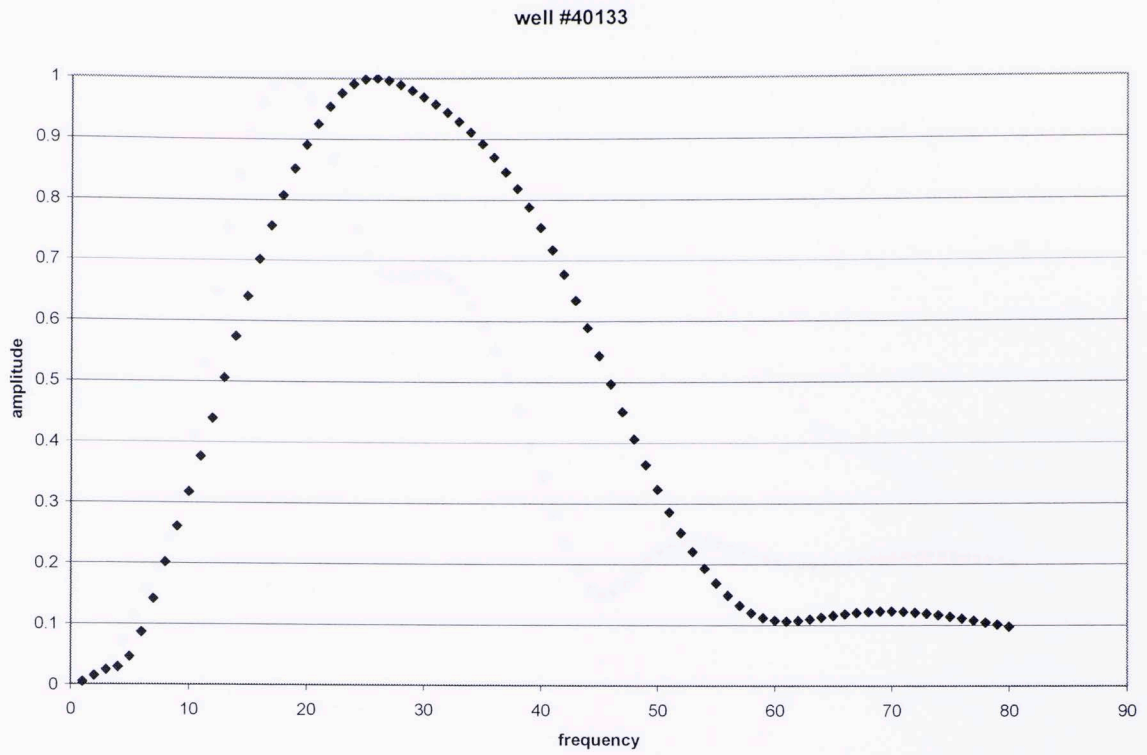
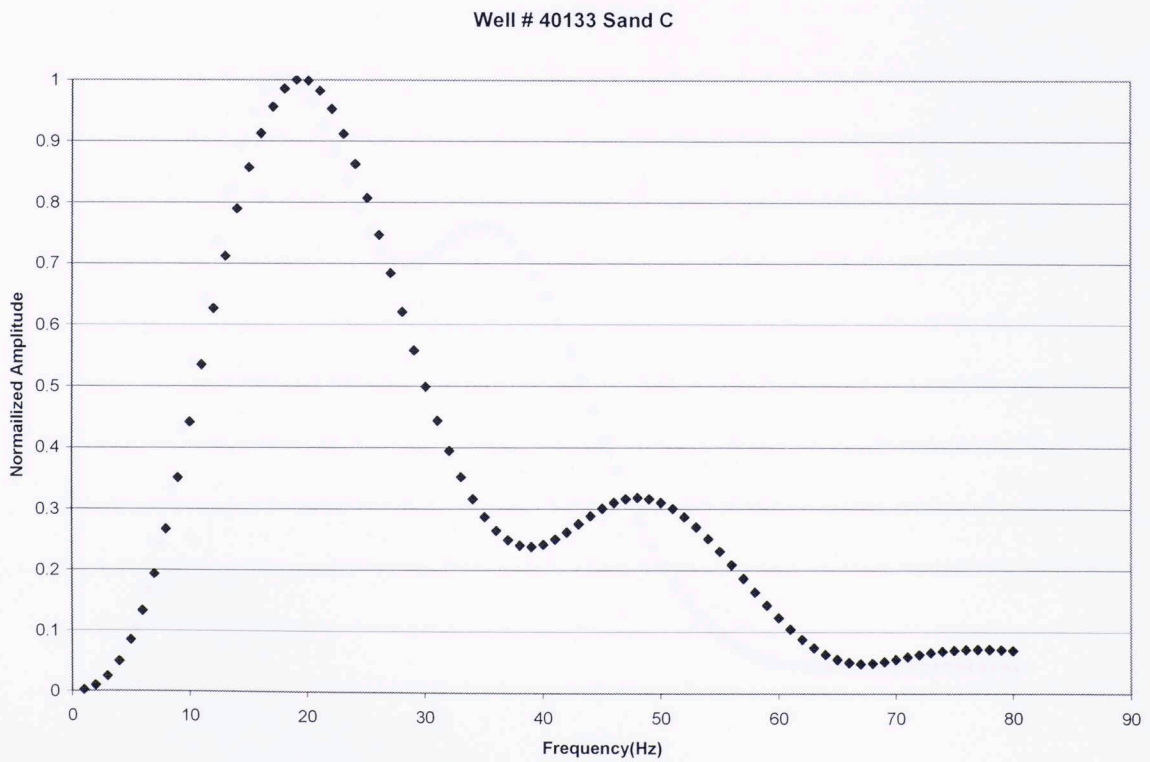


Figure C.12 Frequency Spectrum for Sand C at well # 20066



**Figure C.13** Frequency Spectrum for Sand A at well # 40133



**Figure C.14** Frequency Spectrum for Sand C at well # 40133

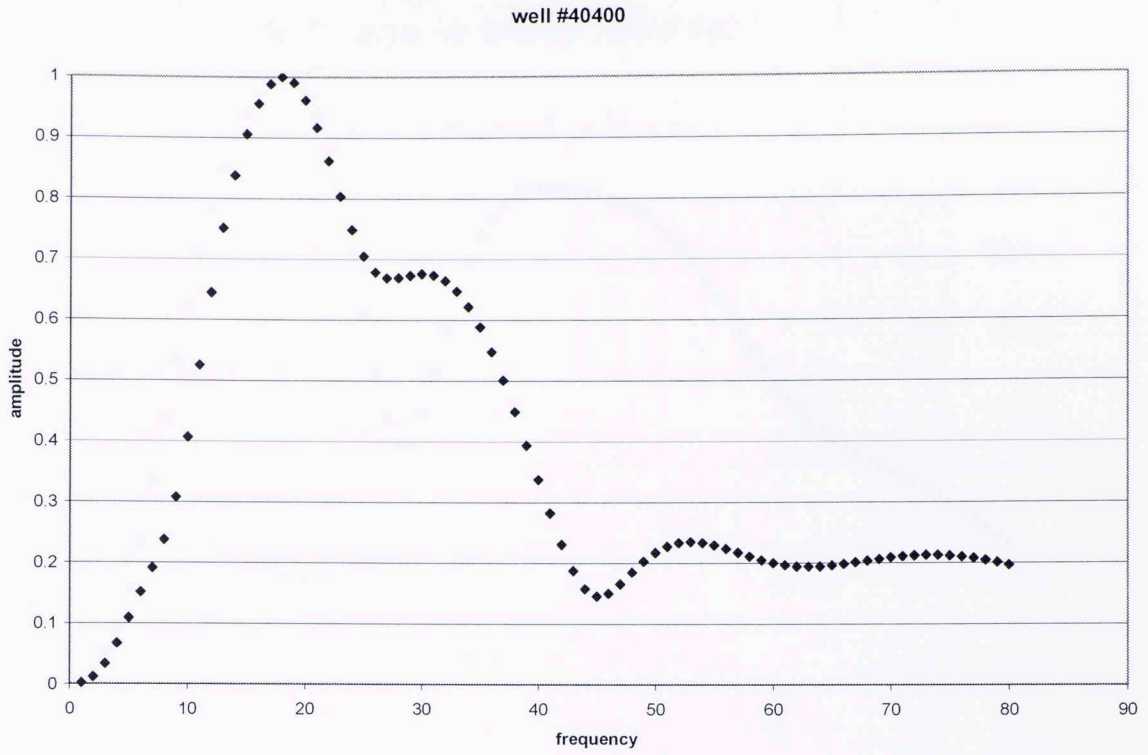


**Figure C.15** Frequency Spectrum for Sand A at well # 40400

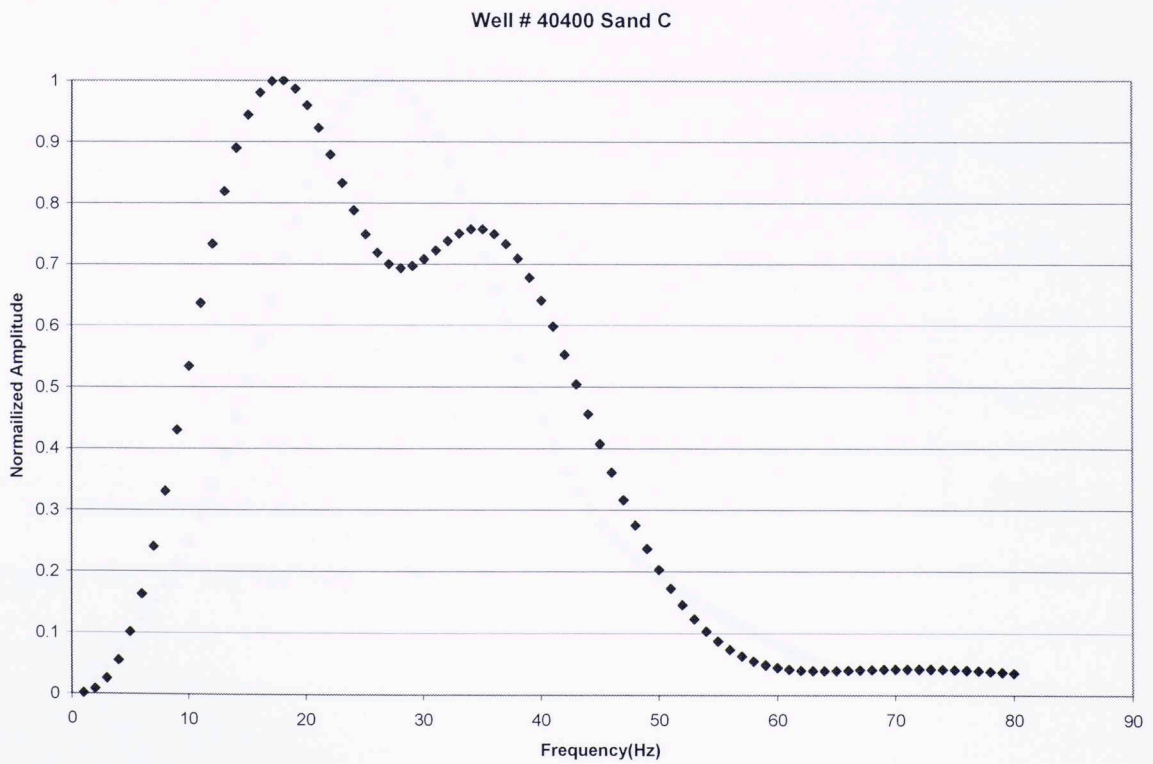


**Figure C.16** Frequency Spectrum for Sand C at well # 40400

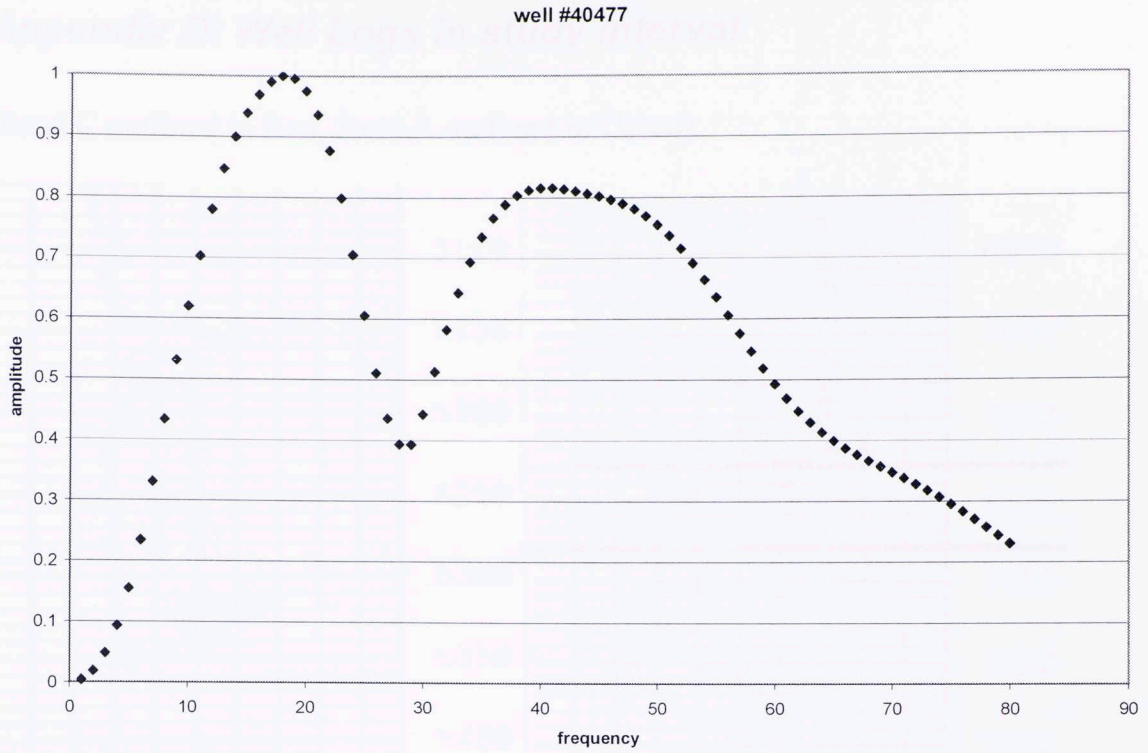


**Figure C.17** Frequency Spectrum for Sand A at well # 40477

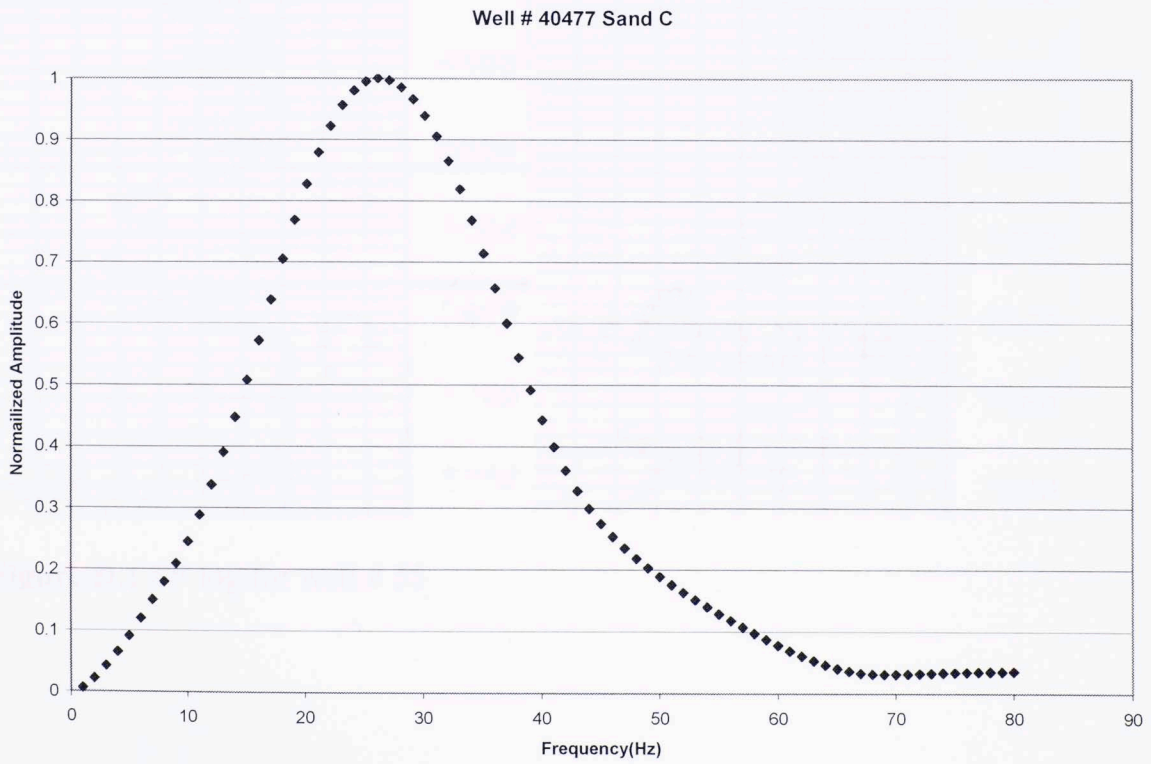


**Figure C.18** Frequency Spectrum for Sand C at well # 40477

## Appendix D: Well Logs in study interval

(Sand C outlined in Red, Sand A outlined in Green)

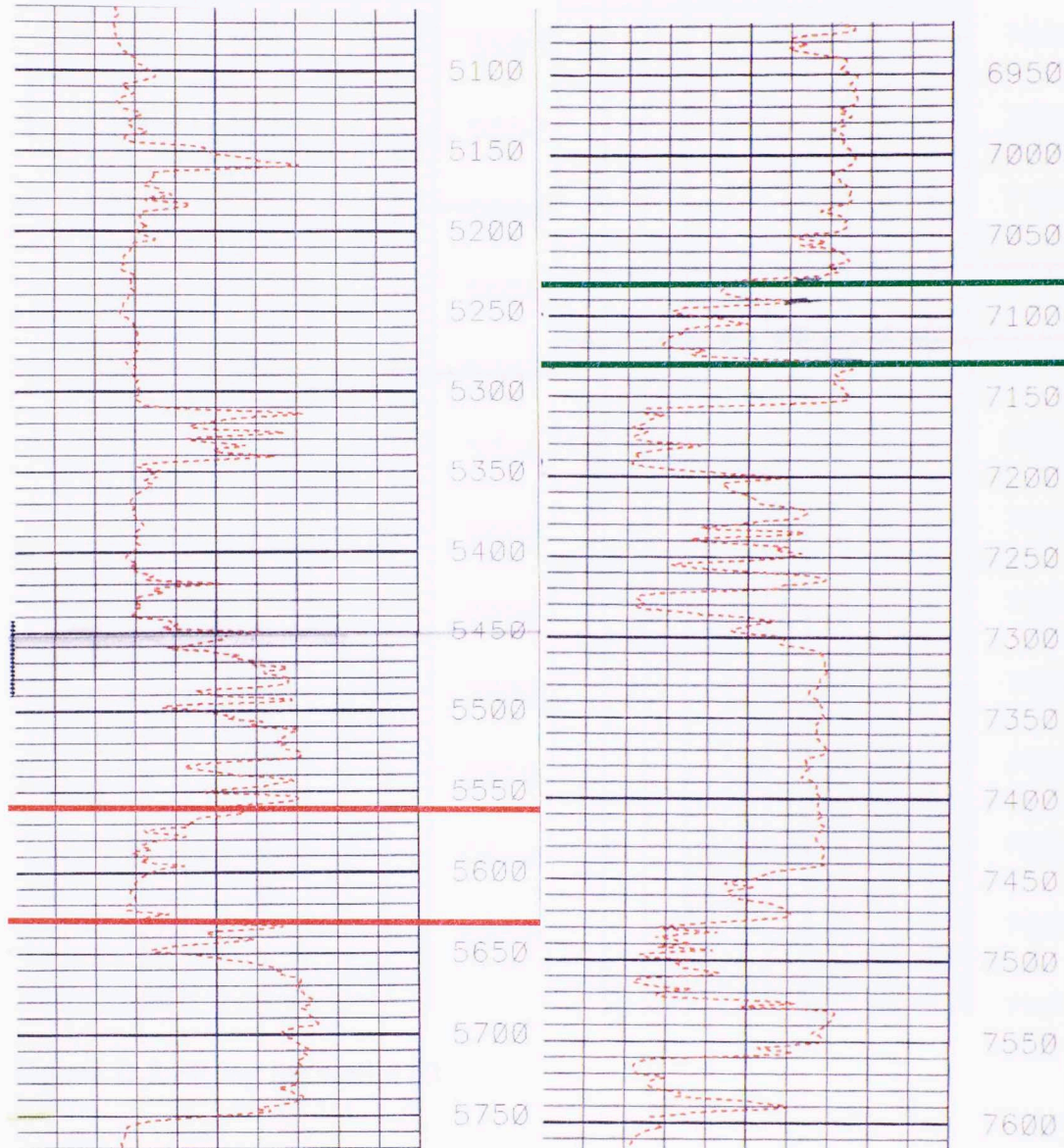
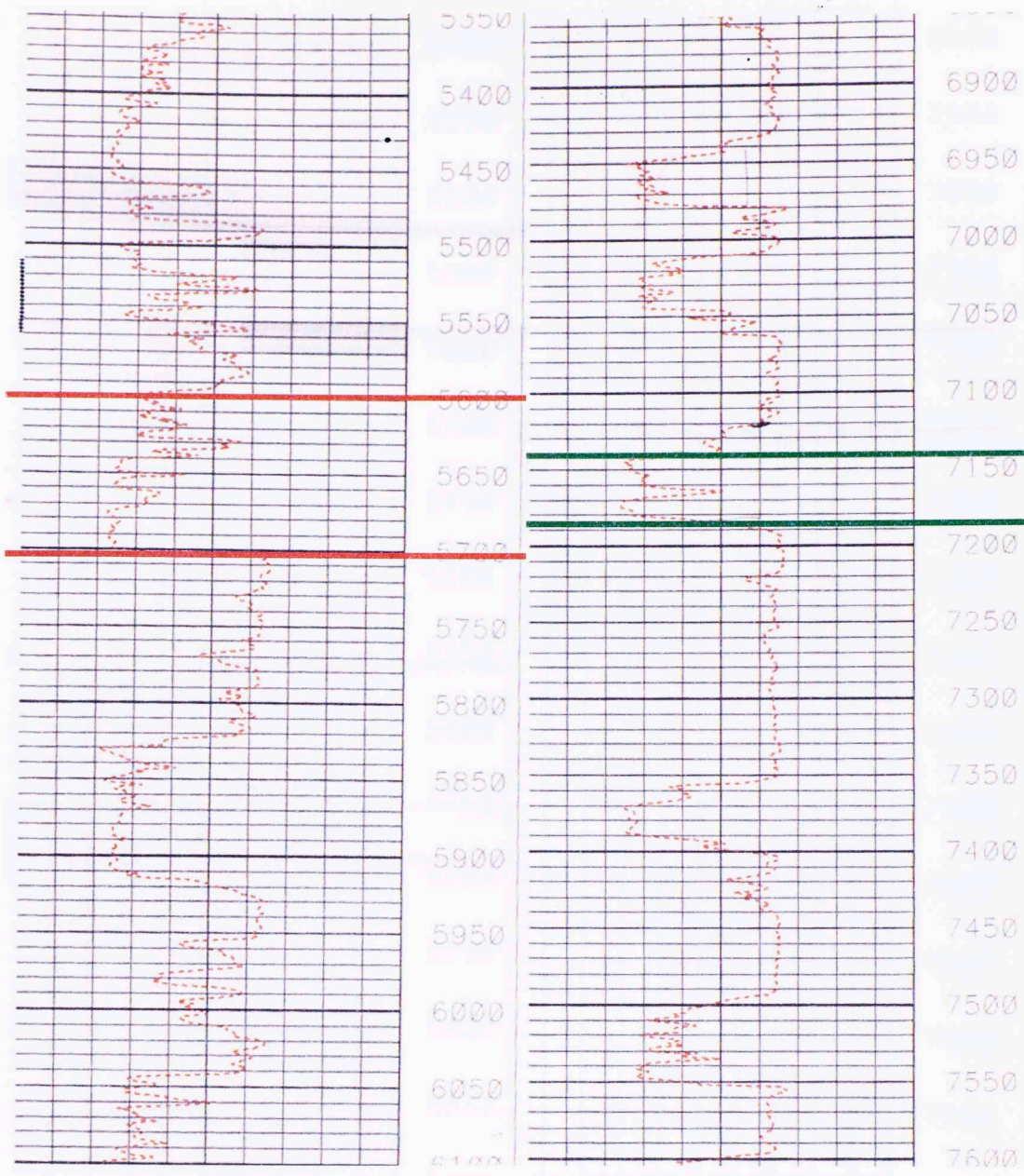
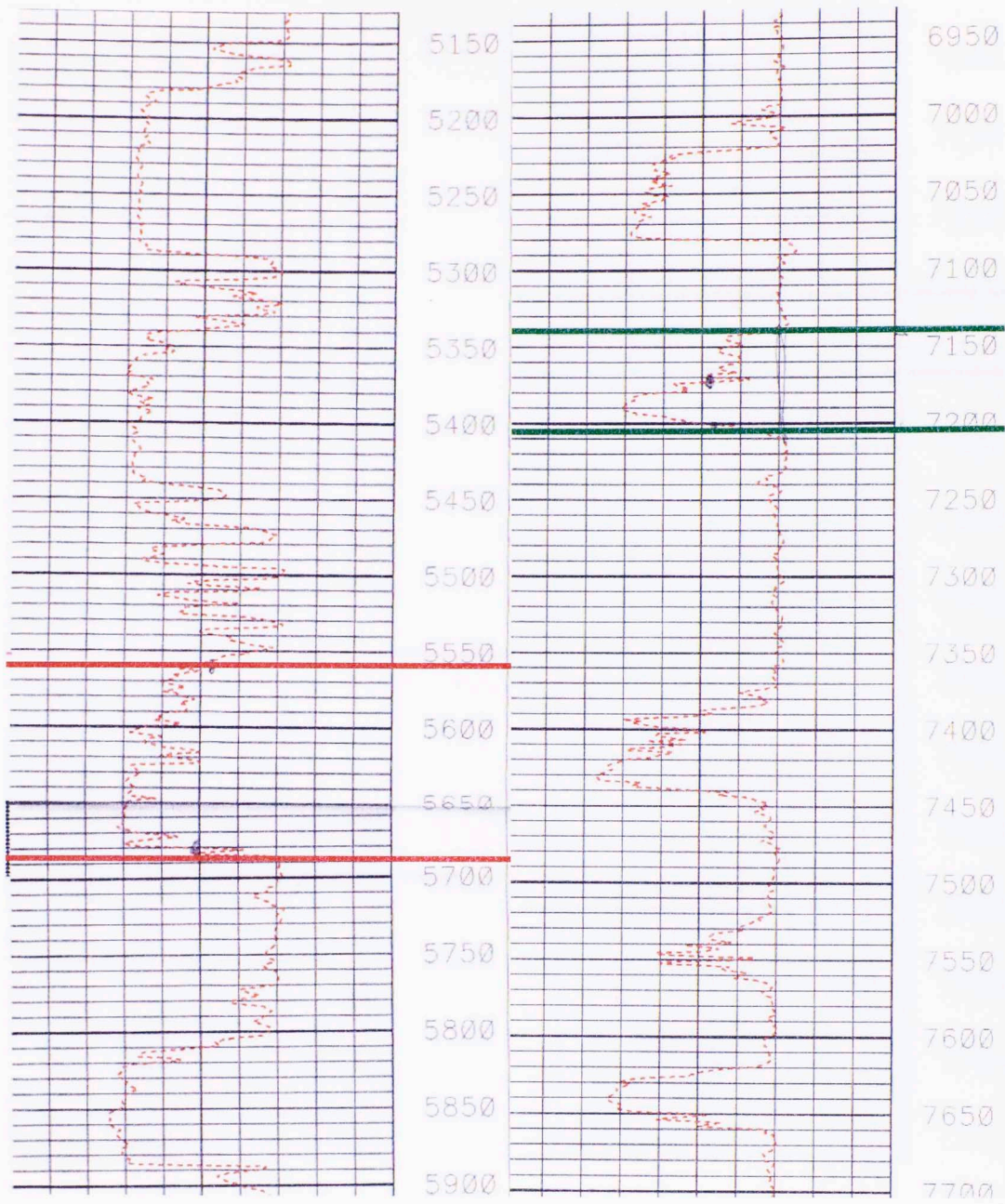


Figure D.1 SP log for well # 55



**Figure D.2** SP log for well # 63



**Figure D.3** SP log for well # 83

**Figure D.4** SP log for well # 84

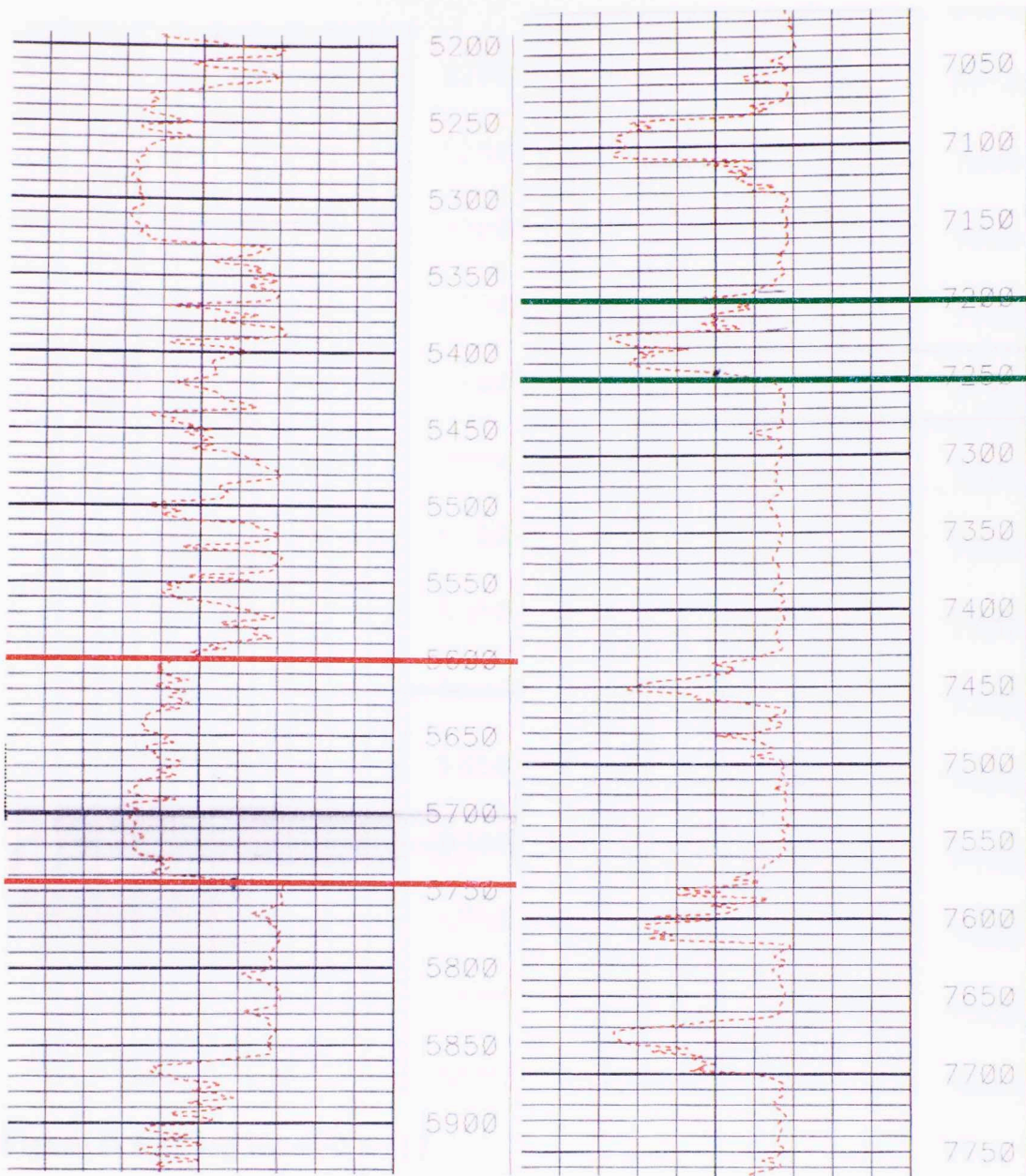


**Figure D.4** SP log for well # 311

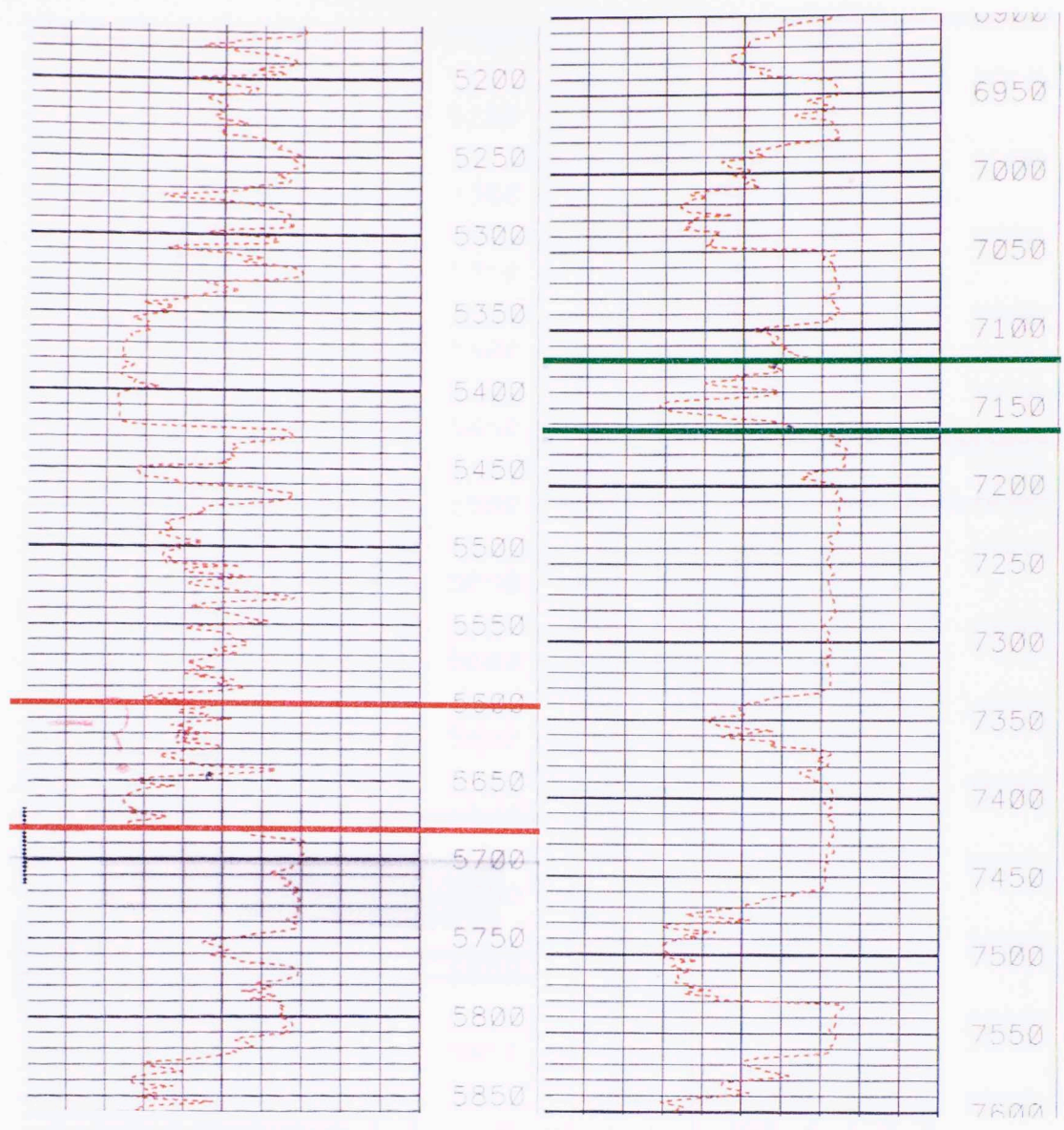


**Figure D.5** SP log for well # 312

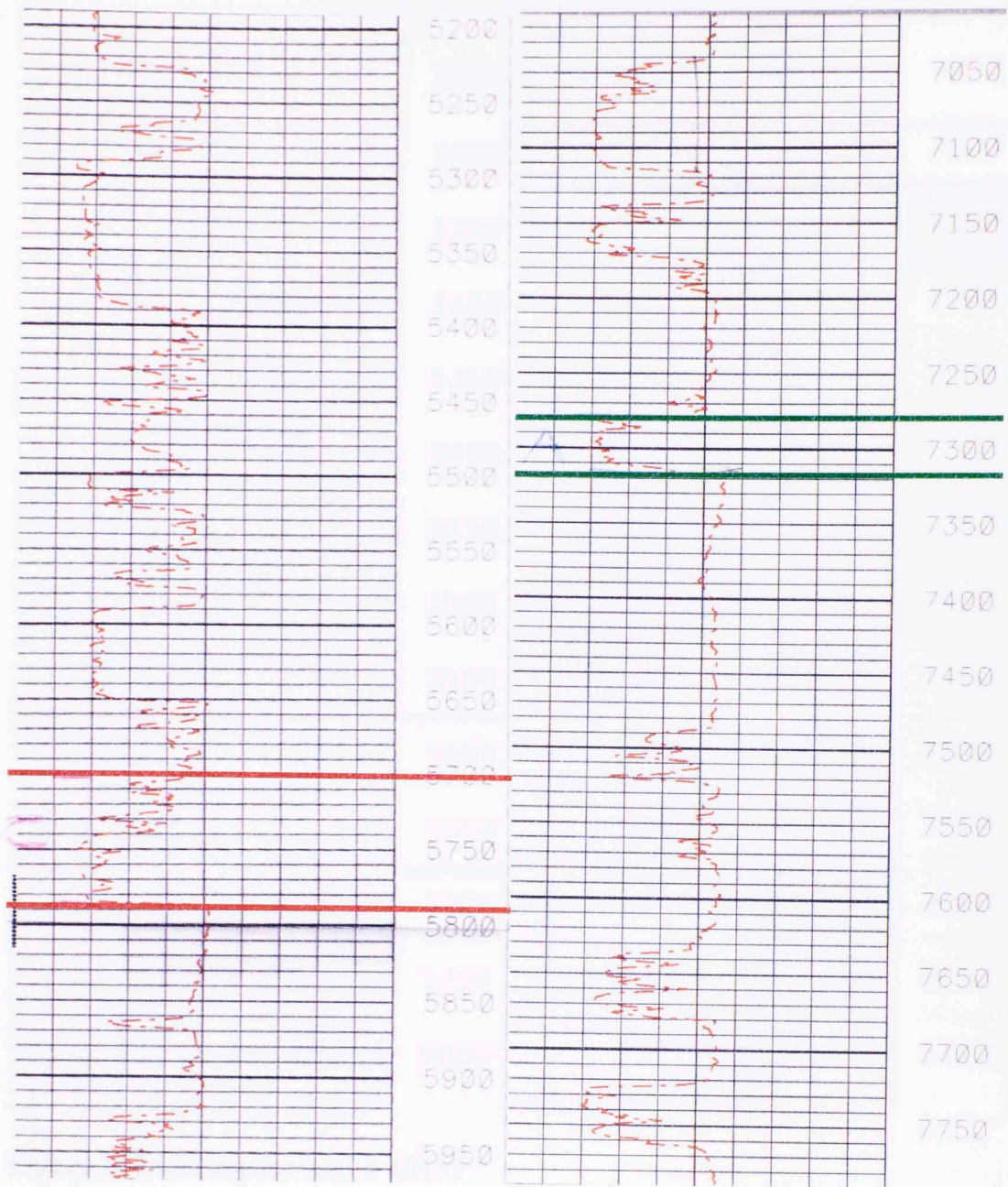
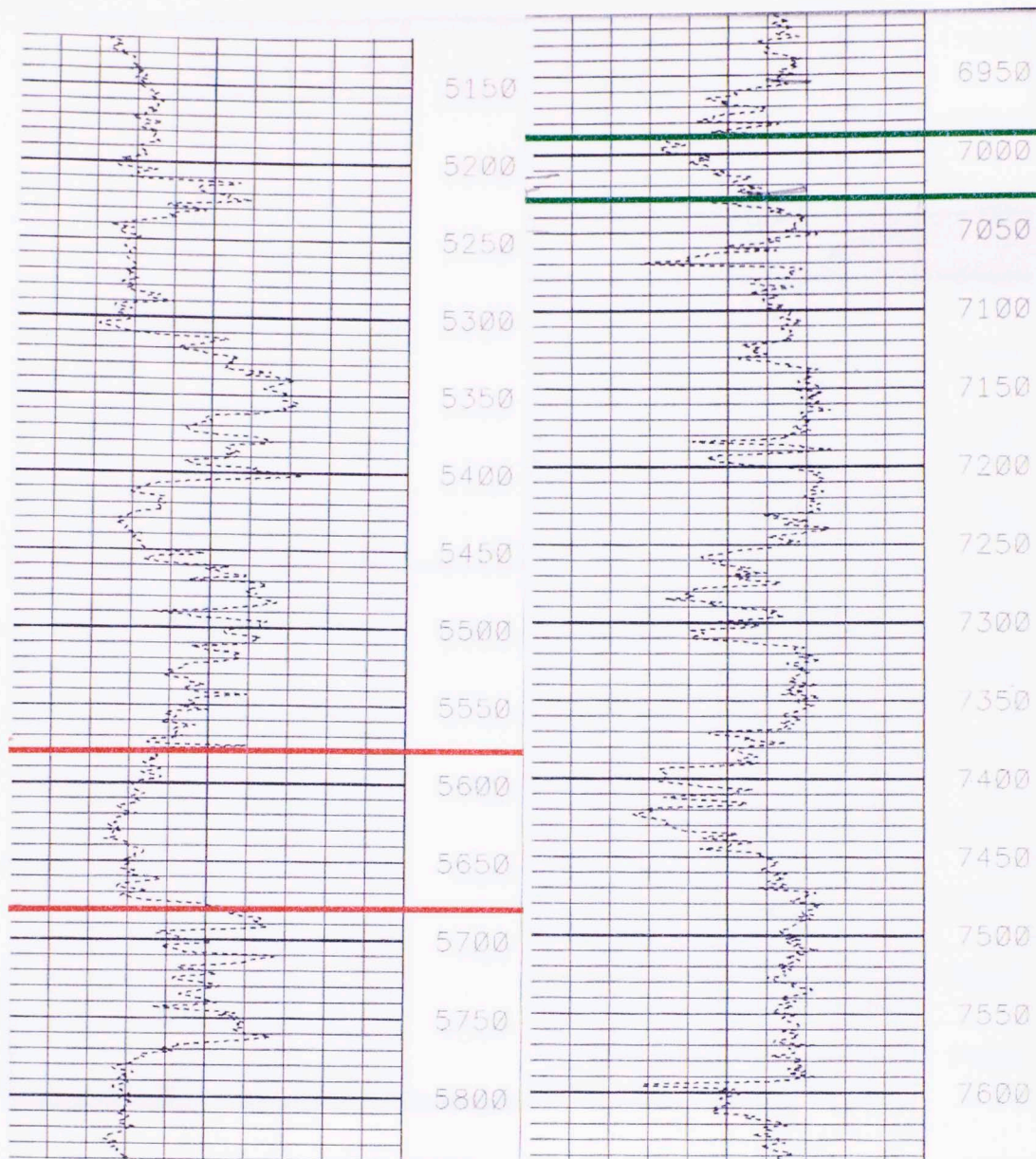
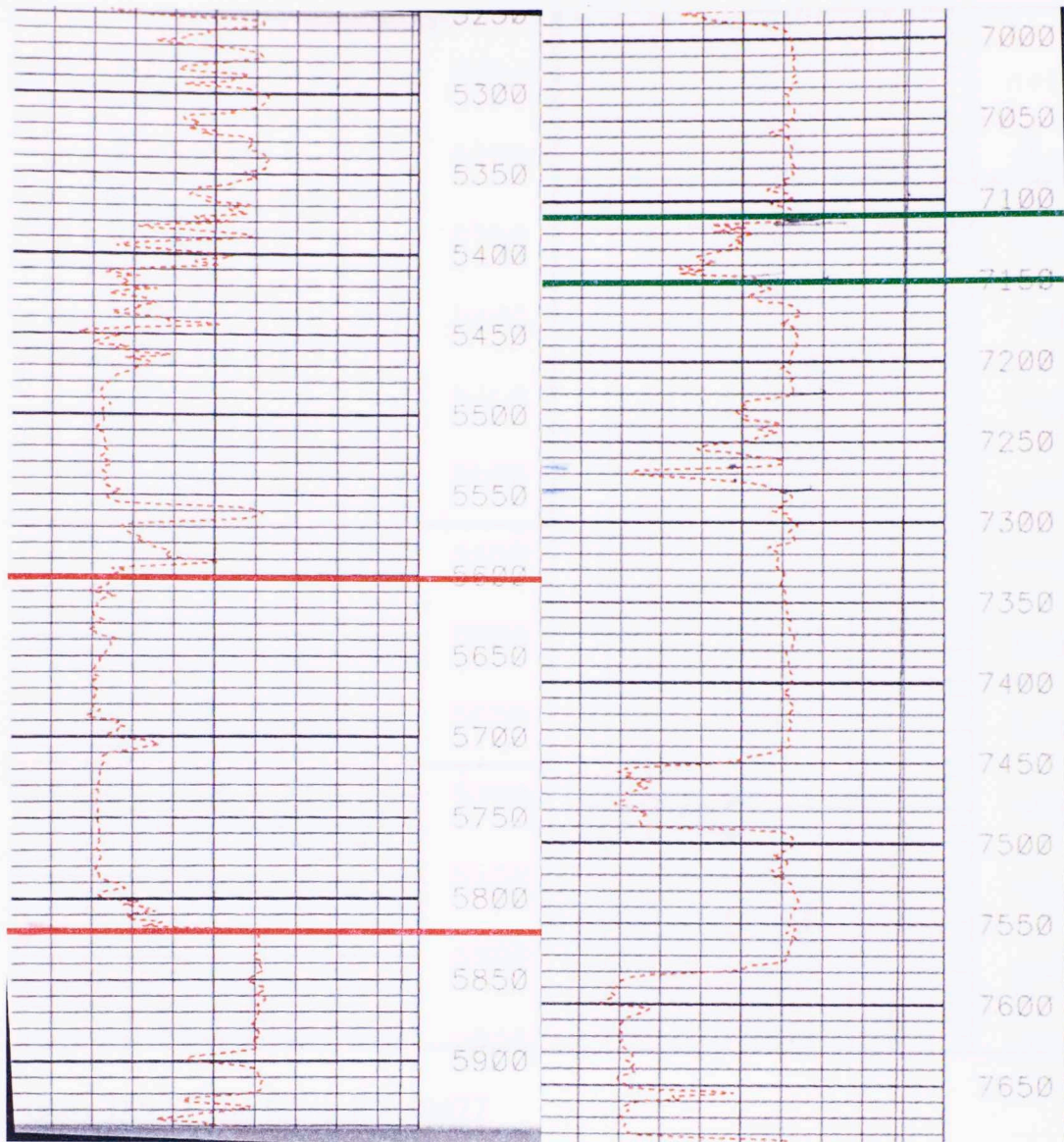


Figure D.6 SP log for well # 20066



**Figure D.7** GR log for well # 40133



**Figure D.8** SP log for well # 40400

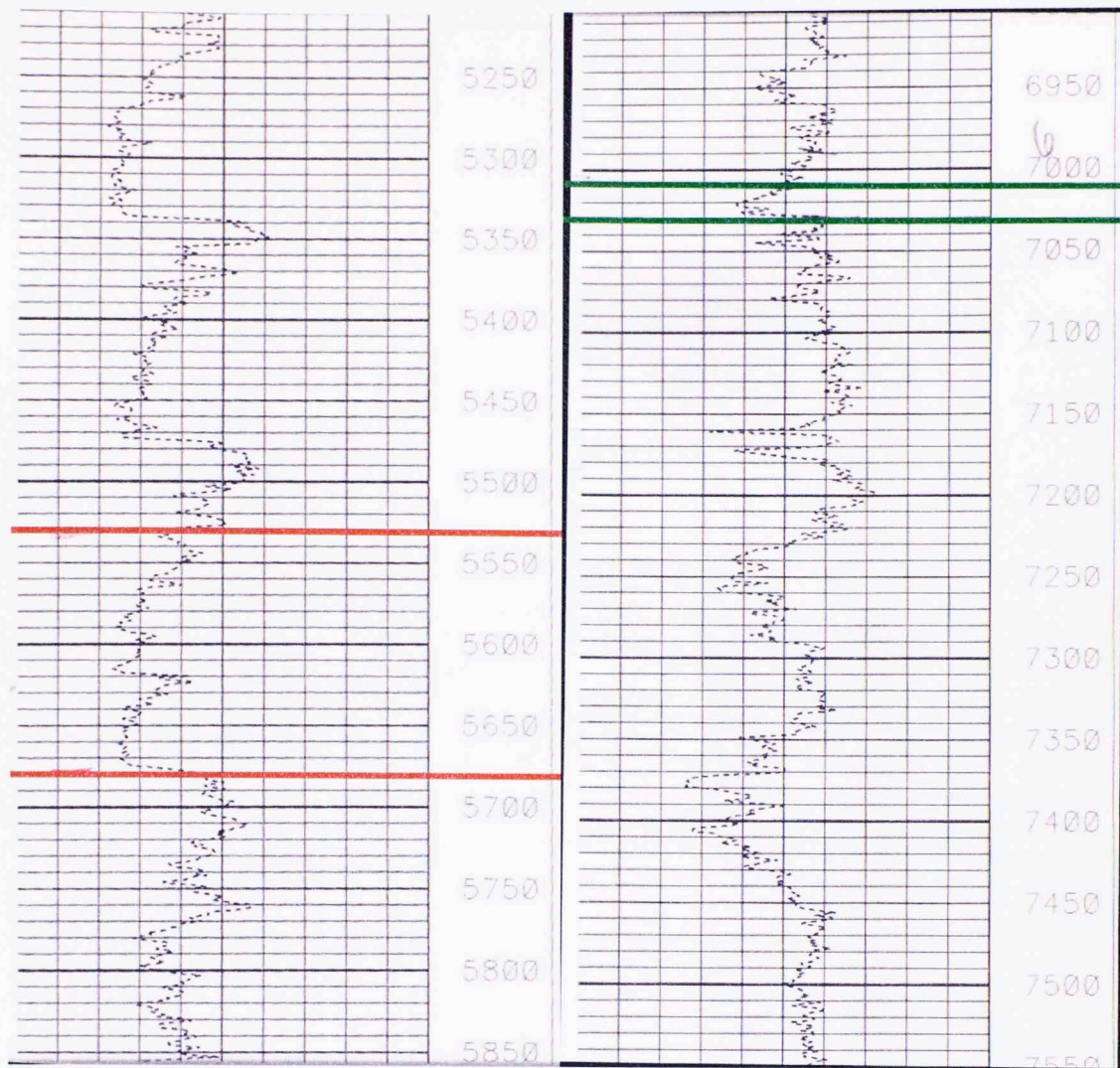


**Figure D.9** SP log for well # 40477

This volume is the property of the University of Oklahoma, but the literary rights of the author are a separate property and must be respected. Passages must not be copied or closely paraphrased without the previous written consent of the author. If the reader obtains any assistance from this volume, he must give proper credit in his own work.

I grant the University of Oklahoma Libraries permission to make a copy of my thesis upon the request of individuals or libraries. This permission is granted with the understanding that a copy will be provided for research purposes only and that requestors will be informed of these restrictions.

NAME

DATE

A library which borrows this thesis for use by its patrons is expected to secure the signature of each user.

This thesis by SARA K. TIRADO has been used by the following persons, whose signatures attest their acceptance of the above restrictions.

NAME AND ADDRESS

DATE

SUBMITTED TO THE GRADUATE FACULTY

in partial fulfillment of the requirements for the

Degree of

Master of Science

Sara K. Tirado

University of Oklahoma

2014